

Effectiveness of Sand Compaction Piles in Improving Soil Bed Formed of Alluvial Deposits of Bangladesh

A thesis by

Md Zillal Hossain

In partial fulfillment of the requirements for the Degree of

Master of Science in Civil Engineering (Geotechnical)



Department of Civil Engineering
Bangladesh University of Engineering and Technology

July 2015

The thesis titled “**Effectiveness of Sand Compaction Piles in Improving Soil Bed Formed of Alluvial Deposits of Bangladesh**”, submitted by Md Zillal Hossain, Student No. 0413042238(F), and Session: April 2013, has been accepted as satisfactory in partial fulfillment of the requirement for the degree of Master of Science in Civil Engineering (Geotechnical) on 25 July 2015.

BOARD OF EXAMINERS

Dr. Md. Zoynul Abedin
Professor
Department of Civil Engineering
BUET, Dhaka-1000

Chairman
(Supervisor)

Dr.A.M.M. Towfiqul Anwar
Professor and Head
Department of Civil Engineering
BUET, Dhaka-1000

Member
(Ex-Officio)

Dr. Abu Siddique
Professor
Department of Civil Engineering
BUET, Dhaka-1000

Member

Dr. Md. Abu Taiyab
Professor
Department of Civil Engineering
DUET, Gazipur

Member
(External)

DECLARATION

It is hereby declared that except for the contents where specific references have been made to the work of others, the studies contained in this thesis are the result of investigation carried out by the author under the supervision of Dr. Md. Zoynul Abedin, Professor, Department of Civil Engineering, Bangladesh University of Engineering and Technology. No part of this thesis has been submitted to any other university or other educational establishments for a degree, diploma or other qualifications (except for publication).

(Signature of the Author)

ACKNOWLEDGEMENTS

The author wishes to express sincere appreciation and deepest gratitude to his supervisor, Dr. Md. Zoynul Abedin, Professor, Department of Civil Engineering, BUET, for his continuous support, guidance and inspiration. His constant direction, advice and supervision encouraged the author to complete the thesis work by overcoming all persistent constraints. Without his sincere effort, vigilant drive and caring attitude, it would not be possible for the part of author alone to complete this colossal task.

The author wants to express his sincere thanks to Dr. Abu Taiyab, Professor, Department of Civil Engineering, DUET, for his support and cooperation, especially for calibrating the Dynamic Cone Penetrometer (DCP) Device. In fact this calibration and its output with necessary analytical comments have formed the core issue of the study.

The author wants to express his sincere thanks to Dr. Md. Towfiqul Anwar, Professor and Head, Department of Civil Engineering, BUET, for his co-operation in allowing the author to work in Geotechnical laboratory. The author wants to express his special thanks to his supervisor, Dr. Md. Zoynul Abedin, Professor, Department of Civil Engineering, BUET, for allowing him to work in Military Institute of Science and Technology (MIST) laboratory. Otherwise, it would be difficult for the author to complete this work in scheduled time.

Author would like to express his special gratitude to Mr. Roman, Mr Kamrujjaman and Mr Khaled laboratory assistants MIST for their excellent support and assistance during author's laboratory work. The author also acknowledges the assistance of Mr. Jahangir Alam and Mr. Shahinur Rahman, office staff of Civil Engineering Department, MIST. Special thanks to Mr. Minhaj for his constant technical support and assistance during the whole tenure of research work.

The author expresses his gratitude to few of his colleagues whose frequent support and inspiration encouraged the author to continue with the persuasion of this research work. They are namely, Col Kalam, Lt Col Mohiuddin, Prof Dr Towhid of MIST, and Prof Dr Zahid of MIST. My special thanks and gratitude to the Head CE Dept of MIST, Col Shah Monirizzaman who had always shown caring attitude and encouraged the author to complete this thesis work.

The author wishes to express his gratitude to his mother, brothers, sisters with all other family members including parents-in-law, brother-in-law and other family members, for their continuous support and sacrifice in completing the thesis work.

The author acknowledges the sincere cooperation, relentless inspiration and support rendered by his wife, Nahar Sultana. The way she sacrificed her time for the author was simply extraordinary. Author's three children Rafsan Mohammad Zahin, Farhan Mohammad Zarif and Zafrin Zahan were also a great source of inspiration in author's day to day thesis work at home.

ABSTRACT

The study was mainly concerned with the effectiveness of Sand Compaction Pile (SCP) in improving the density of alluvial soil deposits of Bangladesh. Miniature sand compaction pile device, miniature dynamic cone penetrometer (DCP), soil tank and sand shower bowl were designed and fabricated for the purpose of the study. Alluvial sandy soil samples were collected from two selected locations of Bangladesh. Soil beds were formed in the soil tank by pouring sand shower from different heights using the specially prepared sand shower bowl so as to achieve sand beds of various densities. The density of soil bed, thus prepared, was measured using density pots and dynamic cone penetration readings were taken to calibrate the soil bed density against cone penetration.

For the purpose of investigating the effectiveness of sand compaction piles in improving the density of loose soil deposits, a sand bed of loose density were formed by sand raining from pre-calibrated height. Initial density of the soil bed was measured using the miniature dynamic cone penetrometer. Sand compaction piles were installed in the soil bed using the miniature sand compaction pile device where a hole was formed in the soil bed by displacing the soil in the lateral direction, and pouring sand in the holes and densified. Square and triangular arrangements of sand compaction piles were used with various spacing. The density of the sand bed with installed sand compaction pile was measured at locations in between the sand piles using the miniature DCP apparatus following the principles outlined in ASTM D6951-09. A term penetration index for the DCP test value was introduced to indicate the density of soil bed.

The data of DCP value and field density thus measured at various depths were analyzed to obtain correlation parameters between dynamic cone resistance (Penetration Index) and relative density of sand. This correlation was used to determine the relative density of improved soil bed due to sand compaction piles of various spacing and arrangements. Results indicated that a triangular arrangement of SCP with a spacing of 2.5 times the diameter of the pile would the most efficient arrangement for improvement of soil bed formed of alluvial soil of Bangladesh. The study yielded useful correlation equations to estimate density from DCP values, and also between SCP spacing and density.

This is perhaps one of the noble studies that attempt to replace the field study of huge SCP construction replaced by physical models in the laboratory.

Keywords: Sand Compaction Pile (SCP) Method, Relative Density, Dynamic Cone Penetrometer.

TABLE OF CONTENTS

	Page
Acknowledgements	iii
Abstract	iv
Table of Contents	v
List of Tables	ix
List of Figures	xi
CHAPTER 1 : INTRODUCTION	1
1.1 General	1
1.2 Soil Improvement Methods	1
1.3 Background of the Present Research	2
1.4 Scopes and Objectives	3
1.5 Outline of Methodology	4
1.6 Overview of the Thesis	4
CHAPTER 2 : LITERATURE REVIEW	6
2.1 General	6
2.2 Relative Density of Sand	6
2.3 Ground Improvement Techniques	8
2.4 Development of SCP Method	10
2.5 Methods of Sand Compaction Pile Installation	14
2.6 Analytical Approach for Bearing Capacity of SCP Treated Ground	15
2.6.1 Bearing Capacity Evaluation by Unit Cell Approach	17
2.6.2 Bearing Capacity Evaluation by Sliding Failure Approach	18
2.6.3 Bearing Capacity Evaluation by General Shear Failure	20

	Approach	
2.6.4	Bearing Capacity Evaluation by Bulging Failure Approach	21
2.6.5	Bearing Capacity Evaluation by Cavity Expansion Approach	22
2.7	Analytical Approach for Settlement of SCP Treated Ground	23
2.7.1	Aboshi and Suematsu's Equilibrium Method	23
2.7.2	Baumann and Bauer's Elastic Method	23
2.7.3	Settlement Relations by Other Investigators	24
2.8	Study and Research on Effectiveness of SCP	25
2.8.1	Replacement Area Ratio	25
2.8.2	Dynamic Cone Penetrometer (DCP) Resistance	26
2.8.3	Effectiveness of SCP against Soil Liquefaction	27
2.8.4	Effectiveness of Granular Pile in Loose to Medium Dense Granular Deposits	29
2.8.5	Effectiveness of SCP against Soil Liquefaction in Ash Pond	30
2.8.6	Evaluation of SCP Treatment	30
2.8.7	Effectiveness of SCP on Foundation Soil as Liquefaction Resistance	32
2.8.8	Dynamic Cone Resistance and Relative Density of Sand	34
2.8.9	Consolidation behavior of Clay Ground Improved by Sand Compaction Piles	34
2.9	Concluding Remarks	35
	CHAPTER 3 : EXPERIMENTAL SETUP, TEST PROGRAMME AND TEST PROCEDURES	36
3.1	General	36
3.2	Design and Fabrication of Miniature SCP Installing Device	37
3.3	Fabrication of Miniature DCP Device	39

3.4	Design and Fabrication of Tank for Housing Sand Bed	43
3.5	Tank for Calibration of DCP	43
3.6	Miniature Device for Dry Air Pluviation of Soil Deposit	44
3.7	Soil Bed and SCP forming Materials	45
3.8	Sand Bed Preparation	46
3.9	SCP Scheme and DCP Location	47
3.10	Installation of Sand Compaction Piling by SCP miniature	50
3.11	Performing Dynamic Cone Penetration(DCP) Test for Density Evaluation	55
3.12	Determination of Bearing Capacity and Shear Strength	57
CHAPTER 4 : RESULTS AND DISCUSSIONS		58
4.1	General	58
4.2	Calibration of Fabricated DCP Miniature	58
4.3	Calibration Correlations	66
4.4	Estimation of Initial Penetration Index, P_{index}	67
4.5	Estimation of Penetration Index, P_{index} for Improved Soil Bed of Turag Sand	67
4.6	Estimation of Penetration Index, P_{index} for Improved Soil Bed of Meghna Sand	72
4.7	Comparison of P_{index} Values of Sand Bed formed of Turag and Meghna Sands	74
4.8	Prediction of Relative Density of Improved Bed	75
4.9	Comparative Study for the Determination of the Most Suitable Method of SCP	78
4.10	Effect of SCP Pattern and Spacing on Soil Improvement	79
4.11	Effect of SCP Pattern on Replacement Ratio for Soil Improvement	82
4.12	Relation between Relative Density , D_r and Replacement Area Ratio, a_s of Soil	82

4.13	Relation between Penetration Index, P_{index} and Relative Density , D_r of Soil	83
4.14	Effect of Grain Characteristics on Soil Improvement due to SCP	83
CHAPTER 5 : CONCLUSIONS AND RECOMMENDATIONS		85
5.1	General	85
5.2	Conclusions	85
5.3	Recommendations for Further Study	86
REFERENCES		88

LIST OF TABLES

		Page
Table 2.1	Typical values of SPT and relative density for sand deposits	7
Table 2.2	Typical values of CPT cone resistance (q_c) and density for sand	8
Table 2.3	Typical values of DCP resistance and density for sand	8
Table 2.4	Ground Improvement Method	9
Table 2.5	SCP applications for on-land construction	11
Table 2.6	SCP application for marine construction	12
Table 3.1	Dimensions of DCP components	42
Table 3.2	Index properties and classification of sands used in the study	46
Table 3.3	Test scheme for the experimental study (Turag Sand)	48
Table 3.4	Test scheme for the experimental study (Meghna Sand)	49
Table 3.5	Characteristics of SCP	50
Table 4.1	Number of Blows and Cumulative Depth of Penetration Data (in mm) for N_{10} and P_{index} Calibration(TURAG SAND)	59
Table 4.2	Number of Blows and Cumulative Depth of Penetration Data (in mm) for N_{10} and P_{index} Calibration (MEGHNA SAND)	62
Table 4.3	Various parameters for Turag sand against pluviation height of fall	64
Table 4.4	Various parameters for Meghna sand against pluviation height of fall	64
Table 4.5	P_{index} value against pile spacing of Turag and Meghna sands for Triangular pattern of SCP	75
Table 4.6	Data for establishing extrapolated calibrated correlation of the DCP miniature between relative density and P_{index} , TURAG sand	76
Table 4.7	Data for establishing extrapolated calibrated correlation of the DCP miniature between relative density and P_{index} , MEGHNA sand	76
Table 4.8	P_{index} and Relative Densities of Sand Bed for Square Pattern for SCP, Turag Sand	78

Table 4.9	P_{index} and Relative Densities of Sand Bed for Triangular Pattern for SCP, Turag Sand	78
Table 4.10	P_{index} and Relative Densities of Sand Bed in Triangular Pattern: Meghna Sand	78
Table 4.11	P_{index} and relative density of sand bed square and triangular patterns of SCP (Turag)	79
Table 4.12	P_{index} and relative densities of Turag and Meghna sands for triangular pattern of SCP	79
Table 4.13	Improvement Indices for Square and Triangular SCP Arrangements (Turag Sand)	80

LIST OF FIGURES

	Page	
Fig. 2.1	Typical improvement purposes of SCP method	11
Fig. 2.2	SCP application for on-land construction	12
Fig. 2.3	SCP application for marine construction	13
Fig. 2.4	Cumulative length of compacted sand piles	14
Fig. 2.5a	SCP machine for on-land construction	16
Fig. 2.5b	SCP barge for marine construction	16
Fig. 2.6	Composer method of SCP installation	16
Fig. 2.7	Non-Vibratory SCP Installation	16
Fig. 2.8	Concept of SCP Ground and Unit Cell	17
Fig. 2.9	Sliding Failure of Composite Ground	19
Fig. 2.10	General Shear Failure of Composite Ground(After, Kitazume)	20
Fig. 2.11	Shear Failure of Composite Ground (After, Barksdale & Bachus)	21
Fig. 2.12	Shear Failure of Composite Ground (After, Barksdale & Bachus)	22
Fig. 2.13	Design Chart for Estimation of Settlement of Improved Soil due to SCP	25
Fig. 2.14	SCP Soil Improvement Pattern	26
Fig. 2.15	(a) Frequency Distribution, (b) Accumulated Frequency Distribution of Relative Density after Improvement (after Moh et al., 1981)	27
Fig. 2.16	Variation of N-values before and after Soil Improvement (After Moh et al. 1981)	28
Fig. 2.17	Relationships between Relative Density and SPT N-Value (after Moh et al., 1981)	28

Fig 2.18	Lateral Displacement of Soil due to Compaction Sand Pile(after Moh et al., 1981)	29
Fig. 2.19	Increases In the Normalised SPT- N_1 Values of Soil (Krishna and Madhav, 2008)	30
Fig. 2.20	The location of Taichung Thermal Power Plant (Ref. [4])	30
Fig. 2.21	Flow Chart of Investigation Assessing Improvement Effect (after Kempfert, 2003)	31
Fig. 2.22	SPT profile before and after the improvement (Kempfert, 2003)	32
Fig. 2.23	Cone resistance before and after improvement (Kempfert, 2003)	32
Fig. 2.24	Plan View of Sampling Locations (After Unnikrishnan And Johnson, 2009)	33
Fig. 2.25	Liquefaction Resistance and Normalized N -Value for Saturated and De-Saturated Improved Sand (after Unnikrishnan and Johnson, 2009)	33
Fig. 2.26	Relative Density and P_{index} and D_{50} for DCP (after Alam et al., 2012)	34
Fig. 3.1	Flow Chart of research Methodology	37
Fig. 3.2	Schematic Diagram of Miniature SCP Mandrel; (a) Open Postion; (b) Closed Position	38
Fig. 3.3	Photograph of Miniature SCP Mandrel	39
Fig. 3.4	Photograph of DCP Miniature Device with Dimensions	40
Fig. 3.5a	Schematic Diagram of Fabricated DCP Miniature Device Assembly	41
Fig. 3.5b	Schematic Diagram of Fabricated DCP Miniature Device Components	42
Fig. 3.5c	Replaceable Point Tip of DCP	42
Fig. 3.6	Sand Bed Housing Tank; (a) Schematic Diagram; (b) Photograph	43
Fig. 3.7	DCP Calibration Tank; (a) Schematic Diagram; (b) Photograph ;	44
Fig. 3.8	Device for Air Pluviation Soil Deposit; (a) Schematic Diagram; (b) Sieve Mesh	44

Fig. 3.9	Grain Size Distribution Curves for Sand Samples used in Investigation	45
Fig. 3.10	Sand Bed Prepared using Dry Air Pluviation Method for SCP	47
Fig. 3.11	Photograph Showing Air Pluviation Method of Sand Deposition	47
Fig. 3.12	Typical Square and Triangular Arrangements of SCP showing DCP Locations	49
Fig. 3.13a	Positioning of Miniature SCP Mandrel	51
Fig. 3.13b	Initial Push to the SCP Mandrel	51
Fig. 3.13c	Driving of SCP Mandrel	52
Fig. 3.13d	Pouring of Coarse Sand in to the Mandrel	52
Fig. 3.13e	Withdrawal of SCP Mandrel	53
Fig. 3.13f	Compacting the SCP Sand	53
Fig. 3.13g	Finished SCP in Square Pattern	54
Fig. 3.13h	Finished SCP in Triangular Pattern	54
Fig. 3.14a	Positioning and Initialization of Miniature DCP Equipment for Testing	55
Fig. 3.14b	Raising the Hammer to the Desired Height	56
Fig. 3.14c	Final Reading Penetration Per Blow	56
Fig. 4.1a	No. of Blows vs Cumul. Penetration Depth (Height of Fall = 15 cm: TURAG SAND)	59
Fig. 4.1b	No. of Blows vs Cumul. Penetration Depth (Height of Fall = 22.5 cm: TURAG SAND)	60
Fig. 4.1c	No. of Blows vs Cumul. Penetration Depth (Height of Fall = 30 cm: TURAG SAND)	60
Fig. 4.1d	No. of Blows vs Cumul. Penetration Depth (Height of Fall = 37.5 cm: TURAG SAND)	61
Fig. 4.1e	No. of Blows vs Cumul. Penetration Depth (Height of Fall = 45 cm: TURAG SAND)	61
Fig. 4.2a	No. of Blows vs Cumul. Penetration Depth (Height of fall = 22.5 cm: MEGHNA SAND)	62
Fig. 4.2b	No. of Blows vs Cumul. Penetration Depth (Height of fall = 30 cm: MEGHNA SAND)	63

MEGHNA SAND)

Fig. 4.2c	No. of Blows vs Cumul. Penetration Depth (Height of fall = 37.5 cm: MEGHNA SAND)	63
Fig. 4.3	Pluviation Height of Fall versus Relative Density of Turag Sand	64
Fig. 4.4	Pluviation Height of Fall versus Relative Density of Meghna Sand	65
Fig. 4.5	Relative Density - Relationship for Turag Sand	65
Fig. 4.6	Relative Density - Relationship for Meghna Sand	66
Fig. 4.7	Estimation of ϕ and ρ_r (SCP Spacing = 30 cm, Square Pattern; TURAG)	68
Fig. 4.8	Estimation of ϕ and ρ_r (SCP Spacing = 22.5 cm, Square Pattern; TURAG)	68
Fig. 4.9	Estimation of ϕ and ρ_r (SCP Spacing = 15 cm, Square Pattern; TURAG)	69
Fig. 4.10	Estimation of ϕ and ρ_r (SCP Spacing = 30 cm, Triangular Pattern; TURAG)	69
Fig. 4.11	Estimation of ϕ and ρ_r (SCP Spacing = 22.5 cm, Triangular Pattern; TURAG)	70
Fig. 4.12	Estimation of ϕ and ρ_r (SCP Spacing = 15 cm, Triangular Pattern; TURAG)	70
Fig. 4.13	Effectiveness of SCP: Piling Spacing Vs. P_{index} , Square Pattern (TURAG)	71
Fig. 4.14	Effectiveness of SCP: Piling Spacing Vs. P_{index} , Triangular Pattern (TURAG)	71
Fig. 4.15	Estimation of ϕ and ρ_r (SCP Spacing = 30 cm, Triangular Pattern; MEGHNA)	72
Fig. 4.16	Estimation of ϕ and ρ_r (SCP Spacing = 22.5 cm, Triangular Pattern; MEGHNA)	73
Fig. 4.17	Estimation of ϕ and ρ_r (SCP Spacing = 15 cm, Triangular Pattern; MEGHNA)	73
Fig. 4.18	Effectiveness of SCP: Piling Spacing Vs. P_{index} , Triangular Pattern (MEGHNA)	74

Fig. 4.19	Comparison of SCP Effectiveness: Comparative Plot of Pile Spacing Vs P_{index} , between the beds formed of TURAG and MEGHNA sand (Triangular Pattern)	75
Fig. 4.20	Extrapolated Correlation between Relative Density and Penetration Index, TURAG	77
Fig. 4.21	Extrapolated Correlation between Relative Density and Penetration Index, MEGHNA	77
Fig. 4.22	Variation of Penetration Index with SCP Spacing ,Turag	80
Fig. 4.23	Variation of Penetration Index with SCP Spacing Ratio, Turag	81
Fig. 4.24	Variation of Penetration Index with Replacement Area Ratio, Turag	81
Fig. 4.25	Variation of Relative Density with Replacement Area Ratio, TURAG	82
Fig. 4.26	Variation of Penetration Index with Relative Density, Turag	83
Fig. 4.27	Comparison of SCP Effectiveness: Comparative Plot of Pile Spacing Vs P_{index} , TURAG and MEGHNA River (Triangular Pattern)	84

CHAPTER 1

INTRODUCTION

1.1 General

It is an obvious truism that structures should be constructed on good quality ground. Ground conditions of construction sites, however, have become worse in recent decades throughout the world. This situation is especially pronounced in Bangladesh, where many construction projects are conducted on soft alluvial clay grounds, reclaimed grounds with dredged soils, highly organic soil grounds, and loose sandy grounds and so on. When any types of infrastructures are constructed on these types of soil large amounts of ground settlement and/or stability failure are likely to be encountered. Apart from clay or highly organic soil grounds, loose sand deposits under a water table cause serious problems of liquefaction under seismic conditions. In such cases, suitable soil improvement techniques are required to improve the physical properties of soft/loose soil in order to cope with these problems. Many soil improvement techniques have been developed in Japan and other countries for these purposes.

The Sand Compaction Pile (SCP) method has been developed and frequently adopted for many construction projects in Japan, in which sand is fed into a ground through a casing pipe and is compacted by either vibration, dynamic impact or static excitation to construct a compacted sand pile in a soft soil ground (Kitazume, 2005). This method was originally developed in order to increase the density of loose sandy ground and to increase the uniformity of sandy ground, to improve its stability or compressibility and/or to prevent liquefaction failure, but now it has also been applied to soft clay ground to assure stability and/or to reduce ground settlement. The principal concept of the SCP method for application to sandy ground is to increase the ground density by placing a certain amount of granular material (usually sand) in the ground. The principal concept for application to clay ground, on the other hand, is reinforcement of composite ground consisting of compacted sand piles and surrounding clay, which is different from that of the Sand Drain method in which sand piles without any compaction are constructed principally for drainage function alone.

1.2 Soil Improvement Methods

Soil improvement methods can be categorized into five groups: replacement, consolidation, densification, solidification and contact pressure reduction. Among the categories, the SCP method can be categorized into 'reinforcement method' and 'densification method' for applications to clay and sandy grounds respectively. The SCP method was practically applied as a densification method in 1957 and as a replacement

method in 1966 that was rather early among the improvement methods (Kitazume, 2005). The present day soil improvement methods are summarized in Chapter 2.

1.3 Background of the Present Research

Construction projects often encounter very soft/loose soil deposits throughout the world, which can pose problems of stability, excessive settlement and/or liquefaction. To solve these problems, a variety of ground improvement techniques have been evolved around the world. The one, sand compaction pile (SCP) method was developed and frequently adopted for improving sandy and clay grounds in Japan. Recently, this method has been adopted in many countries especially in Asia for improving sandy and clay grounds (Samanta et al., 2010; Unnikrishnan and Johnson, 2009; Kitazume, 2005; Kempfert, 2003; Solymar et al., 1986; Moh et al., 1981). Compaction sand piles were used at the site of a steam power plant in the southern part of Taiwan which had high liquefaction potential. The improvement was successful with 100% samples giving over the required 65% relative density, and 92% samples with more than 75% relative density (Moh et al., 1981). The effect of granular pile installation on the modifications induced in loose to medium dense granular deposits is studied by Krishna and Madhav (2008). Performance of ground was improved or enhanced by using granular piles/sand compaction piles as a ground improvement method. It was seen that installation of granular piles densifies the ground and modifies the deformation properties of the soils. SCP was used for assessing improvement effects in an Ash Pond at the site of Taichung Thermal Power Plant, located in the seashore of central Taiwan and neighboring Taichung Harbor, China which suffered serious damage caused by soil liquefaction in the 1999 Chi-Chi earthquake [8]. Their results reveal that the effect of using SCP to improve coal ash deposit is significant except for the shallow layer above the ground water level owing to its low confining stress. The CPT investigation has the highest resolution to identify the improvement effect and is highly recommended to be used in engineering practice. Sand compaction pile (SCP) has been extensively used to ameliorate liquefaction resistance of loose sand deposits. Laboratory tests on high-quality undisturbed samples obtained by the in situ freezing method at six sites were conducted by Okamura et al. [9] where foundation soils had been improved with SCP. The test results revealed that the improved ground was desaturated during the ground improvement. As soils are local materials and the applications are different in various parts of the world, the effectiveness of SCP method will also vary in various parts of the world.

Bangladesh is a riverine country with full of alluvial subsoil having abundance of loose fine sandy silt deposits that needs to be improved for the construction of many civil engineering structures over them. Ground improvement methods are usually complex phenomenon and in most of the occasions are expensive. So, it is the time to concentrate our efforts to examine the application of SCP method for improving the shear strength and bearing

capacity of the alluvial soil deposits in Bangladesh soil condition. SCP method of soil improvement has recently been used in selected locations of approach road of Padma Multipurpose Bridge Project for improving the subsoil conditions. It is noteworthy that these type of highway/mega industrial project based soil improvement techniques are expensive, but it's contribution in the long run are quite significant since it will reduce the problems of stability, deformation, excessive settlement and/or liquefaction. Non-availability of suitable sites for construction is forcing the construction industry to go for such soil improvements and Bangladesh is no exception. Unfortunately, not many works have been done in the past on the aspects of SCP in Bangladesh soil. This calls for carrying out proper research on these important issues of geotechnical engineering in order to find out effective solutions of the problem.

1.4 Scope and Objectives

Based on the above mentioned background, the main objective of this research was to conduct extensive experiments in the laboratory to identify the most effective SCP method in the alluvial soil deposits of Bangladesh. To fulfill the objective, SCPs were conducted on the prepared beds in the laboratory in square and triangular pattern/ category with different spacings. A calibrated DCP miniature based on ASTM standard was used to analyze the effectiveness of SCP. Relative density of improved beds, a governing contributor for determining the effectiveness of SCP was used as a major parameter in this research. Calibrated DCP miniature is used to determine the relative density.

Based on the main goal of this research, the specific objectives of this research are as follows:

- a. To design and fabricate model SCP instruments for conducting tests in the laboratory in order to examine the effectiveness of soil improvement by SCP in the context of Bangladesh soil.
- b. To design and fabricate model dynamic cone penetrometer (DCP) instruments in order to assess the quality of improved soil bed.
- c. To conduct experiments in the laboratory with various soil and SCP pattern/category conditions with an aim to decide on the most effective soil and SCP pattern conditions using representative soil beds of alluvial deposits of Bangladesh.
- d. To analyze the data of the experiments in order to formulate soil and SCP parameters as a means of ground improvement for alluvial soil deposits of Bangladesh.

- e. To identify the most effective SCP scheme for bearing capacity and shear strength of the alluvial soil deposits.

It is expected that the outcome of this research work will facilitate identification of the most effective SCP scheme in the context of the alluvial soil deposits of Bangladesh.

1.5 Outline of Methodology

The total analysis on the effectiveness of SCP method will be done based on the experimental results. The outline methodology of the research work is as follows:

- a. The available literature and SCP guidelines and experiences were reviewed.
- b. Sufficient knowledge on the existing SCP ground improvement techniques, nature and extent of the problems posed by the alluvial soil deposits were gained by conducting detail studies of the previous records/documents/papers.
- c. Miniature SCP and DCP instruments have been designed and fabricated to conduct experiments in the laboratory.
- d. Calibration of the “DCP miniature device” were carried out in the laboratory following the guidelines of investigators (Alam et al., 2012)
- e. Tests were conducted on controlled soil beds of alluvial deposits using various SCP and soil conditions.
- f. Response of the improved/controlled alluvial soil beds depending on various pattern/techniques of SCP method have been assessed with the help of fabricated Dynamic Cone Penetrometer (DCP) miniature device following ASTM and other procedures [Alam et al., 2012; ASTM, 2012a; ASTM, 2012b; ASTM, 2012c; ASTM, 2014a; ASTM, 2014b).
- g. The most suited SCP method as ground improvement technique has been sought out after analyzing the result of the laboratory experiments and other relevant research work on SCP method.

1.6 Overview of The Thesis

Chapter One (Introduction): This chapter introduces the general remarks on SCP method followed by the motivation of this research. This chapter also highlights the main and specific objectives of this study including research methodology followed by this outline.

Chapter 2 (Literature Review): This chapter is devoted to the review of past researches in Bangladesh and other parts of the world more particularly the past researches related to the effectiveness of SCP in improving the beds of alluvial soil. In addition, detail theoretical aspects of SCP method including the development /adoption of SCP method,

categories/techniques of soil improvement, improvement purpose and applications of SCP method etc. are also discussed. Dynamic Cone Resistance and Relative Density of sands are discussed foreseeing its importance in the whole research program.

Chapter 3 (Materials for Soil Deposit, Experimental Setup and Their Calibration): This chapter mainly includes the calibration of a Dynamic Cone Penetrometer (DCP) miniature in a prepared sand bed. Determination of N_{10} and P_{index} value using DCP test are also discussed. In addition, relationships between Cumulative Depth of Penetration (mm) Vs. Number of Blows are presented for different relative density using Dry air pluviation method.

Chapter 4 (Test Programme Procedures and Data Analysis): This chapter includes the Laboratory test programs including laboratory test procedures and numerical analysis. Description of the miniature developed for constructing SCP including procedure of using the miniature is discussed in Chapter 4. Penetration Index () and other associated essential parameters of analytical study and their determination procedures are discussed here.

Chapter 5 (Results and Discussions): In this chapter, SCP miniature together with square & triangular pattern/category with different spacing of SCP, the effectiveness of SCP in improving the representing alluvial sandy soil deposits are discussed. Finally, analyzing different pattern/category of SCP, the most suitable of SCP in context of Bangladesh is evaluated.

Chapter 6 (Conclusions and Recommendations for Further Studies): Findings of the research program and related discussions are presented in this chapter. This chapter also includes scopes for future researches with specific recommendations.

CHAPTER 2 LITERATURE REVIEW

2.1 General

The present study was aimed to investigate the effectiveness of sand compaction pile (SCP) as a tool to improve alluvial soil deposits, the abundant and common soil of Bangladesh, for the construction of civil engineering structures. This chapter presents the basic concepts of SCP, the soil parameters upon which SCP acts and the available literature related to ground improvement techniques especially the past studies on Sand Compaction Piles as a tool of ground improvement.

This chapter also gives an overview of the techniques that are commonly used in various parts of the world to improve the performance of the ground in-situ. Not included are less specialized methods of ground improvement such as surface compaction, or methods that involve the placement of geotextile or geogrid materials in soil fill.

In addition, theoretical aspects of SCP method including the development/adoption of SCP method, categories/techniques of soil improvement, improvement purpose and applications of SCP method etc. are also discussed. Dynamic Cone Resistance and Relative Density of sands are discussed foreseeing its importance in the whole research program. Correlation between Dynamic Cone Resistance/Penetration index and Relative Density of sands is discussed as the result of the Penetration index of the improved bed is utilized to find out the Relative Density of the improved bed to analyse the effectiveness of SCP in improving the beds of alluvial soil deposits which is the main objective of this research program.

2.2 Relative Density of Sand

Relative density of sands refers to the in situ (in-place) void ratio of a sand deposit as referenced to index values of the maximum and minimum void ratio determined in the laboratory from a sample of the natural deposit. By definition, the relative density of a sand deposit, D_r , is calculated as:

$$(\%) = \frac{e_{max} - e}{e_{max} - e_{min}} \times 100 \quad (2.1)$$

The *in situ* void ratio of a sand deposit is affected by the process of deposition as well as the size, shape and gradation of the sand grains. Because the unit weight of a sand deposit is related to the void ratio, the relative density may also be expressed as a ratio of unit weights as:

$$(\%) = \frac{\gamma - \gamma_{min}}{\gamma_{max} - \gamma_{min}} \times 100 \quad (2.2)$$

If all of the sand grains in a deposit are idealized as uniformly sized perfect spheres and they are packed in their loosest possible state, the maximum void ratio would be approximately $e = 0.90$. If these same idealized grains are packed in their densest possible state, the minimum void ratio would be approximately $e = 0.35$. Natural sand deposits often times contain a range of particle sizes, with particle shapes ranging from nearly rounded to very angular. When the sand grain sizes are not uniform, smaller grains will fill in the gaps between larger grains and thus the minimum void ratio may be reduced to around 0.25 in the dense state. When the sand grains are angular they tend to form looser structures than rounded grains, resulting in higher void ratios. If the sand deposit is compacted by vibration accompanied with surcharge loading, a dense structure with minimized void ratio can be obtained.

As the void ratio/unit weight of a sand changes, strength characteristics of the deposit will also change. On the basis of relative density, sandy soils may be qualitatively classified from Very Loose to Very Dense state. Natural deposits of sands are commonly sampled/tested using the standard penetration test (SPT) or the static cone penetration test (CPT). V.N.S Murthy (2002) presented approximate relationships between relative density of sands, the SPT results, and the internal friction angle of the sand in his book “Geotechnical Engineering: Principles and practices of soil “ as given in Table 2.1 for sands with both rounded and angular grains.

Table 2.1: Typical values of SPT and relative density for sand deposits (After Murthy 2002)

	Compactness	Dr (%)	rounded	angular
0 – 4	Very Loose	0-15	<27	<30
4 – 10	Loose	15-35	27-30	30-35
10 – 30	Medium	35-65	30-35	35-40
30 – 50	Dense	65-85	35-38	40-45
> 50	Very Dense	>85	>38	>45

The load bearing capacity of a non-reinforced sand deposit is also related to its relative density. In general, as the relative density increases, the internal friction angle of the sand increases as does the ability of the sand to support loads without failure or excessive settlement. When a soil layer is reinforced, the increased load bearing capacity is related to the depth and number of reinforcing layers, the aerial extent of the reinforcement, and strength properties of the reinforcing material(s).

Look (2007) presented a simplified version of strength assessment of coarse grained soil from cone penetration resistance from Cone Penetration Test (CPT) as given in Table 2.2.

Table 2.2: Typical values of CPT cone resistance (q_c) and density for sand (After Look, 2007)

(MPa)	Compactness	Dr (%)	Typical values of
< 2.5	Very Loose	0-15	<30
2.5 – 5.0	Loose	15-35	30 – 35
5.0 –10.0	Medium	35-65	35 – 40
10.0 –20.0	Dense	65-85	40 – 45
> 20	Very Dense	>85	> 45

Look (2007) also mentioned of the strength parameters as estimated from Dynamic Cone Penetration (DCP) test. According to him the standard cone penetrometer has energy of approximately $1/3^{\text{rd}}$ as compared to that of SPT. He presented a chart, Table 2.3, to correlated DCP values with soil strength of sandy soil.

Table 2.3: Typical values of DCP resistance and density for sand (After Look, 2007)

– (blows/100 mm)	Compactness	Typical values of
0 – 1	Very Loose	<30
1 – 3	Loose	30 – 35
3 –8	Medium	35 – 40
8 –15	Dense	40 – 45
> 15	Very Dense	> 45

2.3 Ground Improvement Techniques

According to improvement principles, soil improvement methods can be categorized into five groups: replacement, consolidation, densification, solidification and contact pressure reduction. Among the categories, the SCP method can be categorized into ‘reinforcement method’ and ‘densification method’ for applications to clay and sandy grounds respectively. The SCP method was practically applied as a densification method in 1957 and as a replacement method in 1966 that was rather early among the improvement methods. Table 2.4 summarizes various soil improvement techniques and the period in which practical application of each method was introduced as presented by Kitazume (2005).

The densification category includes other sand pile constructions methods such as 'vibro-compaction' for sandy grounds and 'vibro-replacement' and 'vibro-displacement' for clay grounds, which have been applied in many countries. The procedure of constructing compacted sand piles in these methods is somewhat different from the SCP method: the sand piles in these methods are constructed by feeding sand in the cavity outer surface of

the casing pipe. However the shape and function of compacted sand piles in a ground are similar to those of the SCP method.

Table 2.4: Ground improvement methods (After Kitazume, 2005)

Improvement principle	Engineering method	Work examples	Period practical application introduced										
Replacement	Excavation Replacement	Dredging replacement method											
	Forced Replacement	Sand compaction pile method				1966							
Consolidation	Preloading	Preloading method	1928										
	Preloading with vertical drain	Sand drain method			1952								
		Packed sand drain method				1967							
		Board drain method				1963							
	Dewatering	Deep well method		1944									
		Well point method			1953								
		Vacuum consolidation method					1971						
	Chemical dewatering	Quick lime pile method				1963							
	Densification	Dewatering compaction	Sand compaction pile method			1957							
			Grand compaction pile method				1965						
compaction		Vibration compaction			1955								
		Impact compaction					1973						
Solidification (Admixture stabilization)	Agitation mixing	Shallow mixing method					1972						
		Deep mixing method					1974						
	Jet mixing	Jet mixing method						1981					
Contact pressure reduction	Load Distribution	Fascine mattress											
		Sheet net method				1962							
		Sand net method											
		Surface solidification method					1970						
	Balancing loads												

2.4 Development of SCP Method

To solve the problems of stability, excessive settlement and/or liquefaction due to very soft/loose soil deposits encountered by the construction projects, a variety of ground improvement techniques have been evolved around the world. One of them, the Sand Compaction Pile (SCP) method has been developed and frequently adopted for many construction projects in Japan and frequently adopted in many countries especially in Asia for improving sandy and clay grounds in which sand is fed into a ground through a casing pipe and is compacted by either vibration, dynamic impact or static excitation to construct a compacted sand pile in a soft/loose soil ground (Samanta et al., 2010; Unnikrishnan and Johnson, 2009; Kitazume, 2005; Kempfert, 2003; Solymar et al, 1986; Moh et al., 1981).

This method was originally developed in order to increase the density of loose sandy ground and to increase the uniformity of sandy ground, to improve its stability or compressibility and/or to prevent liquefaction failure, but now it has also been applied to soft clay ground to assure stability and/or to reduce ground settlement (Kitazume, 2005).

The principle concept of the SCP method for application to sandy ground is to increase the ground density by placing a certain amount of granular material (usually sand) in the ground. The principle concept for application to clay ground on the other hand, is reinforcement of composite ground consisting of compacted sand piles and surrounding clay, which is different from sand drain method in which sand piles without any compaction are constructed principally for drainage function alone (Kitazume, 2005).

In Japan, the Sand Compaction Pile (SCP) method has been applied to improve soft clays, organic soils and loose sandy soils for various purposes and in various ground conditions. Figure 2.1 shows typical improvement purposes of the SCP. Tables 2.5 and 2.6 describe the purpose of SCP under various structures constructed on land and marine sites respectively. They are also shown schematically in Figures 2.2 and 2.3.

According to the wide varieties of SCP application together with the development of SCP machines, the maximum improvement depth of the method increased to 70 m in 1993. The cumulative length of compacted sand piles also increased very rapidly in the 1970s, 1980s and 1990s, and reached 350 thousand km in 2001, as summarized in Figure 2.4. Nowadays, the SCP method has been used to improve many kinds of ground including clay ground, sandy ground and fly ash ground for various improvement purposes.

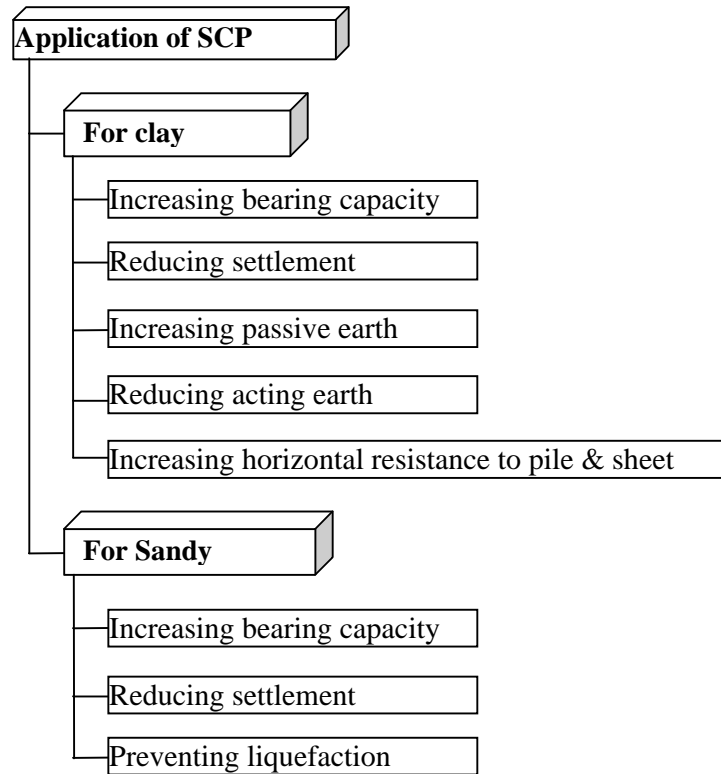


Figure 2.1: Typical improvement purposes of SCP method (After Kitazume, 2005)

Table 2.5: SCP applications for on-land construction (After Kitazume, 2005)

Item	Structure	Purpose of using SCP
(a)	Embankments for road & highway	Prevention of sliding failure of bearing capacity, reduction of settlement
(b)	Filling behind bridge foundation	Prevention of sliding failure of bearing capacity, reduction of settlement, prevention of liquefaction.
(c)	Storage yard for power station	Prevention of sliding failure of bearing capacity, reduction of settlement
(d)	River embankment	Prevention of sliding failure of bearing capacity, reduction of settlement, prevention of liquefaction.
(e)	Foundation of building and factory	Prevention of sliding failure of bearing capacity, reduction of settlement
(f)	Underground structure	Increase of bearing capacity, prevention of liquefaction, reduction of earth pressure, increase of k_0 -value
(g)	Foundation of tank, silo and retaining wall	Prevention of sliding failure, increase of bearing capacity, reduction of settlement, prevention of liquefaction, increase of K_0 -value

Table 2.6: SCP application for marine construction (after Kitazume, 2005)

Item	Structure	Purpose of using SCP
(a)	Concrete caisson type breakwater	Increase of stability, increase of bearing capacity, reduction of settlement
(b)	Concrete block type sea revetment	Increase of stability, improvement of bearing capacity, reduction of settlement
(c)	Cellular block type	Increase of stability, reduction of settlement, improvement of bearing capacity
(d)	Steel sheet pile type sea revetment	Increase of stability, reduction of settlement, increase of K_o -value
(e)	Pile type pier, jacket type structure	Increase of stability, reduction of settlement, increase of K_o -value
(f)	Sloping sea revetment	Increase of stability increase of bearing capacity, reduction of settlement

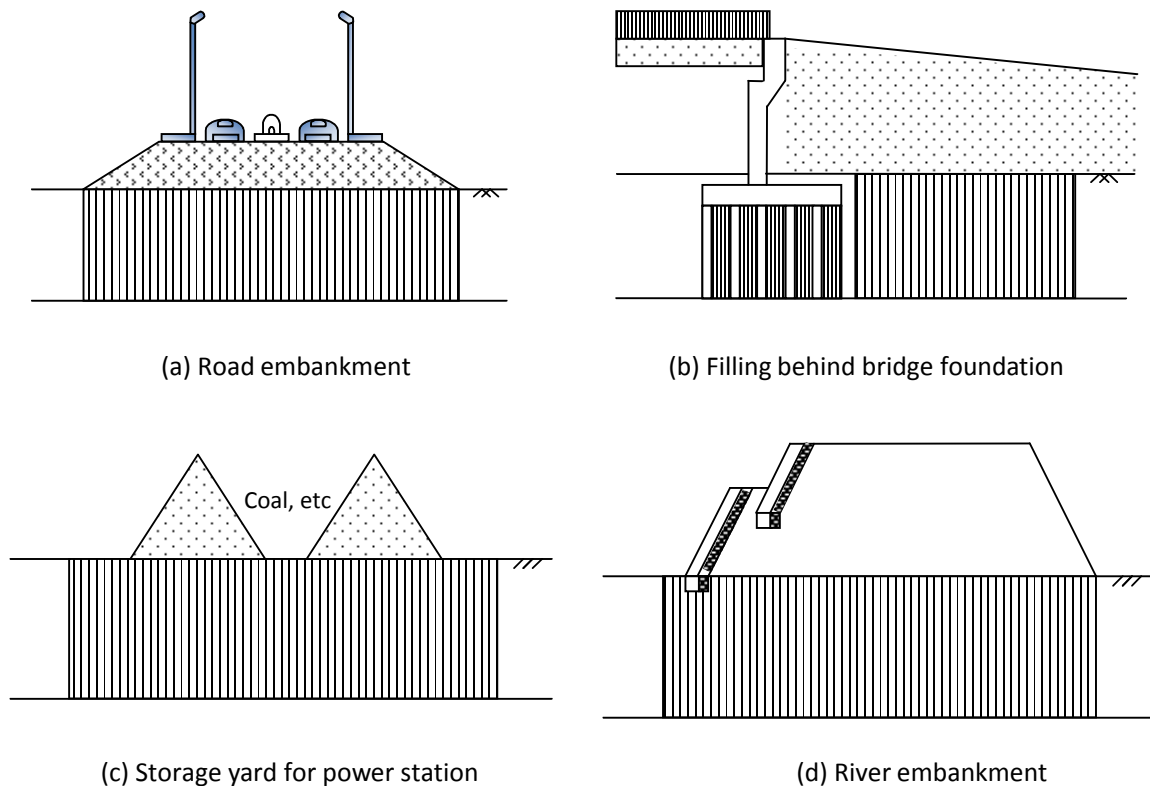
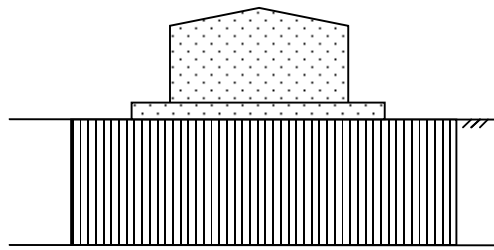
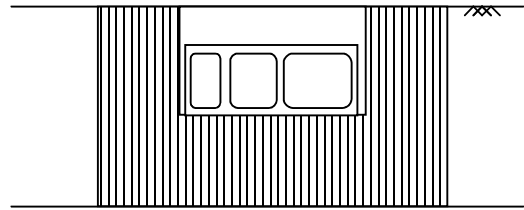


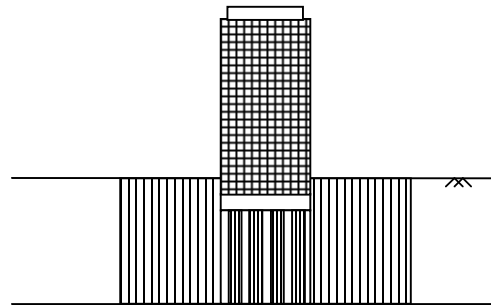
Figure 2.2: SCP applications for on-land construction (after Kitazume, 2005)



(e) Foundation of building and factory

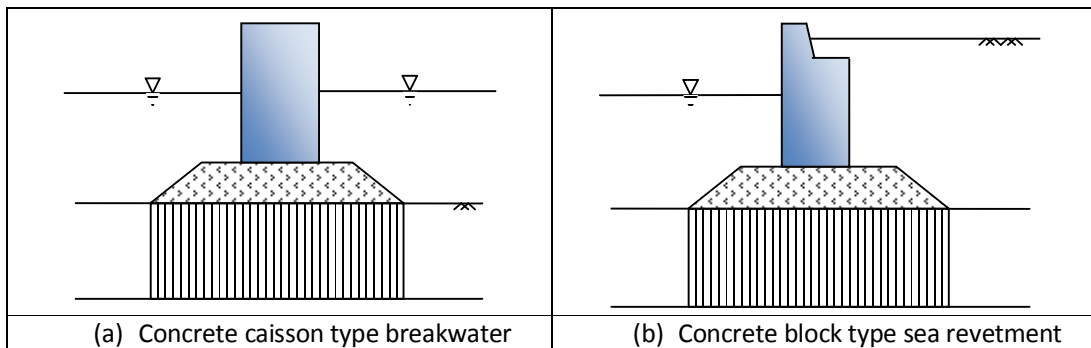


(f) Underground structures



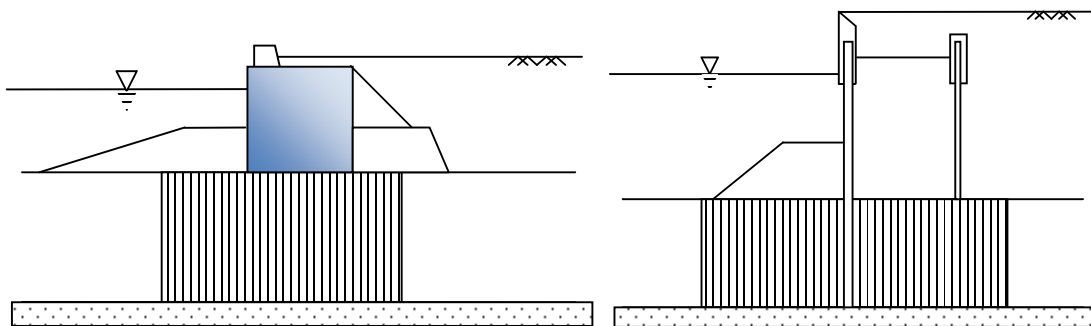
(g) Foundation of tank, silo and retaining wall

Figure 2.2 (contd.): SCP applications for on-land construction (after Kitazume, 2005)



(a) Concrete caisson type breakwater

(b) Concrete block type sea revetment



(c) Cellular block type

(d) Steel sheet pile type sea revetment

Figure 2.3: SCP applications for marine construction (after Kitazume, 2005)

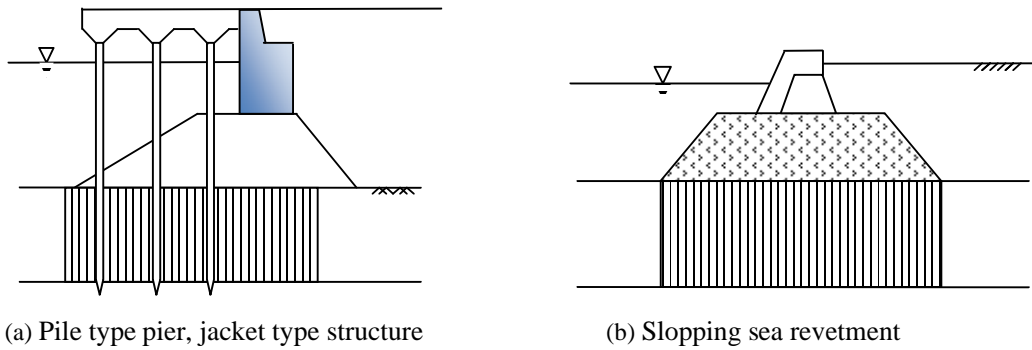


Figure 2.3 (contd.): SCP applications for marine construction (after Kitazume, 2005)

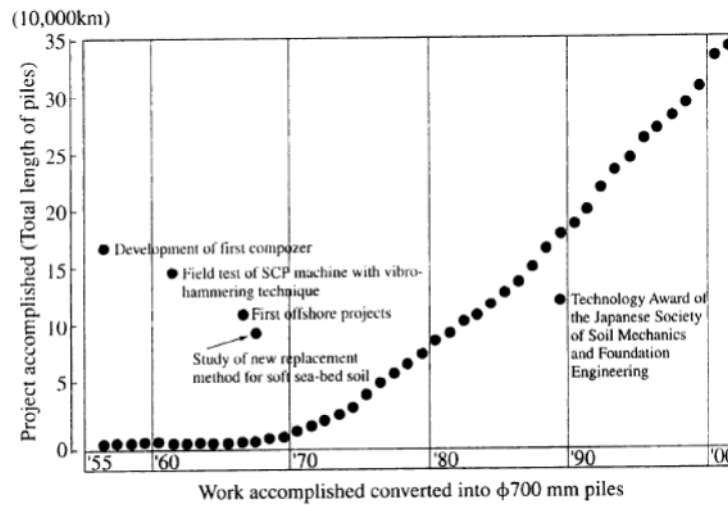


Figure 2.4: Cumulative length of compacted sand piles (after Kitazume, 2005)

2.5 Methods of Sand Compaction Pile Installation

According to Weber (2004), sand compactions piles are widely used in practice in order to improve soft ground, such as soft clay or peat. In particular, when less settlement-sensitive structures such as embankments are designed, the more cost effective method of sand piles is often preferred, in comparison to creating a piled embankment with reinforced concrete piles.

The most commonly practiced construction method of SCP is the composer method (Aboshi and Suematsu, 1985). Figures 2.5(a) and 2.5(b) illustrate the typical equipment for on-land and near-shore constructions, respectively, using the composer method. The construction procedure of the composer method consists of several steps as depicted in Figure 2.6. The steel casing is first positioned to the prescribed locations, collimation of which in marine construction is assisted by the transit apparatus optical finder, or GPS. Under excitation from the vibro-hammer, the casing pipe is then driven downwards into the ground. Sand is continually in-filled into the casing pipe during its penetration. In case

of stiff soil layer, compressed air may be used to assist in the penetration. After arriving at the desired depth, the casing pipe is hoisted upwards by certain height to discharge and feed sand into the ground. Afterwards, the casing pipe is partially re-driven downwards to squash and compact the discharged sand, which also enlarges the diameter of sand column. The above procedure of withdrawal followed by partially re-driving is repeated up to the soil surface. At the end, a well-compacted sand column with a diameter larger than the casing pile is constructed in soil (e.g. Aboshi and Suematsu, 1985, Kitazume, 2005). Due to the use of vibro-hammer, the preceding execution procedure is inevitably accompanied with some noise and disturbance, which may restrict the use of SCP construction in urban areas.

To mitigate the noise problem, a non-vibratory compaction technique was recently developed in Japan (Tsuboi et al., 2003). As shown in Figure 2.7, the non-vibratory compaction technique utilizes a rotary motor, instead of vibro-hammer, to facilitate penetration and withdrawal. The use of rotary motor can substantially reduce the amount of noise and vibration generated during SCP construction and retain favorable compaction efficacy.

2.6 Analytical Approach for Bearing Capacity of SCP Treated Ground

Jiangtao (2009) reports of Terashi et al. (1991a, 1991b) who presented a concise note on the design methodology of the SCP treated ground. The mechanical performance of the SCP-improved soft clay ground (or the "composite ground") is fairly complex. It is influenced by a number of factors which, as summarized by Terashi et al. (1991a, 1991b), include:

- (i) the shear strength of sand piles as well as the strength profile of the soft clay,
- (ii) the area replacement ratio " " which is defined as the ratio of the area occupied by sand piles to the overall area of the improved ground,
- (iii) the geometric conditions such as the ratio of the width of improved area over the width of foundation,
- (iv) the ratio of the length of sand piles over the thickness of soft soil layer, and
- (v) the external loading conditions (e.g. loading rate, load eccentricity and inclination).

A number of design approaches have been proposed in the literature to evaluate the bearing capacity, settlement and stability of the composite ground. Due to the complexity of the problem, most of these methods are developed on semi-empirical or empirical basis, instead of first principle analysis. The following sections give an overview of various SCP design methodologies.

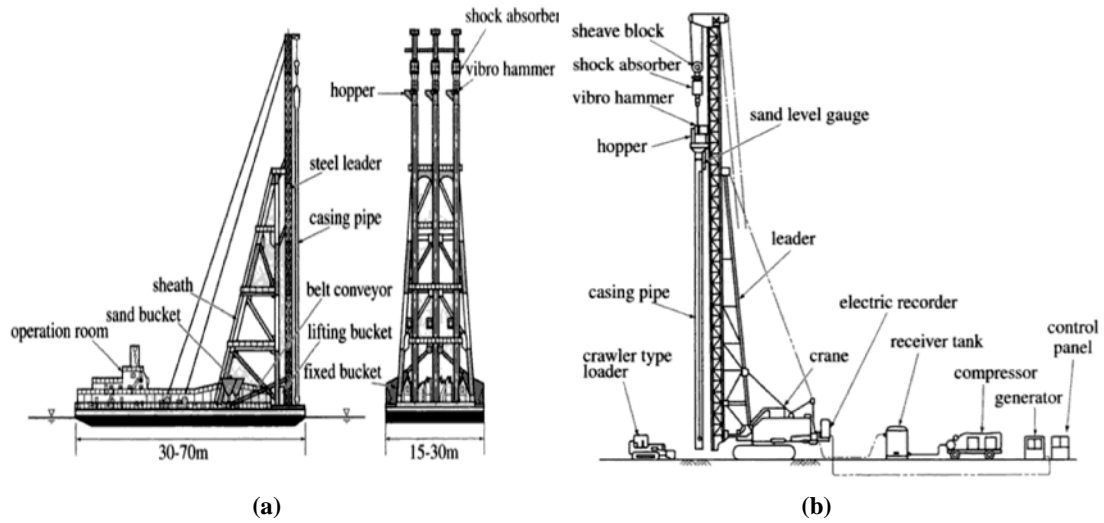


Figure 2.5: (a) SCP machine for on-land construction; (b) SCP barge for marine construction (after Kitazume, 2005; Aboshi and Suematsu, 1985)

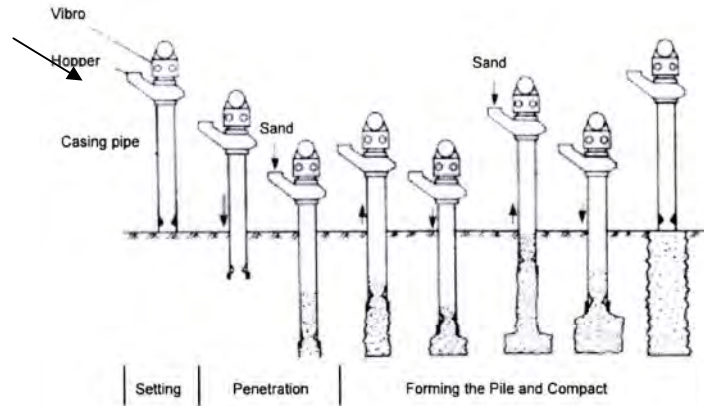


Figure 2.6: Composer method of SCP Installation (after Aboshi and Suematsu, 1985)

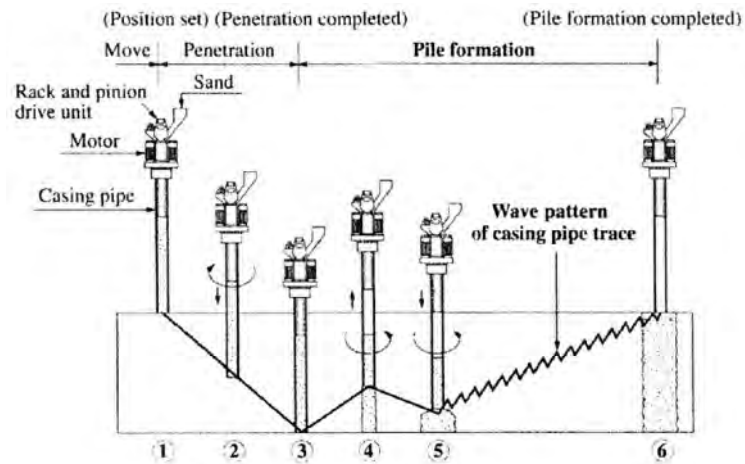


Figure 2.7: Non-vibratory SCP Installation (after Tsuboi et al. 2003)

2.6.1 Bearing Capacity Evaluation by Unit Cell Approach

When subjected to widespread load, the composite ground can be viewed as an assemblage of identical cells and analyzed using the unit cell approach. As shown in Figure 2.8, each cell is made up of a single SCP column surrounded by its "tributary" clay. The mechanical behavior of cell is assumed to be representative of the composite ground. It therefore simplifies the analysis of the whole soil domain into one soil unit.

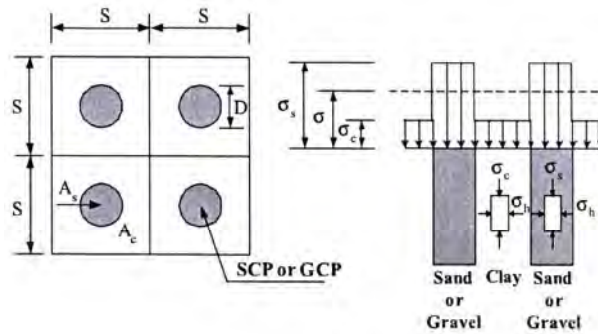


Figure 2.8: Concept of SCP Ground and Unit Cell (Aboshi and Suematsu, 1985)

Within the unit cell, applied load is collectively taken by the stiff sand column and the soft tributary clay.

$$\sigma_s = \sigma_c + \sigma_h \quad (2.3)$$

$$\sigma_s A_s + \sigma_c (A_c - A_s) = \sigma_c A_c \quad (2.4)$$

Where,

σ_s = applied external load

σ_c = average loading intensity

A_c = cross-sectional area of unit cell

A_s = cross-sectional area of sand pile within unit cell

$A_c - A_s$ = cross-sectional area of clay soil within unit cell

σ_c = vertical stress on clay

σ_s = vertical stress on sand pile

$\alpha = A_s / A_c$ = area replacement ratio = —

Owing to the stiffness disparity, stress concentration is expected to be present in the unit cell, with more stress on the stiff sand column and less stress on the clay. The ratio of stress acting on the sand column, σ_s , over the stress on the clay, σ_c , is defined as stress concentration ratio, σ_s / σ_c . Stress equilibrium and stability within the unit cell (Murayama, 1962; Aboshi and Suematsu, 1985) leads to:

$$\sigma_s / \sigma_c \geq \frac{1}{1 - \alpha} \quad (2.5)$$

$$\leq + \quad (2.6)$$

Where,

- = lateral confining stress on the cylindrical surface of sand pile,
- = angle of internal friction of sand, and
- = upper yield stress of clayey ground.

If one further assumes that the stress conditions of clay and sand in the unit cell are fully passive and active, respectively, the combination of above Equations (2.5) and (2.6) produces the stress concentration ratio as follows:

$$= - = \frac{1}{1 + } \quad (2.7)$$

The ultimate bearing capacity is therefore evaluated as:

$$= = \frac{1}{() ()} (+) \quad (2.8)$$

Where,

- = maximum load on the composite ground
- = ultimate bearing capacity

As Equation (2.8) indicates, the bearing capacity of composite ground that can be estimated based on the soil and sand strength parameters and , and stress concentration ratio . The stress concentration ratio , in the above equation, usually needs to be determined empirically or based on the field measurement data. Aboshi and Suematsu (1985) suggested a reasonable range of 4 to 7, from experimental data and field measurements.

2.6.2 Bearing Capacity Evaluation by Sliding Failure Approach

Another approach for ultimate bearing capacity estimation of the composite ground is based on the sliding failure mode, as depicted in Figure 2.9 (e.g. Aboshi et al., 1979; Cho et al., 2005; Kitazume, 2005). Again, load acting on composite ground is shared by both clay and sand pile, giving:

$$= = \frac{1}{()} \quad (2.9)$$

$$= = \frac{1}{()} \quad (2.10)$$

Where,

- = ratio of sand pile stress to average loading intensity = -
- = ratio of clay soil stress to average loading intensity = -

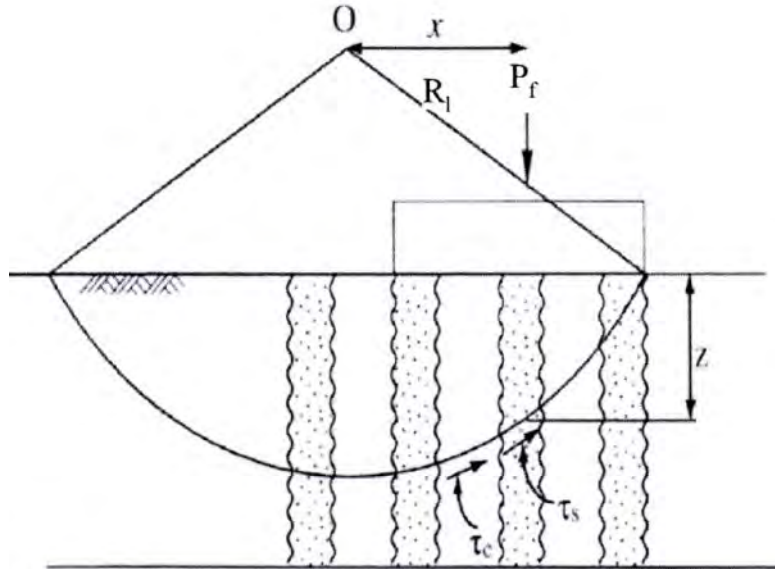


Figure 2.9: Sliding Failure of Composite Ground (After, Kitazume, 2005)

The shear strength of composite ground can be estimated by taking the weighted-average of the strength of the soft soil and sand with respect to the area replacement ratio (Aboshi et al., 1979):

$$\tau_c = (1 - R_f) \tau_s + (R_f + \gamma_s z) \tan \alpha \cos \alpha \quad (2.11)$$

Where,

τ_c = shear strength of the composite ground

γ_s = unit weight of sand pile

z = depth below ground surface

α = inclination of the failure surface measured from the horizontal plane, and

τ_s = undrained shear strength of clay

In cases where load is gradually applied on the composite ground in stages (e.g. the construction of embankment), Aboshi and Suematsu (1985) suggested taking into account the additional shear strength increase due to the application of surcharge as follows:

$$\tau_c = \tau_s + (\tau_s - \tau_{s0}) \frac{1 - C_u}{1 - C_u} \quad (2.12)$$

Where,

τ_{s0} = initial strength of clay soil,

C_u = degree of consolidation, and

$\frac{1 - C_u}{1 - C_u}$ = ratio of undrained shear strength increase due to surcharge

Knowing the shear strength of composite ground (Equations 2.11 and 2.12); the bearing capacity the slip circle analysis can be given by (Kitazume, 2005):

$$= \frac{\sum (c \Delta)}{F} \quad (2.13)$$

Where,

x = horizontal distance of load to the centre of rotation, Figure 2.9

λ = degree of consolidation

Δ = arc of slip circle

r = radius of slip circle, and

F = factor of safety.

2.6.3 Bearing Capacity Evaluation by General Shear Failure Approach

In scenarios wherein the ground is improved by short end-bearing sand piles, general shear failure (as depicted in Figure 2.10) is likely to be the controlling failure mode of the composite ground. Sogabe (1981) estimated the bearing capacity of composite ground failed by general shear failure, by invoking Terzaghi's bearing capacity theory:

$$q_f = \frac{1}{2} \gamma B + (1 - \lambda) q_{f0} \quad (2.14)$$

Where,

B = width of foundation,

γ = unit weight of sand pile, and

q_{f0} , λ = bearing capacity factors for self-weight and cohesion, respectively.

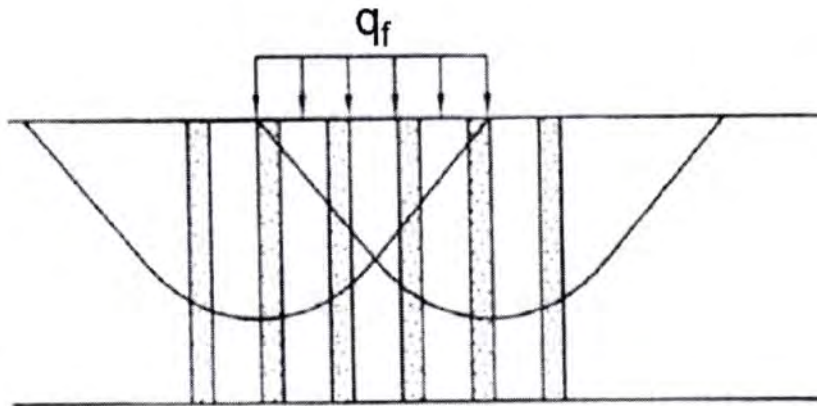


Figure 2.10: General Shear Failure of Composite Ground (After, Kitazume, 2005)

Barksdale and Bachus (1983) also developed another approach to assess the bearing capacity of composite ground based on general shear failure, as illustrated in Figure 2.12. In this simplified mechanism, the failure surface is represented by two straight rupture surfaces. Analyzing the force equilibrium of the wedge formed by the two straight rupture surfaces produced the ultimate bearing capacity in the following forms:

$$q_f = 2(1 - \lambda) \gamma B \tan \alpha + \frac{1}{2} \gamma B \tan^2 \alpha + 2 c \tan \alpha \quad (2.15)$$

$$= 45 + \frac{(\quad)}{\quad} \quad (2.16)$$

Where,

= unit weight of clay

= ratio of stress on sand pile to the average loading intensity

= angle of internal friction of sand, and

= angle between the postulated failure surface and foundation, Figure 2.11.

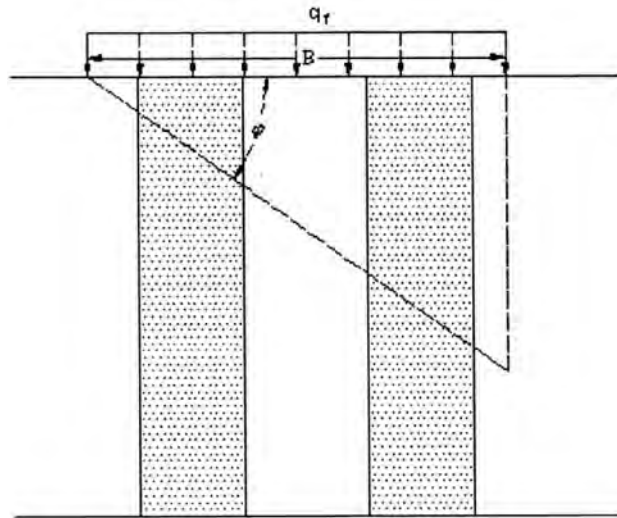


Figure 2.11: Shear Failure of Composite Ground (After, Barksdale and Bachus, 1983)

2.6.4 Bearing Capacity Evaluation by Bulging Failure Approach

For granular columns (e.g. SCP) extended to the underlying firm stratum, there is tendency for columns to bulge and mobilize passive earth pressure from the surrounding clay (Greenwood, 1970). Bulging, or local, failure of columns may control the bearing capacity of the composite ground as shown in Figure 2.12. In such situations, Greenwood (1970) proposed the following relationship for the estimation of lateral earth pressure resisting the bulging column:

$$= \quad + \quad + 2 \quad \text{---} \quad (2.17)$$

Where,

= passive earth pressure coefficient of tributary clay, and

= surcharge per unit area.

If it is assumed that the column is fully active, the bearing capacity of column can be calculated and expressed as follows:

$$= \text{---} \quad (2.18)$$

$$= + 2 \quad + \quad \text{---} \quad (2.19)$$

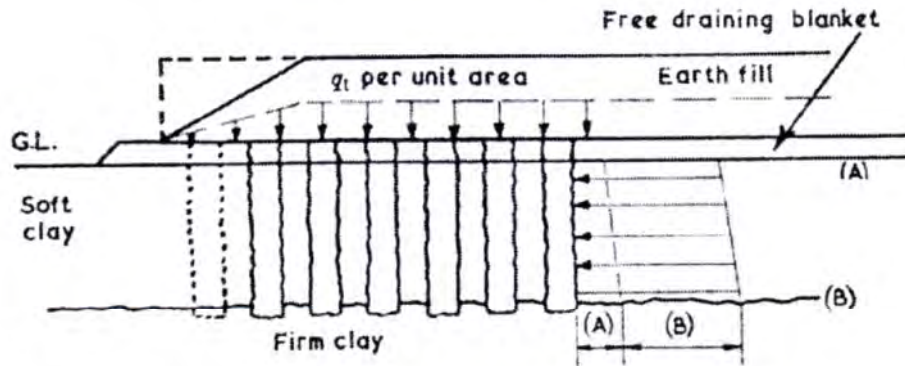


Figure 2.12: Shear Failure of Composite Ground (After, Barksdale and Bachus, 1983)

2.6.5 Bearing Capacity Evaluation by Cavity Expansion Approach

Using the analogy between the bulging of granular column and the expansion of cylindrical cavity, Hughes and Withers (1974) introduced the elasto-plastic cavity expansion theory into analyzing the bulging failure of granular column. The limiting internal pressure on the expanding cavity was related to the radial stress of the soil around bulging granular column. Hughes and Withers (1974) formulated the horizontal (or radial) stress of the soil with respect to the in-situ total horizontal stress and undrained shear strength of soil :

$$= + 4 \quad (2.20)$$

The ultimate bearing capacity of sand column can then be estimated by:

$$= \text{---} \quad (2.21)$$

Another similar solution was proposed by Brauns (1978), who re-casted the total horizontal stress a_h as the function of Vesic's rigidity index, I (Vesic, 1972):

$$= + (1 + \log \quad) \quad (2.22)$$

Bhandari (1983) commented that Hughes and Withers's method may probably underestimate the ultimate load of granular columns. Hansbo (1994) suggested increasing the value of multiplier for in Equation 2.19 from 4 to 5 based on field data:

$$= + 5 \quad (2.23)$$

2.7 Analytical Approach for Settlement of SCP Treated Ground

2.7.1 Aboshi and Suematsu's Equilibrium Method

Aboshi and Suematsu (1985) proposed a simple approach named equilibrium method to estimate the (long-term) settlement of the composite ground. It was assumed that both the sand column and the surrounding clay settled by the same amount when loaded. The settlement of composite ground can be calculated as the product of original ground settlement and the settlement reduction factor:

$$s_c = s_o \cdot R_f \quad (2.24)$$

Where, s_o is the original (unimproved) ground without improvement and R_f is the settlement reduction factor. The settlement reduction factor can be deduced from the stress reduction mechanism, and the original ground settlement can be readily determined by using the classic one-dimensional consolidation calculation

$$s_o = \frac{C_c}{1 + e_o} \cdot \frac{H}{\gamma_w} \cdot \log \left(\frac{\sigma'_{v2}}{\sigma'_{v1}} \right) \quad (2.25)$$

$$R_f = \frac{1}{1 + \frac{C_c}{1 + e_o} \cdot \frac{H}{\gamma_w} \cdot \log \left(\frac{\sigma'_{v2}}{\sigma'_{v1}} \right)} \quad (2.26)$$

Where, C_c is the coefficient of volume change of clay and H is the thickness of subsoil.

2.7.2 Baumann and Bauer's Elastic Method

The elastic method for settlement analysis of composite ground was proposed and developed by Baumann and Bauer (1974) and Priebe (1976, 1995). Baumann and Bauer (1974) assumed both intervening soil and granular columns experienced the same amount of settlement under loading. The sand column was assumed to be incompressible, deforming with no volume change. Hence the settlement or vertical shortening of column could be directly linked with its radial deformation which could be estimated by the elastic cavity expansion theory. By doing so, Baumann and Bauer (1974) arrived at the following relation for the estimation of stress concentration:

$$\sigma'_c = \frac{1}{1 + \frac{2(1 - \mu_s)}{D}} \cdot \sigma'_v \quad (2.27)$$

Where,

μ_s = coefficients of earth pressure in the sand column

μ_c = coefficients of earth pressure in clay

D = diameter of the sand column

= Young's modulus of the sand

= Young's modulus of the clay.

The ground settlement, s , was solved and expressed in the following correlation,

$$s = \frac{\Delta}{E_c} \ln \left(\frac{C_1}{C_2} \right) \quad (2.28)$$

Where, Δ is the difference of lateral pressure increases between sand column and clay, i.e. $\Delta = p_{s1} - p_{c1}$.

A similar relation was derived by Priebe (1976) on the following assumptions:

- (i) column extends to the underlying rigid layer
- (ii) column deforms with constant volume
- (iii) self-weight of the column and soil can be neglected
- (iv) shearing of column material takes place from the beginning while the surrounding soil reacts elastically-
- (v) coefficient of earth pressure is 1.0.

Based on the theory of elasticity, Priebe obtained the following expression for the settlement reduction factor α :

$$\alpha = 1 + \frac{(\nu_c - \nu_s)}{(\nu_s + \nu_c)} \quad (2.29)$$

Where,

$$(\nu_s, \nu_c) = \frac{(\nu_s)(\nu_c)}{(\nu_s + \nu_c)} \quad (2.30)$$

$$= \tan^2 45^\circ - \mu \quad (2.31)$$

Where, ν_s is the Poisson's ratio of clay. Solutions of Equations (2.29) for the Poisson's ratio of 0.33 were plotted as a design chart (Figure 2.13). Priebe (1995) subsequently refined the preceding solutions by considering the compressibility of granular column and self-weight of clay and granular material.

2.7.3 Settlement Relations by Other Investigators

Other investigators also introduced relations for settlement of SCP ground considering various assumptions (Gounour, 1983; Van Impe and De Beer, 1983). For more details of the methods reference can be made to Jiangtao (2009).

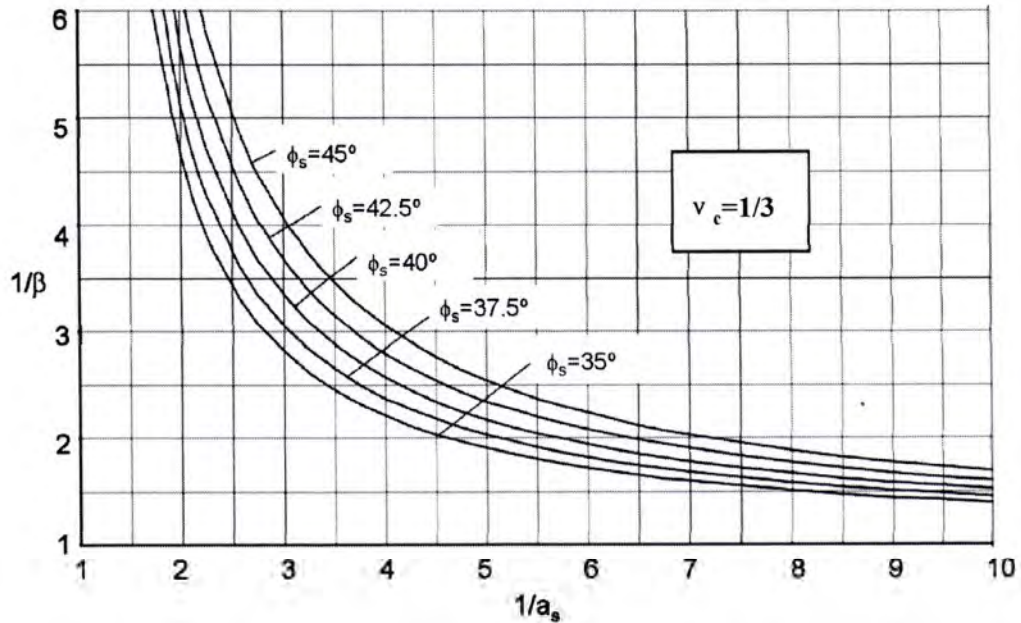


Figure 2.13 Design Chart for Estimation of Settlement of Improved Soil due to SCP

2.8 Study and Research on Effectiveness of SCP

Few researchers carried out in depth researches in different parts of the world on the effectiveness of SCP in different fields of investigation. They introduced the various effectiveness measurement tools and carried out field and laboratory investigations. Important investigations and related principles are highlighted in subsequent paragraphs.

2.8.1 Replacement Area Ratio

In principles, sand compaction pile is a replacement method of soil compaction. The principal parameter used in the design of sand compaction pile is the replacement area ratio. The replacement area ratio, is defined by Kitazume (2005) as the ratio of the sectional area of the sand pile to the hypothetical cylindrical area, which is formulated as Equation (2.32).

$$\text{Replacement area ratio, } = \text{---} \quad (2.32)$$

Equations 2.33(a), 2.33(b), 2.33(c) show the formulas for square patterns, equilateral triangular patterns and rectangular patterns respectively.

For square patterns:

$$= \text{---} = \text{---} \quad (2.33a)$$

For Equilateral triangular patterns:

$$= \text{---} = \frac{\sqrt{3}}{2} \text{---} = \frac{\sqrt{3}}{2} \text{---} \quad (2.33b)$$

For rectangular patterns:

$$= - = - - - - - \quad (2.33c)$$

Where,

- = replacement area ratio
- = cross sectional area of sandy ground and sand pile (m^2)
- = sectional area of sand pile (m^2)
- = diameter of sand pile (m)
- = intervals of sand piles (m)
- = intervals of sand piles for rectangular pattern (m), Figure 2.15 (c)
- = intervals of sand piles for rectangular pattern (m), Figure 2.15 (c)
- = angle of sand piles arrangement for rectangular pattern

Figure 2.14 (a), 2.14(b), 2.14(c) shows the figures for square patterns, equilateral triangular patterns and rectangular patterns respectively. The replacement area ratio for applications to sandy ground is typically less than 0.3, and for clay ground the ratio ranges from 0.3 to 0.8. In the case of the replacement area ratio of about 0.78, sand piles are in contact with each other. The SCP improved ground can be divided into ‘low’ , ‘medium’ and ‘high’ for a replacement area ratio of less than 0.3, 0.3 to 0.5, and higher than 0.5.

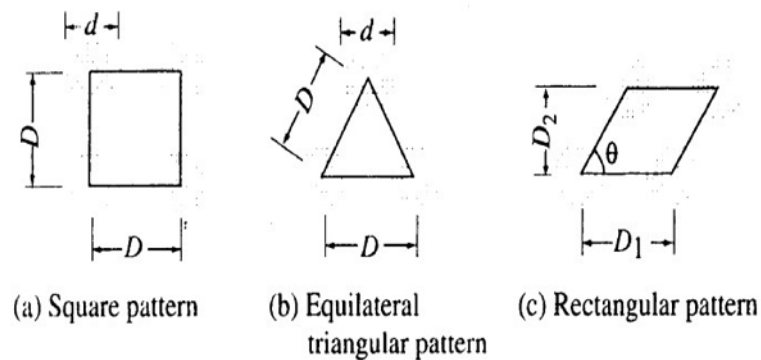


Figure 2.14: SCP Soil Improvement Pattern (Kitazume, 2005)

2.8.2 Dynamic Cone Penetrometer (DCP) Resistance

Standard test method of DCP in shallow pavement application covers the measurement of the penetration rate of the Dynamic Cone Penetrometer with an 8- kg hammer (8-kg DCP) through undisturbed soil and/or compacted materials. The penetration rate may be related to in situ strength such as an estimated in situ CBR (California Bearing Ratio). A soil density may be estimated if the soil type and moisture content are known. The DCP described in this test method is typically used for pavement applications. The test method provides for an optional 4.6-kg sliding hammer when the use of the 8-kg sliding mass produces excessive penetration in soft ground conditions.

The operator drives the DCP tip into soil by lifting the sliding hammer to the handle then releasing it. The total penetration for a given number of blows is measured and recorded

in mm/blow, which is then used to describe stiffness, estimate an in situ CBR strength from an appropriate correlation chart, or other material characteristics.

This test method is used to assess in situ strength of undisturbed soil and/or compacted materials. The penetration rate of the 8-kg DCP can be used to estimate in-situ CBR (California Bearing Ratio), to identify strata thickness, shear strength of strata, and other material characteristics. Other test methods exist for DCPs with different hammer weights and cone tip sizes, which have correlations that are unique to the instrument.

2.8.3 Effectiveness of SCP against Soil Liquefaction

Moh et al. (1981) conducted experimental research on sand compaction piles using triangular pattern to improve the subsoil condition by densification at the site of a steam power plant in the southern part of Taiwan. The top 6 m of the subsoil was a loose fine sand deposit which had high liquefaction potential, factor of safety against liquefaction in the upper sand layer under a 4 m of fill were generally lower than 2. Since the power plant was located in a seismic active zone, it was necessary to improve the subsoil condition by densification and thereby to increase the factor of safety against liquefaction. In their experiment, they used compaction sand piles of 45 cm diameter, 7.5 m long placed at 1.8 m center to center spacing in a triangular pattern distribution.

A land area of 3500 sq m was improved in the first stage of construction. For the evaluation of the effectiveness of the ground improvement, soil sampling and Standard Penetration Tests (SPT) were performed at random locations both prior to and after the improvement. The test results indicate that the improvement was successful with 100% samples giving over the required 65% relative density and 92% samples with more than 75% relative density (Figure 2.15). Liquefaction potential of the site was therefore greatly reduced.

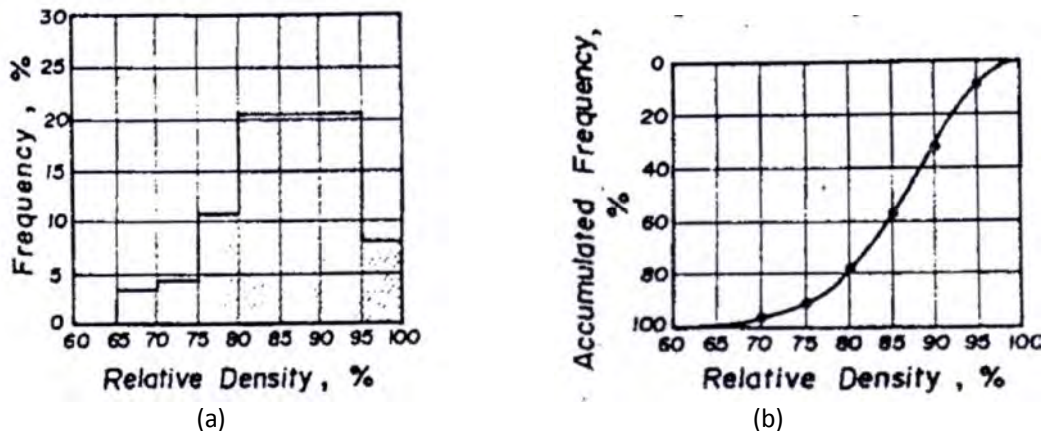


Figure 2.15: (a) Frequency Distribution, (b) Accumulated Frequency Distribution of Relative Density after Improvement (after Moh et al., 1981)

According to Moh et. al. (1981) standard penetration tests were found to be an effective way for the field control work. They established correlations between the SPT values and relative density that are presented in Figures 2.16 and 2.17.

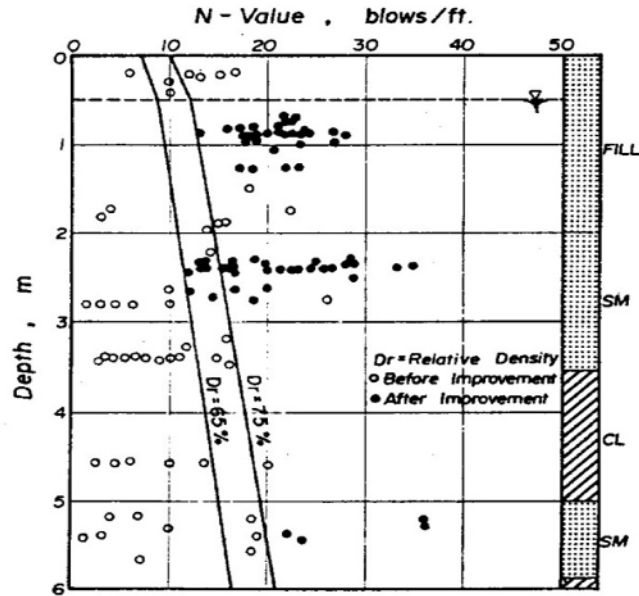


Figure 2.16: Variation of N-values before and after Soil Improvement (After Moh et al., 1981)

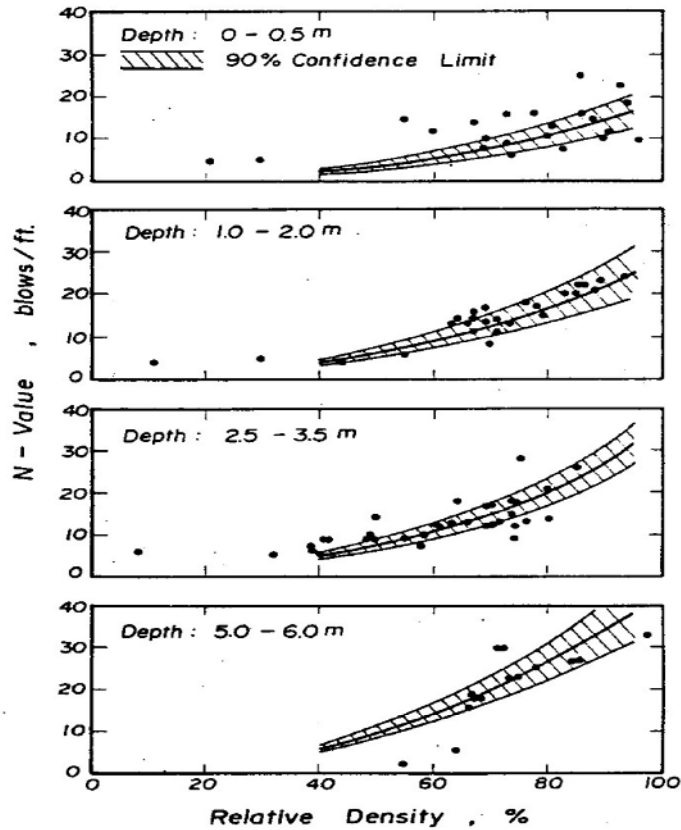


Figure 2.17: Relationships between Relative Density and SPT N-Value (after Moh et al., 1981)

According to Moh et al. (1981), within the depth of improvement, both sand and clay layers developed excess pore pressure during installation of the compaction sand piles. This excess pressure took 3 to 4 weeks time to dissipate which is a factor to be considered in foundation design. After improvement, the lateral resistance of sandy soils increases but there is no effect on cohesive soils (Figure 2.18).

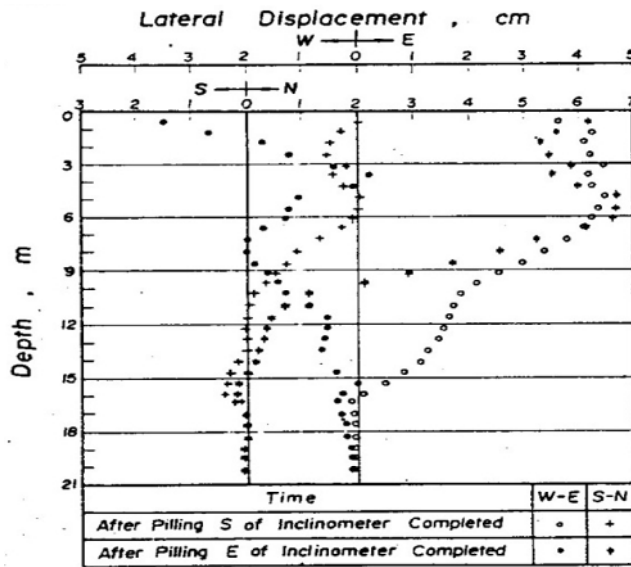


Figure 2.18: Lateral Displacement of Soil due to Compaction Sand Pile (after Moh et al., 1981)

2.8.4 Effectiveness of Granular Pile in Loose to Medium Dense Granular Deposits

The effects of granular pile installation on the modifications induced in loose to medium dense granular deposits were studied by Krishna and Madhav (2008). SPT N_1 values of the ground before and after the treatment are measured to evaluate the improvement of the virgin in situ soil. Expressions for modified SPT N_1 values for different soils, i.e., different initial SPT N_1 values, were determined as functions of replacement ratio from the available field data, as shown in Equation (2.34).

$$N_{1m} = N_{1u} + \frac{R}{100} (N_{1p} - N_{1u}) \quad (2.34)$$

Where, N_{1m} is the modified SPT N_1 value of the treated soil; R is the replacement ratio expressed in percentage; and A and B are the parameters that depend on SPT N_1 value of untreated soil (N_{1u}) as,

$$A = 1.23 \cdot N_{1u}^{-0.5} \quad (2.35a)$$

$$B = 0.03 \cdot N_{1u} \quad (2.35b)$$

Improvements in the ground are represented in the form of modified SPT N_1 values versus replacement ratio charts as shown in Figure 2.19, which then can be used to design the required degree of treatment for the expected improvement or to estimate the improved values of treated ground for different initial states of sand.

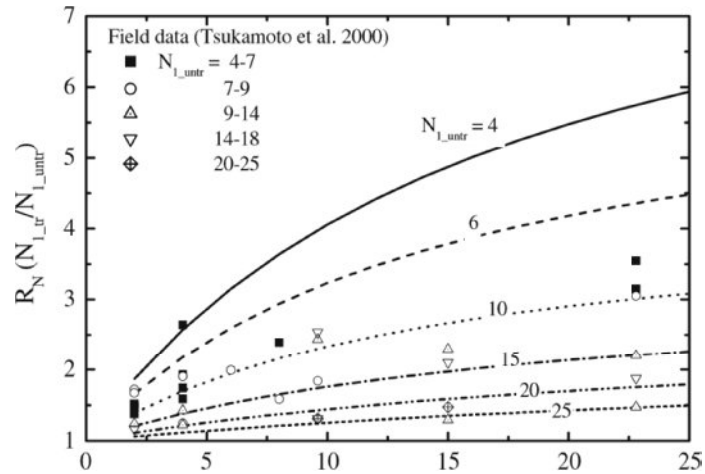


Figure 2.19: Increases In the Normalised SPT- N_1 Values of Soil (Krishna and Madhav, 2008)

2.8.5 Effectiveness of SCP against Soil Liquefaction in Ash Pond

Detail study on “Assessing Improvement Effects of Sand Compaction Pile in an Ash Pond” in the Taichung Thermal Power Plant located in the seashore of central Taiwan and neighbouring Taichung Harbour was carried out by Hwang and Yeh (2012) as shown in Figure 2.20, which suffered serious damage caused by soil liquefaction in the 1999 Chi-Chi earthquake, Kempfert(2003)

The SCP used in the test area is 10 m long and in triangular layout. The diameter of SCP is 0.7 m and the center spacing between two SCPs is 1.5m. The replacement ratio of SCP is 0.35 for this ash site which is higher than the ratio of 0.1-0.2 generally used in ordinary sandy soils, such as the original alluvial sea bed deposit.



Figure 2.20: The location of Taichung Thermal Power Plant (Ref. [4])

2.8.6 Evaluation of SCP Treatment

To evaluate the improving performance of SCP in ash pond, three methods, including in-situ penetration tests, laboratory tests on undisturbed ash samples, and piezometer and

inclinometer measurements are used. The investigation works were carried out according to the flow chart shown in Figure 2.21, Kempfert (2003). Improvement effect of SCP is accurately evaluated by SPT and SCPT investigation methods through a careful planning and execution, shown in Figure 2.22 and 2.23 respectively.

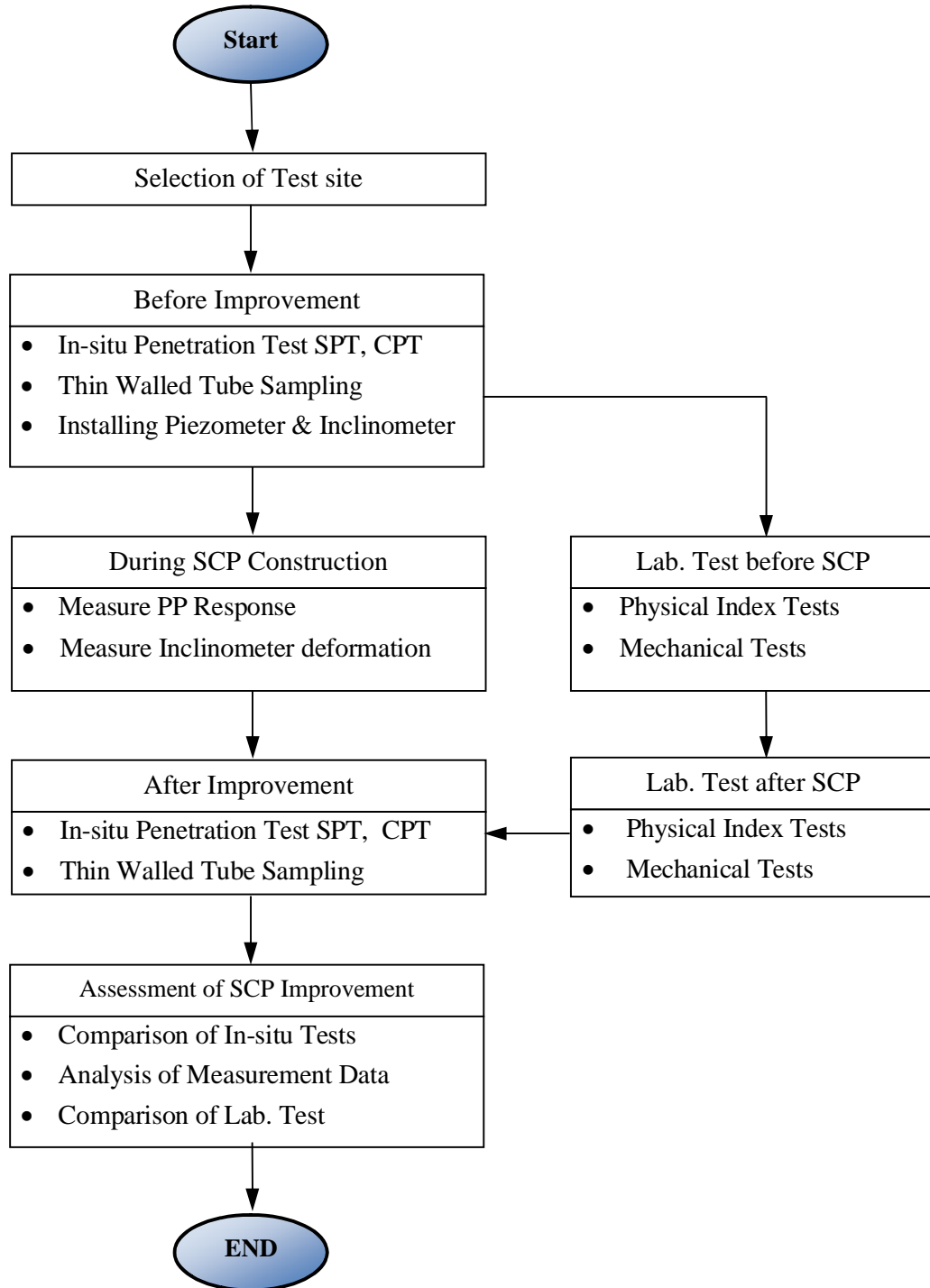


Figure 2.21: Flow Chart of Investigation Assessing Improvement Effect (after Kempfert, 2003)

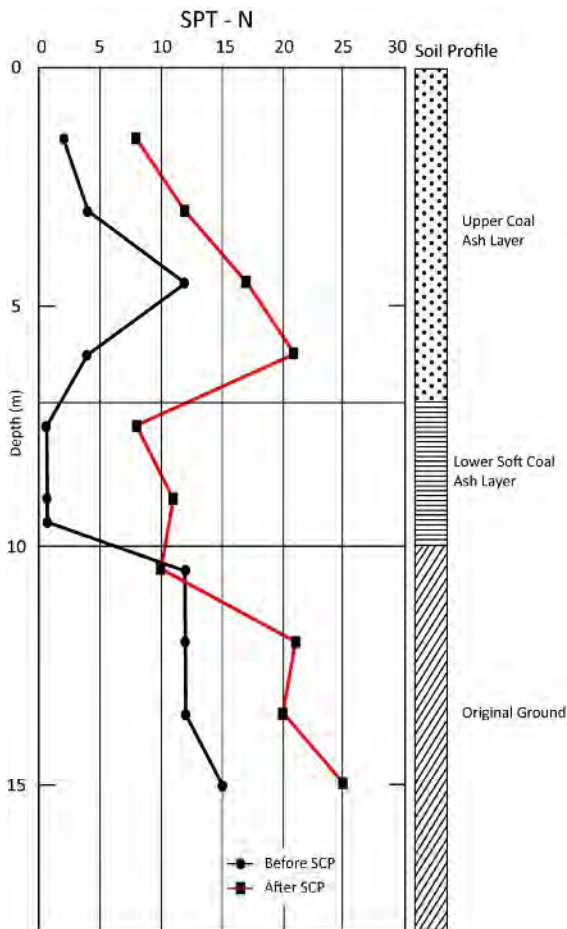


Figure 2.22: SPT profile before and after the improvement (Kempfert, 2003)

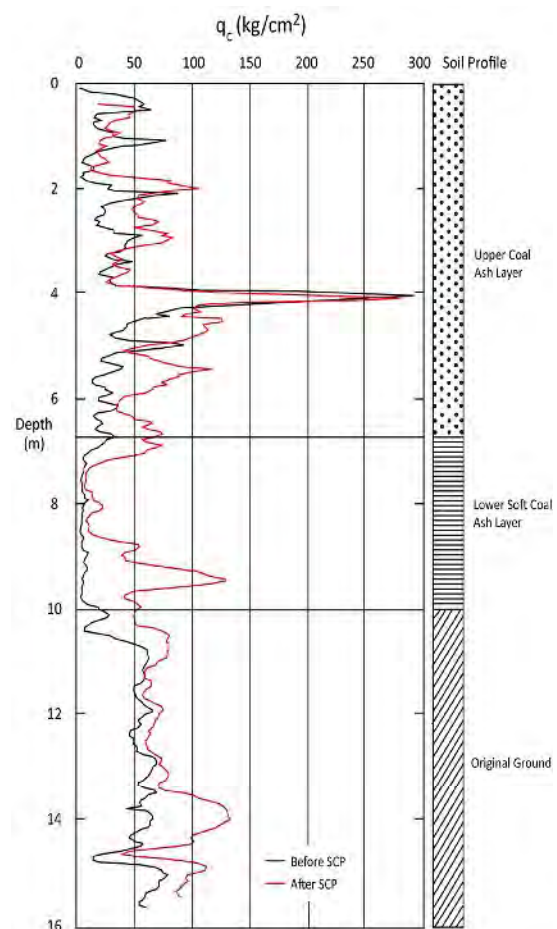


Figure 2.23: Cone resistance before and after improvement (Kempfert, 2003)

2.8.7 Effectiveness of SCP on Foundation Soil as Liquefaction Resistance

Ocamura et al. (2006) conducted laboratory tests on high-quality undisturbed samples obtained by the in situ freezing method at six sites where foundation soils had been improved with SCP. The in situ ground freezing method is a sampling method capable of obtaining high-quality undisturbed soil samples, especially for sands and gravels with less fines content (Yoshimi et al. 1978, 1994). The plan view of each site, showing arrangement of sand piles and sampling locations are shown in Figure 2.24. Inspection of samples revealed that the improved ground was de-saturated during the ground improvement. Inspection of samples as well as the primary wave velocity testing conducted at a site confirmed that the improved ground contained air exhausted from casing pipe during SCP installation. Degree of saturation S_r in the improved area was lower than 77% for the sand piles and 91% for the improved sand layers, while S_r was approximately 100% for improved clayey and silty soils. Degree of saturation of improved soils depend primary on the soil grain size but other factors including distance from sand pile, depth, and replacement ratio have little effect on .

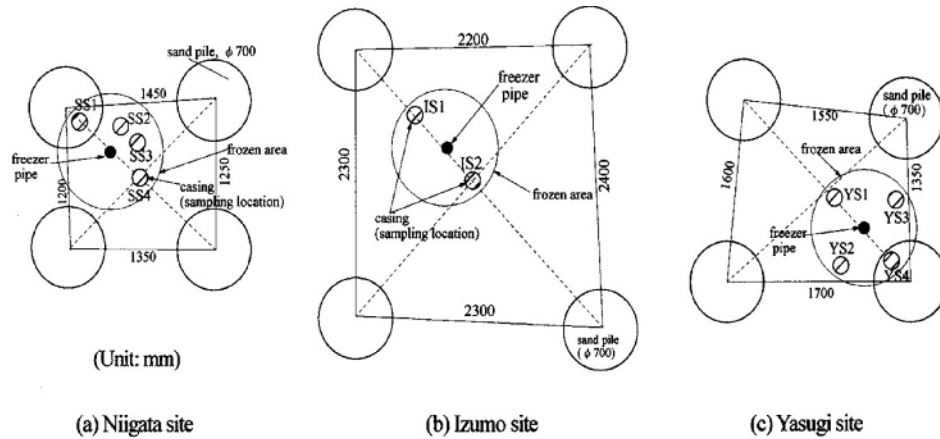


Figure 2.24: Plan View of Sampling Locations (After Unnikrishnan And Johnson, 2009)

A good correlation was found between N_1 and 5% diameter of the soil; the larger 5% diameter of soils, the lower the degree of saturation. It appeared that the variation of N_1 with d_{50} for soils within a month after the ground improvement work was quite similar in trend to that after more than several years. Degree of saturation of soils after several years was noticeably, but not significantly, higher as compared with that shortly after ground improvement, at most about 10%, indicating longevity of air bubbles injected in the improved soil. Undrained cyclic shear tests were also carried out on both saturated and unsaturated improved soil specimens and effects of desaturation on undrained cyclic shear strength were studied. The test results were summarized in a form of liquefaction resistance with reference to normalized SPT N_1 , as shown in Figure 2.25. The liquefaction resistance of the unsaturated specimens was found to be considerably higher than saturated specimens with lower N_1 -value. The liquefaction resistance of unsaturated specimens is in a relatively small range between 0.4 and 0.5 irrespective of N_1 -value and the degree of saturation.

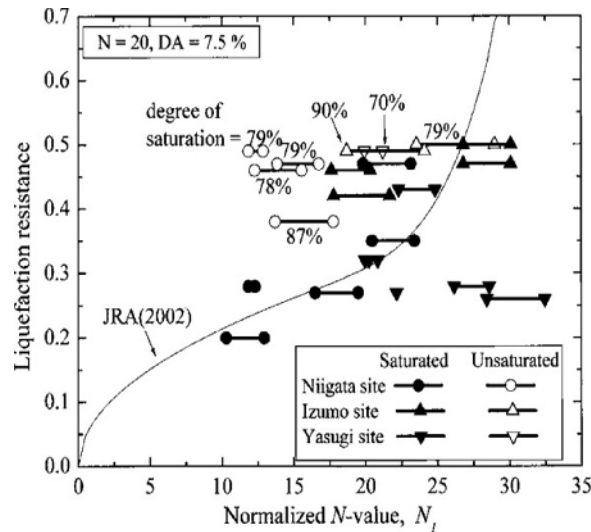


Figure 2.25: Liquefaction Resistance and Normalized N_1 -Value for Saturated and De-Saturated Improved Sand (after Unnikrishnan and Johnson, 2009)

2.8.8 Dynamic Cone Resistance and Relative Density of Sand

Sand fill is required for many purposes, for example, backfill of earth retaining structures, backfill in foundation trenches, reclamation of low lands and construction of road embankments etc. In all these situations good compaction of fill should be ensured to avoid future subsidence, failure of foundation and moreover liquefaction. Relative density is the most appropriate index to control the compaction of sand fill. Generalized correlation between dynamic cone resistance and relative density of sand was developed by Alam et al. (2014) which is shown in Figure 2.26.

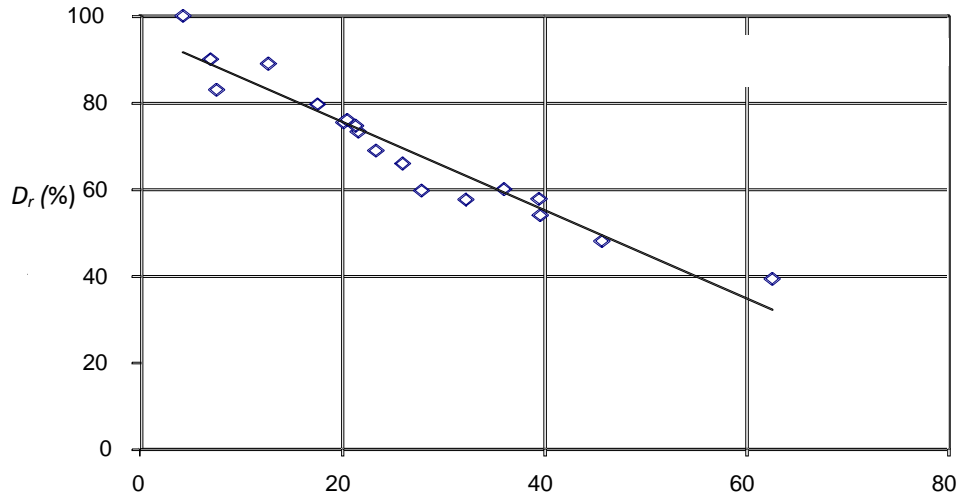


Figure 2.26: Relative Density and P_{index} and D_{50} for DCP (after Alam et al., 2012)

They observed that penetration index increases exponentially with decrease of relative density. By fitting the data in an exponential equation, a generalized correlation for DCP was found as:

$$P_{index} = 3.09 + 97.4 \frac{1}{D_r} \quad (2.36)$$

Where,

- D_r = Relative Density (%)
- P_{index} = Penetration Index (mm/blow)
- D_{50} = Mean Diameter of sand particles in mm

2.8.9 Consolidation behavior of Clay Ground Improved by Sand Compaction Piles

Jung et. al. (1999) carried out model tests for clay ground improved by fully or partially penetrated sand compaction pile (SCP) in order to investigate the effect of the penetration ratio, the depth and replacement ratio of the SCPs. They observed that the stress concentration ratio varied with depth and penetration ratio of SCPs. The stress

concentration ratio decreased with an increase in penetration ratio and strongly dependent upon the process of consolidation and the replacement area ratio.

2.9 Concluding Remarks

The literature review revealed that sand compaction pile is as an effective tool of ground improvement especially of soft and loose soils. As compared to the importance of the topic, the study and research on the topic are relatively few. Studies have been made in the past on the various aspects of SCP with varying soil properties. However, the study on the effectiveness of the use of SCP in alluvial soil conditions is not reported yet. As such, it is felt necessary to carry out a research on the effectiveness of SCP for the purpose of improving alluvial soils of Bangladesh.

CHAPTER THREE

EXPERIMENTAL SETUP, TEST PROGRAMME AND TEST PROCEDURES

3.1 General

The present study was aimed at investigating the effectiveness of sand compaction pile (SCP) in improving loose alluvial soil deposits of Bangladesh. The investigation was done in the laboratory using models of prototype equipments/apparatus through different patterns/techniques. This is perhaps one of the noble studies that attempt to replace the field study of huge SCP construction replaced by physical models in the laboratory. In SCP, a column of sand is introduced in to the ground thus inducing stresses within the soil mass that eventually results in densification. The evaluation of densification is usually done by performing any of the penetration tests. The present chapter describes the experimental set up, test programme and test procedures that were carried out in order to fulfill the objectives of this study. To execute the SCP scheme in the laboratory a soil tank to house the artificially prepared sand bed, a sand deposition apparatus, a miniature SCP machine and a dynamic cone penetrometer were designed and fabricated. The experimental study scheme mainly consisted of preparation of sand bed, installation of SCP using both square and triangular patterns with varying spacing of SCP and Dynamic Cone Penetration (DCP). Two types of sand samples were used to form and investigate sand beds having varying deposits. DCPs were carried out on both intact soil bed and the bed after insertion of SCPs. DCP tests on improved soil bed were carried out at the centre locations in between the SCPs. The relative density of the improved bed was evaluated introducing term of $r_{d, \text{max}}$ as suggested by Alam et al. (2012). Using the determined relative density the compactness, corrected SPT-N value, angle of internal friction and hence the bearing capacity and shear strength of the SCP improved sand bed are evaluated following table 2.1. A flow diagram of the whole experimental program is presented in Figure 4.1

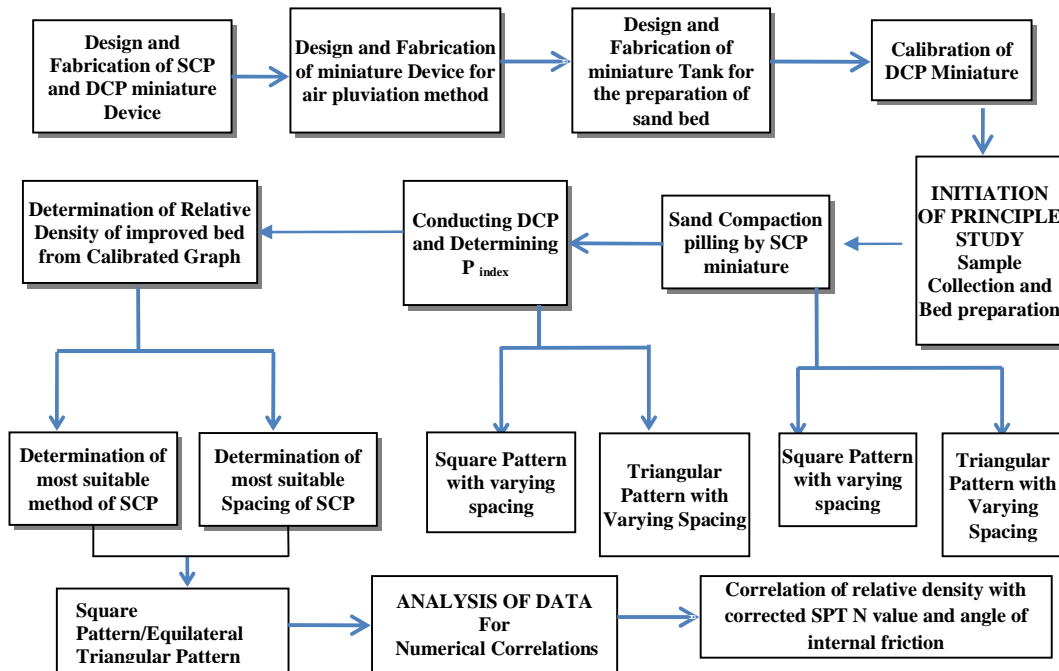


Figure 3.1: Flow Chart of Research Methodology

3.2 Design and Fabrication of Miniature SCP Installing Device

The most commonly practiced construction method of SCP is the composer method (Aboshi and Suematsu, 1985). The construction procedure of the composer method consists of several steps as depicted in Figure 2.6. The installation equipment consists of a steel casing that is first positioned to the prescribed locations, collimation of which is assisted by the transit apparatus, the casing pipe is then driven downwards into the ground. Sand is continually in-filled into the casing pipe during its penetration. After arriving at the desired depth, the casing pipe is hoisted upwards by certain height to discharge and feed sand into the ground. Afterwards, the casing pipe is partially re-driven downwards to squash and compact the discharged sand, which also enlarges the diameter of sand column. The above procedure of withdrawal followed by partially re-driving is repeated up to the soil surface. At the end, a well-compacted sand column with a diameter larger than the casing pile is constructed in the soil. The casing is usually driven in to the ground either by using a vibro-hammer or non-vibratory pushing techniques using a rotary motor. However, the miniature type of SCP composer can be operated in mechanical means.

In the present study, a push in type manual SCP machine was designed and fabricated. The device mainly consists of a mild steel frame or mandrel with a conical shape splitted bottom tip and a handle at the top that is used to push down or move up the conical bottom tip at desired position using a specially devised driving rod. The schematic diagram of the fabricated SCP miniature device with the components in both open and closed positions is shown in Figure 3.2. A photograph of the SCP miniature device is shown in Figure 3.3.

The main frame or mandrel of SCP miniature device was constructed of a mild steel tube having a wall thickness of 2.15 mm. The length and diameter of the SCP mandrel were 91.44 cm (3 feet), 7.62 cm (3 inches) respectively. End of the miniature is conical in shape. One mechanical lever is fixed inside the miniature through welding. Mechanical arrangement has been made in such a way that while pushing the miniature into the sand bed the end of the miniature will be closed, while the end of the miniature will be opened once the miniature will be pulled upward.

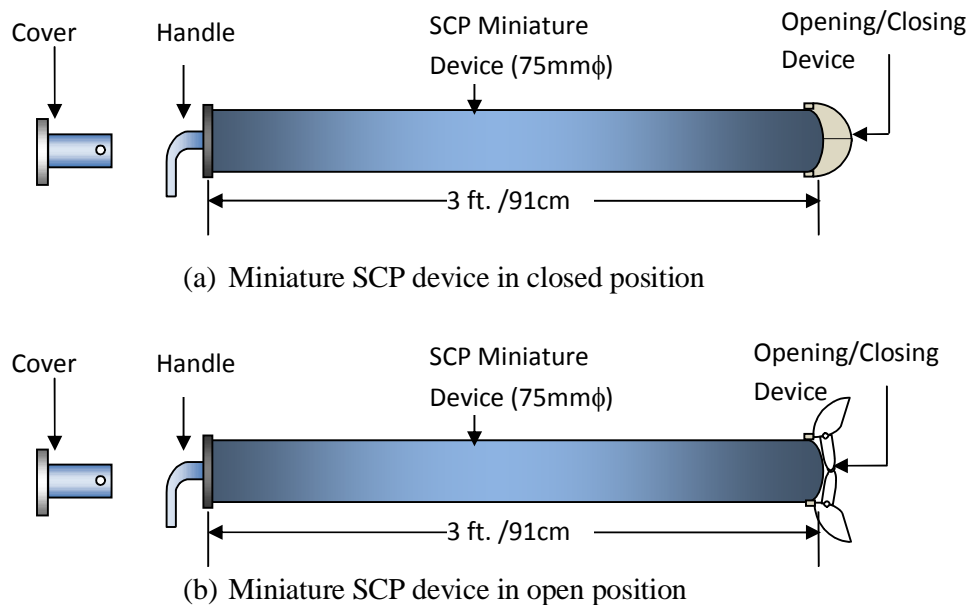


Figure 3.2: Schematic Diagram of Miniature SCP Mandrel; (a) Open Position; (b) Closed Position

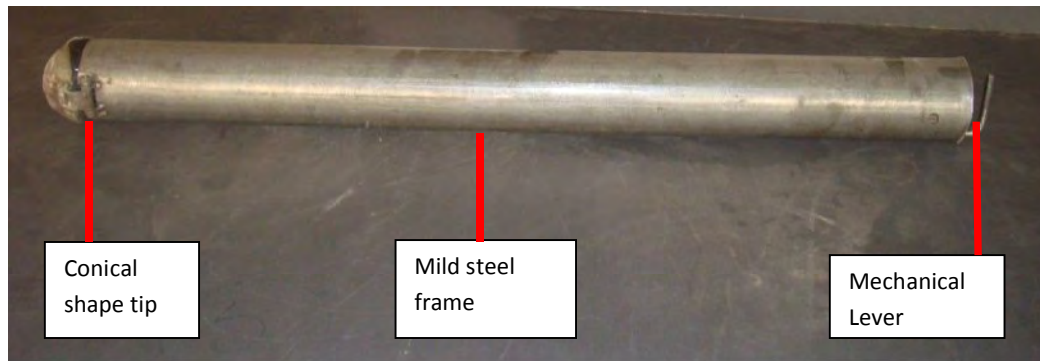


Figure 3.3: Photograph of Miniature SCP Mandrel

3.3 Fabrication of Miniature DCP Device

Standard test method of dynamic cone penetration (DCP) are frequently used in shallow pavement application that covers the measurement of the penetration rate of a cone of designated dimensions with an 8 kg hammer (8kg DCP) through undisturbed soil and/or compacted materials. The penetration rate may be related to in situ strength of soil or in situ CBR (California Bearing Ratio). A soil density may be estimated if the soil type and moisture content are known. The test method provides for an optional 4.6 kg sliding hammer when the use of the 8 kg sliding mass produces excessive penetration in soft ground conditions.

The operator drives the DCP tip into soil by lifting the sliding hammer to the handle then releasing it. The total penetration for a given number of blows is measured and recorded in mm/blow, which is then used to describe stiffness, estimate an in situ CBR strength from an appropriate correlation chart, or other material characteristics.

This test method is used to assess in situ strength of undisturbed soil and/or compacted materials. The penetration rate of the 8 kg DCP can be used to estimate in-situ CBR (California Bearing Ratio), to identify strata thickness, shear strength of strata, and other material characteristics. Other test methods exist for DCPs with different hammer weights and cone tip sizes, which have correlations that are unique to the instrument.

For the purpose of present study, a modified miniature DCP is fabricated following “ASTM Designation: D 6951 – 03(2006). A photograph of the miniature DCP device is shown in Figure 3.4. The schematic diagrams of the fabricated DCP miniature device with necessary dimension are shown in Figures 3.5 (a) and 3.5(b). The geometry of the replaceable tip is an important component of DCP device. A schematic diagram of the tip with dimensions is shown in Figure 3.5 (c). The dimensions are also listed in Table 3.1.

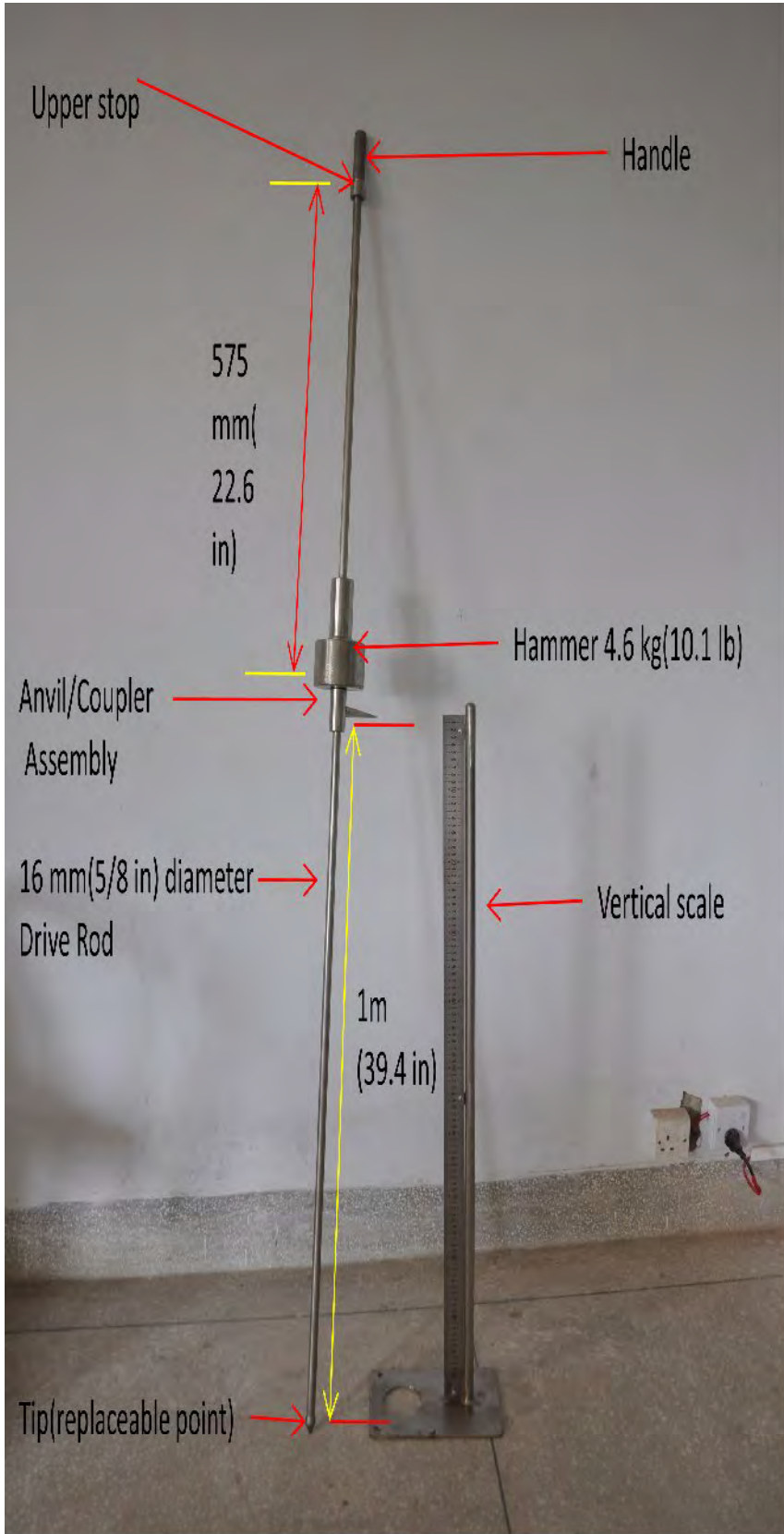


Figure 3.4 Photograph of DCP Miniature Device with Dimensions

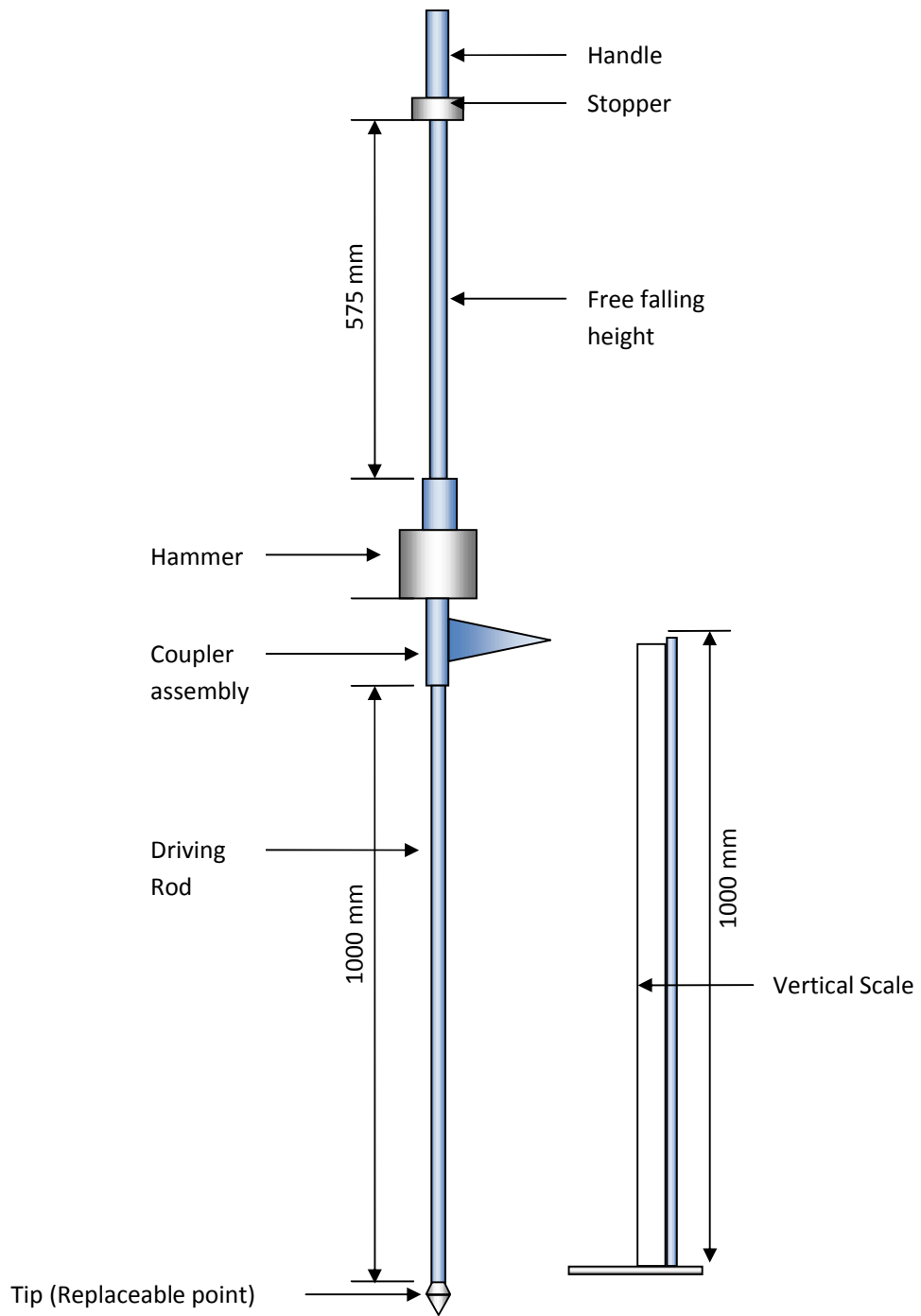


Figure 3.5(a): Schematic Diagram of Fabricated DCP Miniature Device Assembly

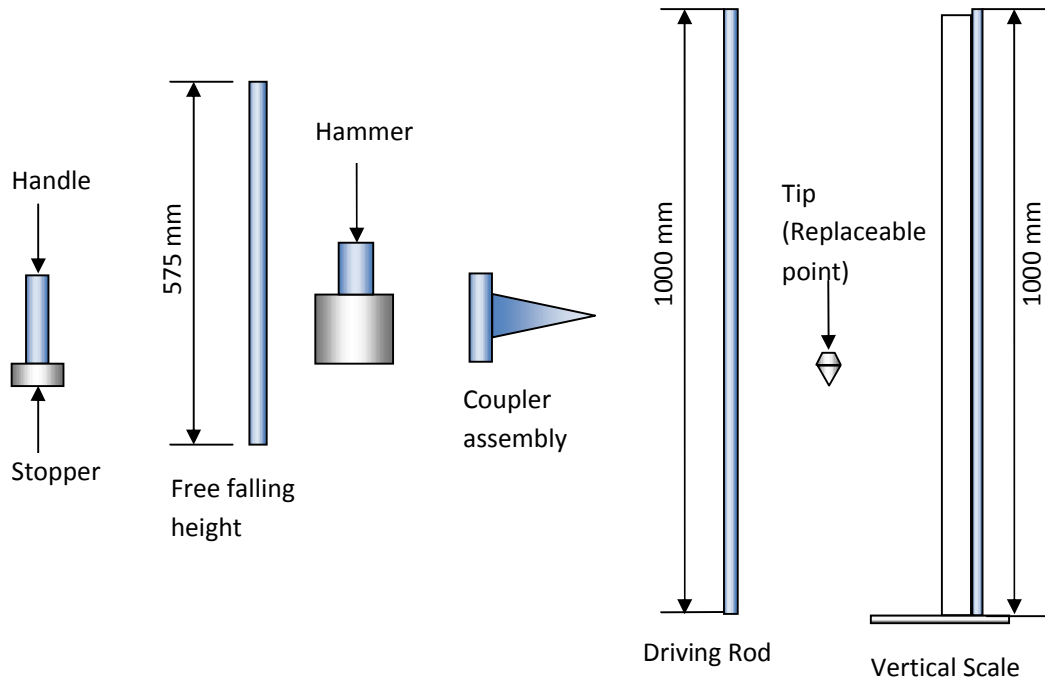


Figure 3.5(b): Schematic Diagram of Fabricated DCP Miniature Device Components

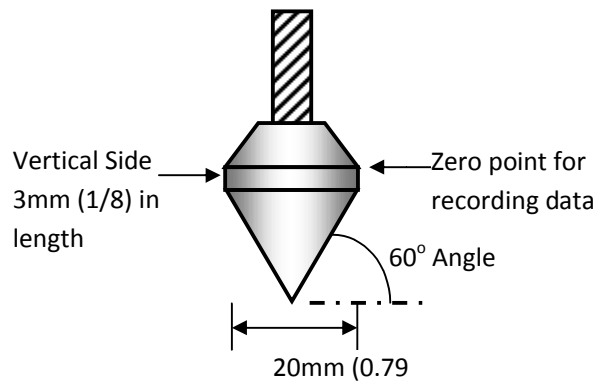


Figure 3.5 (c): Replaceable Point Tip of DCP

Table 3.1: Dimensions of DCP components

Item No	Parameters	Material/ Dimension
1	Hammer	Steel
2	Height of fall	575 mm
3	Cone Diameter	20 mm
4	Apex angle of cone	60 degree
5	Length of Guide Rod	1000 mm
6	Hammer Weight	4.6 kg or 10.1 lb
7	Tip	Replaceable point

3.4 Design and Fabrication of Tank for Housing Sand Bed

A metallic tank designed and fabricated using steel frame fenced with 10 mm thick glass plate that was used as the container to retain the soil formed of alluvial soil deposits. Thus the tank is known as the tank for soil bed formation. The inside dimension of the tank was same to make a cubic sand bed having length, width and depth dimensions of 600 mm. The schematic diagram of the sand bed tank is shown in Figure 3.6(a). A photograph of the fabricated tank is also shown in Figure 3.6(b).

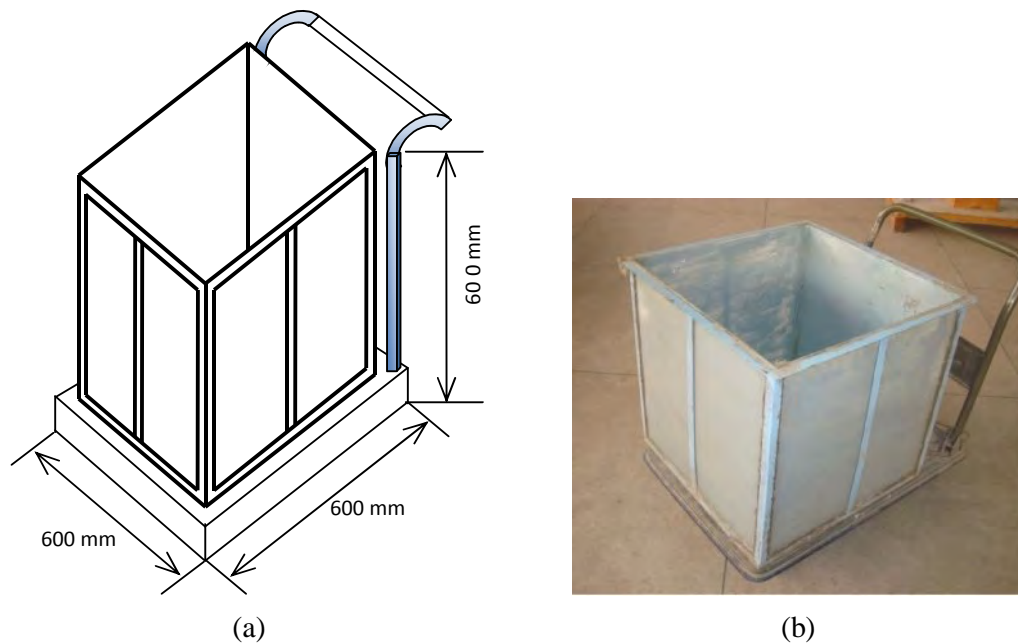
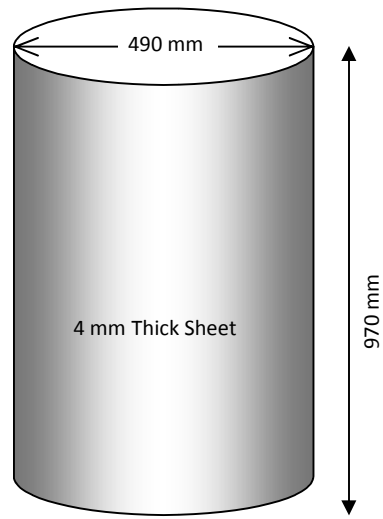


Figure 3.6: Sand Bed Housing Tank; (a) Schematic Diagram; (b) Photograph

3.5 Tank for Calibration of DCP

For the calibration of DCP a deeper tank was required to be procured. A steel cylindrical drum of diameter 490 mm, height 970 mm and thickness 4 mm was used as a calibration chamber. The schematic diagram and photograph of cylindrical drum is shown in Figure 3.7(a) and 3.7(b) respectively. Top of the cylinder was open while bottom of the cylinder is closed. Sand samples from Turag River (F.M. 0.66) and Meghna River (F.M. 0.89) were taken as the representative alluvial sand. For calibration of DCP in two types of soil, the tank was filled with sand in a controlled manner so that uniform sand deposits formed. The density of the soil was determined using calibrated pots and drive cylinder. The penetrometer was driven in to the deposit used to develop the correlation between dynamic cone resistance and relative density of sand. The calibration procedure is described in the next Chapter.



(a)

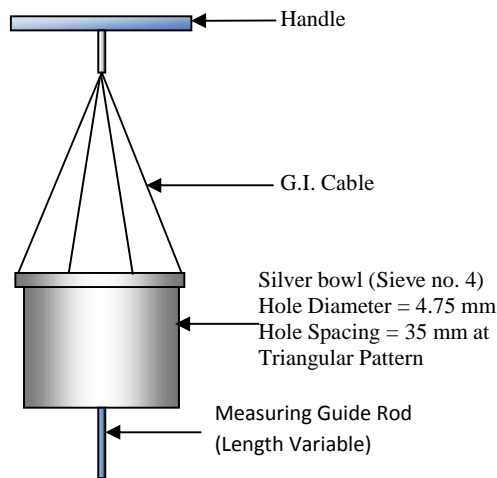


(b)

Figure 3.7: DCP Calibration Tank; (a) Schematic Diagram; (b) Photograph

3.6 Miniature Device for Dry Air Pluviation of Soil Deposit

A miniature device has been designed and fabricated for the preparation of sand bed of uniform density by dry air pluviation method as suggested by Alam et al. (2012). The schematic diagram of the air pluviation device and photograph showing the opening of the mesh are shown in Figures 3.8(a) and 3.8(b).



(a)



(b)

Figure 3.8: Device for Air Pluviation Soil Deposit; (a) Schematic Diagram; (b) Sieve Mesh

The air pluviation bowl was designed in such a manner that it can pour shower of sand in to the tank to form a uniform deposit. For the purpose, the base of plastic or silver bowl was slotted in such a manner that the slot opening was exactly equal to the opening of No. 4 ASTM sieve (4.75 mm). A hanger system was provided with the bowl connected to a handle such that the bowl can be moved all around the tank and shower of sand could be dropped from a desired height. A guide rod was used to measure height of fall of sand shower.

3.7 Soil Bed and SCP forming Materials

Two types of sand samples from river bed deposits of Turag and Meghna rivers of Bangladesh were collected and used in the present investigation as the sand bed materials. Coarse grained sand, namely Sylhet sand, was used as the SCP material. Relevant physical properties like specific gravity, maximum and minimum densities, coarseness (Fineness modulus) and grain size distribution tests of the samples were done using ASTM Standard test procedures. The grain size distribution curves of the soil samples are presented in Figure 3.9, and relevant physical properties are listed in Table 3.2.

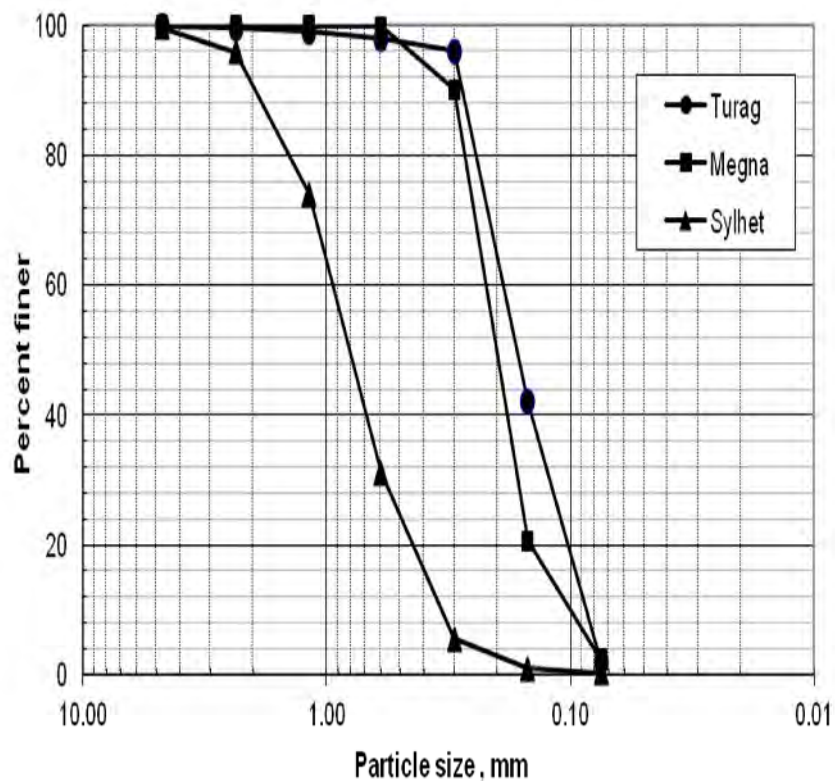


Figure 3.9: Grain Size Distribution Curves for Sand Samples used in Investigation

Table 3.2: Index properties and classification of sands used in the study

Item No.	Properties	Values of Parameters		
		Turag	Meghna	Sylhet
1	Fineness Modulus	0.66	0.89	2.93
2	Specific Gravity ()	2.73	2.68	-
3	D ₁₀ (mm)	0.09	0.10	0.35
4	D ₃₀ (mm)	0.12	0.16	0.58
5	D ₅₀ (mm)	0.17	0.20	0.80
6	D ₆₀ (mm)	0.19	0.22	0.95
7	Uniformity Coefficient,	2.19	1.22	2.71
8	Coefficient of Curvature,	0.91	2.22	1.01
9	Maximum Void Ratio,	1.04	-	-
10	Minimum Void Ratio,	0.81	-	-
11	Maximum Index Density, (KN/m ³)	14.76	-	-
12	Minimum Index Density, (KN/m ³)	13.1	-	-
13	Percent Fines	2.3	2.4	0.0
14	USCS Classification	SP	SP	SP
15	USCS Soil Description	Poorly Graded Sand	Poorly Graded Sand	Poorly Graded Sand

3.8 Sand Bed Preparation

Sand bed was prepared in the fabricated steel framed experimental cubic tank. Dry air pluviation method was used to fill the experimental tank so that uniform relative density was achieved. Fabricated No. 4 sieve silver bowl was used for the preparation of loose sand bed of uniform relative density keeping a height of fall approximately 200 mm so that density of the prepared sand bed remains low. This helped to evaluate the

effectiveness of SCP for sand bed improvement effectively. Same sieve was also used for the calibration of DCP miniature. The sand bed thus prepared is shown in Figure 3.10. The procedure of the preparation of sand bed is shown in Figure 3.11.



Figure 3.10: Sand Bed Prepared using Dry Air Pluviation Method for SCP



Figure 3.11: Photograph Showing Air Pluviation Method of Sand Deposition

3.9. SCP Scheme and DCP Location

A total 62 numbers of SCP were installed and 30 DCP tests were done. The test scheme is presented in Table 3.3 and Table 3.4. Typical Square and Triangular arrangements of SCP showing DCP locations are shown in Figure 3.12.

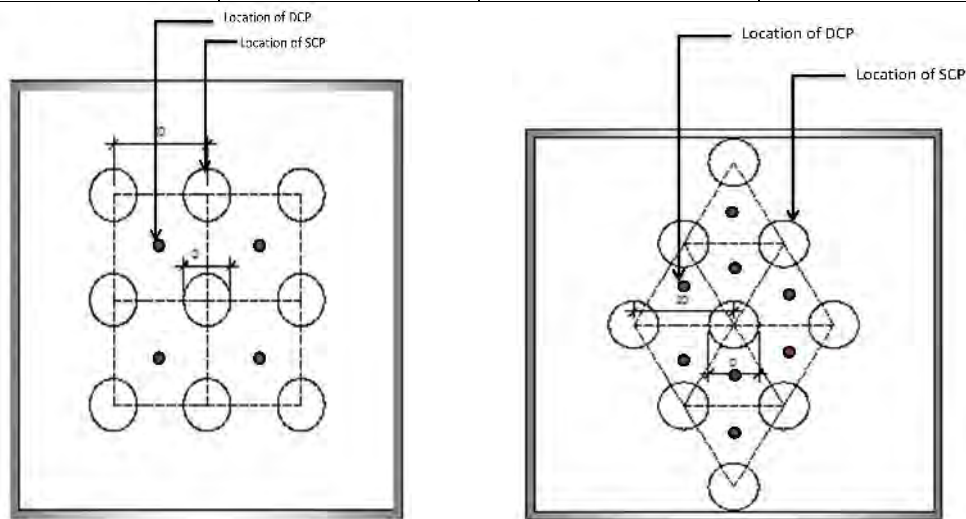
Table 3.3: Test scheme for the experimental study (Turag Sand)

Arrangement of SCP	Spacing of SCP	SCP Designation	DCP Designation
Square	2D = 15 cm	SCP-1	DCP-1 DCP-2
		SCP-2	
		SCP-3	
		SCP-4	
		SCP-5	
		SCP-6	
		SCP-7	
		SCP-8	
		SCP-9	
	3D = 22.5 cm	SCP-10	DCP-3 DCP-4 DCP-5 DCP-6
		SCP-11	
		SCP-12	
		SCP-13	
		SCP-14	
		SCP-15	
		SCP-16	
4D = 30 cm	SCP-17	DCP-7 DCP-8 DCP-9	
	SCP-18		
	SCP-19		
	SCP-20		
Triangular	2D = 15 cm	SCP-21	DCP-11 DCP-12 DCP-13 DCP-14 DCP-15
		SCP-22	
		SCP-23	
		SCP-24	
		SCP-25	
		SCP-26	
		SCP-27	
		SCP-28	
		SCP-29	
	3D = 22.5 cm	SCP-30	DCP-16 DCP-17 DCP-18 DCP-19
		SCP-31	
		SCP-32	
		SCP-33	
		SCP-34	
		SCP-35	
		SCP-36	
4D = 30 cm	SCP-37	DCP-20 DCP-21 DCP-22	
	SCP-38		
	SCP-39		
	SCP-40		

Table 3.4: Test scheme for the experimental study (Meghna Sand)

Arrangement of SCP	Spacing of SCP	SCP Designation	DCP Designation
Triangular	2D = 15 cm	SCP-41	DCP-23 DCP-24 DCP-25
		SCP-42	
		SCP-43	
		SCP-44	

		SCP-45	DCP-26 DCP-27 DCP-28 DCP-29
		SCP-46	
		SCP-47	
		SCP-48	
		SCP-50	
	3D = 22.5 cm	SCP-51	
		SCP-52	
		SCP-53	
		SCP-54	
		SCP-55	
		SCP-56	
4D = 30 cm	SCP-57	DCP-30	
	SCP-58		
	SCP-59		
	SCP-60		
	SCP-61		
	SCP-62		



(a) Square Arrangement

(b) Triangular Arrangement

Figure 3.12: Typical Square and Triangular Arrangements of SCP showing DCP Locations

3.10 Installation of Sand Compaction Piling by SCP Miniature

Sand compaction pilings were done on the prepared sand bed in the laboratory with the help of SCP miniature device. The sand beds were prepared by both Turag sand sample and Meghna sand sample. The sand pilings were done with 15.0 cm, 22.5 cm and 30 cm centre to centre spacing both in square and triangular patterns for Turag sand and in triangular pattern with similar spacing for beds formed of Meghna sand.

Coarse sand namely Sylhet sand was used for sand compaction piles. Grain size analysis curve and data of Sylhet sand is shown earlier in Figure 3.9 and Table 3.2. The depth of

piles was of 350 mm (14 inch). And diameter of the piles was of 75 mm (3 inch). Details of the piling are enumerated in Table 3.5.

Table 3.5: Characteristics of SCP

SL No	Items	Notation	Dimension / Description
1	Pile Diameter	D	75 mm
2	Depth	d	350 mm
3	Cross-sectional area of pile	a	4418 mm ²
4	Weight of sand per pile	W	3 kg
5	Type of sand used for Piling	–	Coarse sand (Sylhet sand; F.M. = 2.93)
6	Pattern of SCP	–	Square and Triangular
7	Spacing of SCP	s	15.0 cm,22.5 cm,30.0 cm c/c

SCP miniature was pushed manually into the sand bed up to a depth of 350 mm. The conical end of SCP miniature was kept closed during pushing with the help of the mechanical lever so that no sand can enter in to the cylindrical hollow SCP miniature. The sand was then poured into the hollow cylindrical SCP miniature from the top. The conical end of SCP miniature was then opened with the help of the mechanical lever and the miniature was pulled upward slowly for about 15 cm which allowed the sand to fall freely and fill the hole below. The end of SCP miniature was then closed with the help of the mechanical lever and SCP miniature was pushed downward to compact the free falling sand below. To make the compaction effective hammer blows are applied with a hammer of 4.6 kg. This procedure of pulling upward and pushing downward and thus compaction of sand continued till the completion of sand piles of desired depth. A sequential procedure of SCP installation can be seen in the photographs of Figure 3.13.



Figure 3.13 (a): Positioning of Miniature SCP Mandrel



Figure 3.13 (b): Initial Push to the SCP Mandrel



Figure 3.13 (c): Driving of SCP Mandrel



Figure 3.13 (d): Pouring of Coarse Sand in to the Mandrel



Figure 3.13 (e): Withdrawal of SCP Mandrel



Figure 3.13 (f): Compacting the SCP Sand



Figure 3.13 (g): Finished SCP in Square Pattern



Figure 3.13 (h): Finished SCP in Triangular Pattern

3.11 Performing Dynamic Cone Penetration (DCP) Test for Density Evaluation

Dynamic Cone Penetration Test was performed following ASTM test procedure D 6951. The procedure consists of driving a cone in to the soil by using a hammer from desired height. Detailed data of DCP including weight and height of fall of the hammer is provided in Table 3.1.

The DCP was held vertically and the tip seated such that the top of the widest part of the tip was flush with the sand surface. An initial reading was obtained from the graduated drive rod or a separate vertical scale/measuring rod. The distance was measured to the nearest 1-mm. The sliding reference attachments allowed the scale/measuring rod to be set/marked at zero when the tip was at the zero point. The whole testing in sequential order is presented in photographs of Figures 3.14(a) to 3.14(c).



Figure 3.14 (a): Positioning and Initialization of Miniature DCP Equipment for Testing



Figure 3.14 (b): Raising the Hammer to the Desired Height



Figure 3.14 (c): Final Reading Penetration per Blow

3.12 Determination of Bearing Capacity and Shear Strength

Penetration index is determined from dynamic cone penetration test. Penetration index is then used to determine the relative density from the calibrated graph of the penetration index vs. relative density relationship of the calibrated DCP miniature. Relative density determined in this way is used to find out the compactness, corrected SPT-N value and hence the bearing capacity, angle of internal friction and hence the shear strength of the SCP improved sand bed using Table 2.1.

CHAPTER FOUR

RESULTS AND DISCUSSIONS

4.1 General

The present study was aimed at investigating the effectiveness of Sand Compaction Pile (SCP) in improving the density characteristics of alluvial soil deposits of Bangladesh. Models of SCP installing equipment, density measuring equipment DCP and sand bed tank and other accessories were developed in order to perform this study in the laboratory. It is understood that SCP installing equipment in actuality is very massive, the parameters involved in the densification process are many and degree of the complexity of the compaction phenomenon is very high. As such, conducting investigation in the field involving all these parameters may lead to costly and time-consuming procedures, and idealization of soil in the field appeared to be as difficult as complexities. As such, first step of the present study was to attempt obtaining a reasonable procedure to carry out the investigation in the laboratory on loose sandy soil having controlled deposition.

The first step of this study of design, fabrication and use of the models appeared to be reasonably successful as the tests done using the models yielded some interesting results.

Using model SCP and DCP miniatures with square and triangular SCP pattern/category and different spacing of SCP, the effectiveness of SCP in improving the representing alluvial sandy soil deposits were evaluated in Chapter 3. The results are reported and discussed in the following sections.

4.2 Calibration of Fabricated DCP Miniature

The calibration tank was placed on a level ground. To calibrate the miniature DCP, sands were discharged in to the calibration tank from the air pluviation bowl maintaining a constant height of fall, throughout, to make uniform relative density of the soil. Sand deposits of preselected relative densities were thus prepared with different constant height of fall of sand shower. DCP test was performed on the sand deposit of known relative density of calibration sand bed for each of the relative density. Penetration of cone was recorded for every blow of hammer. and values of DCP tests were determined from Cumulative Depth of Penetration (mm) Vs. Number of Blows plot. N_{10} is the number of blows per 10 cm of penetration of dynamic cone and is the penetration rate of cone in mm/blow. Tables 4.1 shows the data obtained for determining and from

Cumulative Depth of Penetration (mm) vs. Number of Blows plot for 15 cm (6 inch), 22.5 cm (9 inch), 30 cm (12 inch), 37.5 cm (15 inch), 45 cm (18 inch) height of falls respectively for Turag Sand.

Table 4.1: Number of Blows and Cumulative Depth of Penetration Data (in mm) for and Calibration (TURAG SAND)

No of Blows	Height of Fall in cm				
	15.0	22.5	30.0	37.5	45.0
1	297	147	215.7	151.5	113.3
2	463.5	278.2	369.4	252.5	204.6
3	627	399	469.1	358.5	289.6
4	745.5	536.5	583.8	456.5	377.6
5	-	645.3	654.3	541.5	463.9
6	-	-	-	-	556.2
7	-	-	-	-	634.9

Figures 4.1(a), 4.1(b), 4.1(c), 4.1(d) and 4.1(e) show the graphical procedure of obtaining and from Cumulative Depth of Penetration (mm) vs. Number of Blows plot for 15 cm (6 inch), 22.5 cm (9 inch), 30 cm (12 inch), 37.5 cm (15 inch), 45 cm (18 inch) pluviation height of falls respectively.

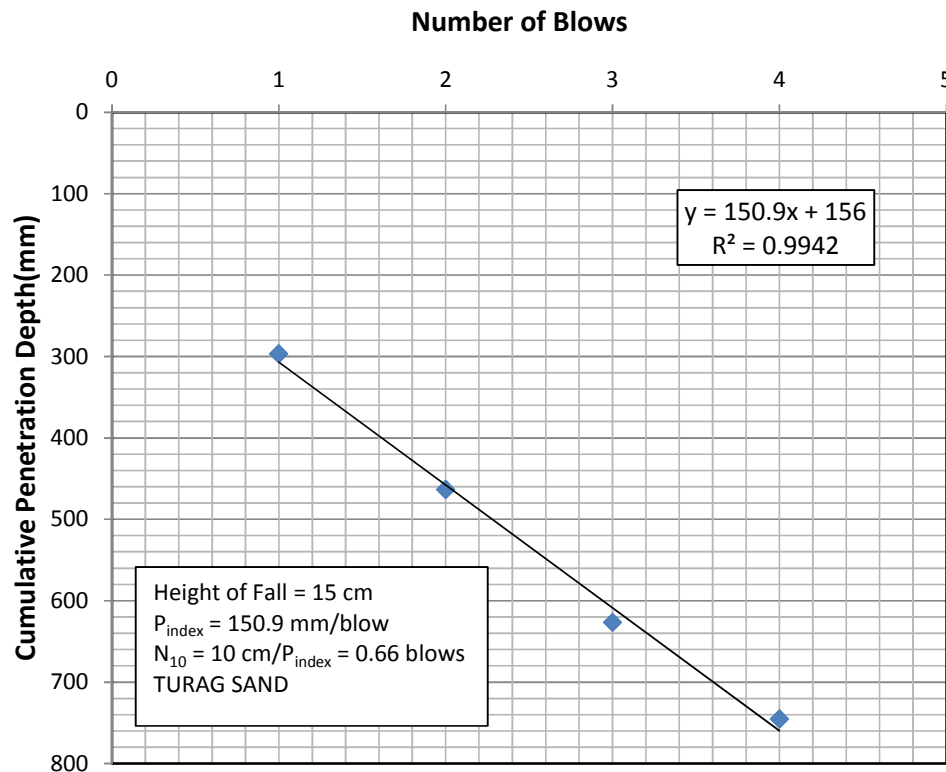


Figure 4.1(a): No. of Blows vs Cumul. Penetration Depth (Height of fall = 15 cm: TURAG SAND)

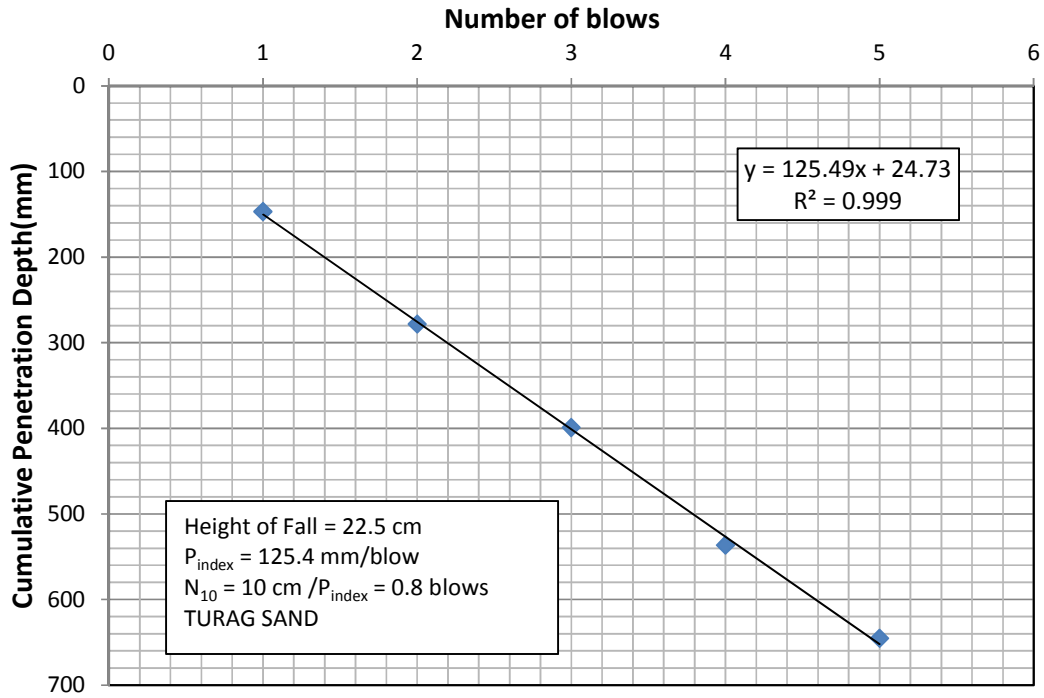


Figure 4.1(b): No. of Blows vs Cumul. Penetration Depth (Height of fall = 22.5 cm: TURAG SAND)

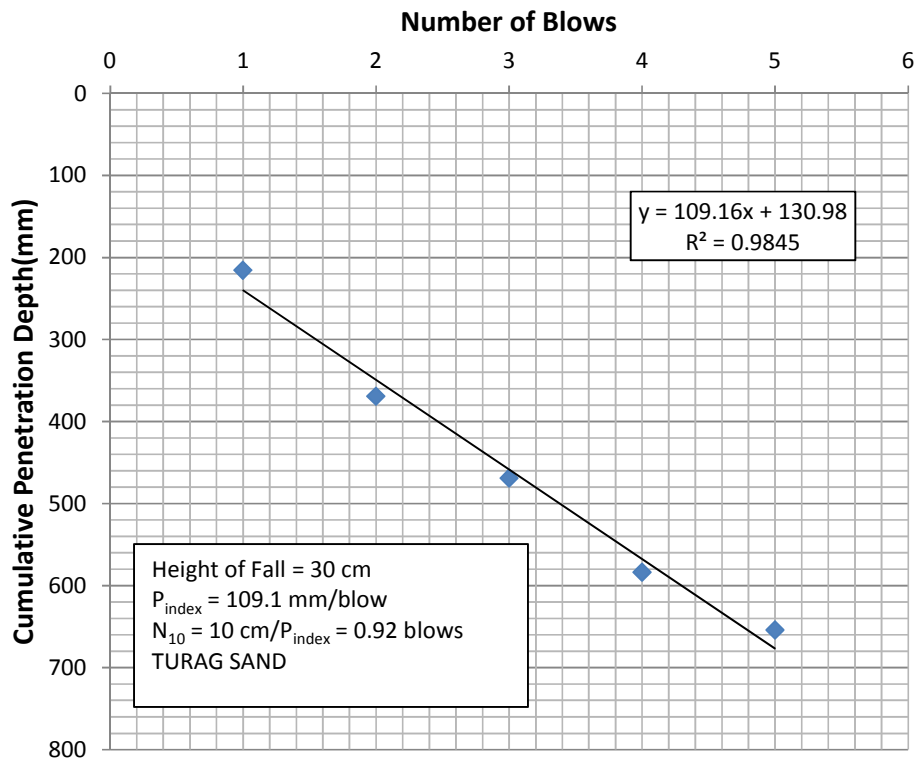


Figure 4.1(c): No. of Blows vs Cumul. Penetration Depth (Height of fall = 30 cm: TURAG SAND)

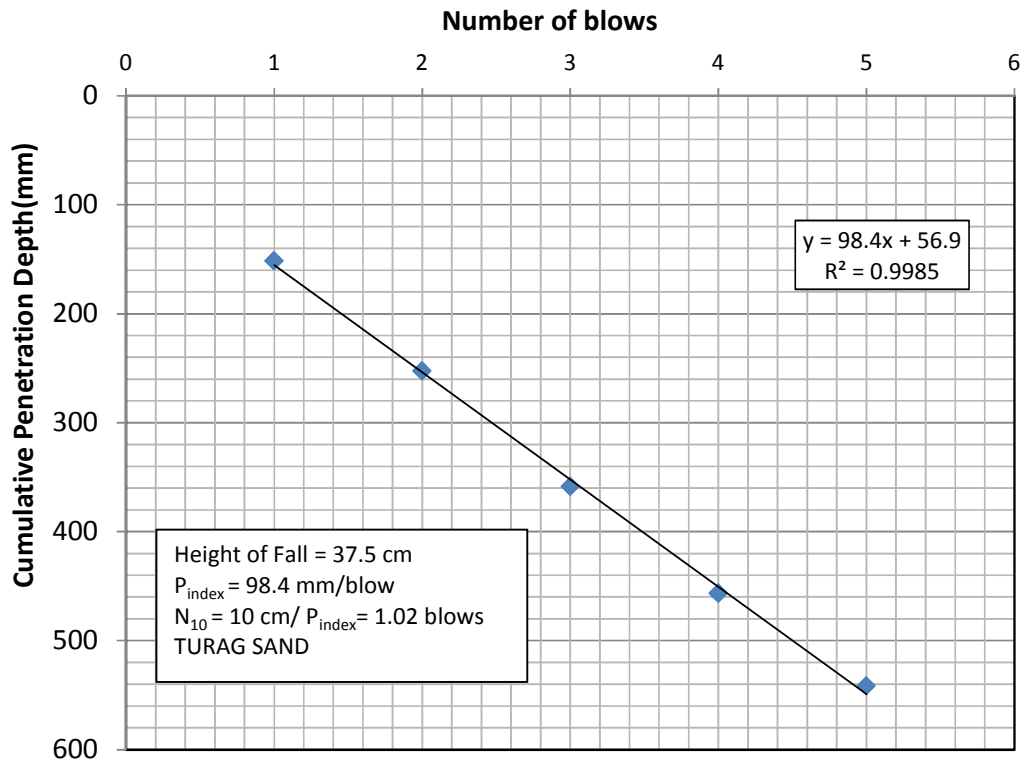


Figure 4.1(d): No. of Blows vs Cumul. Penetration Depth (Height of fall = 37.5 cm: TURAG SAND)

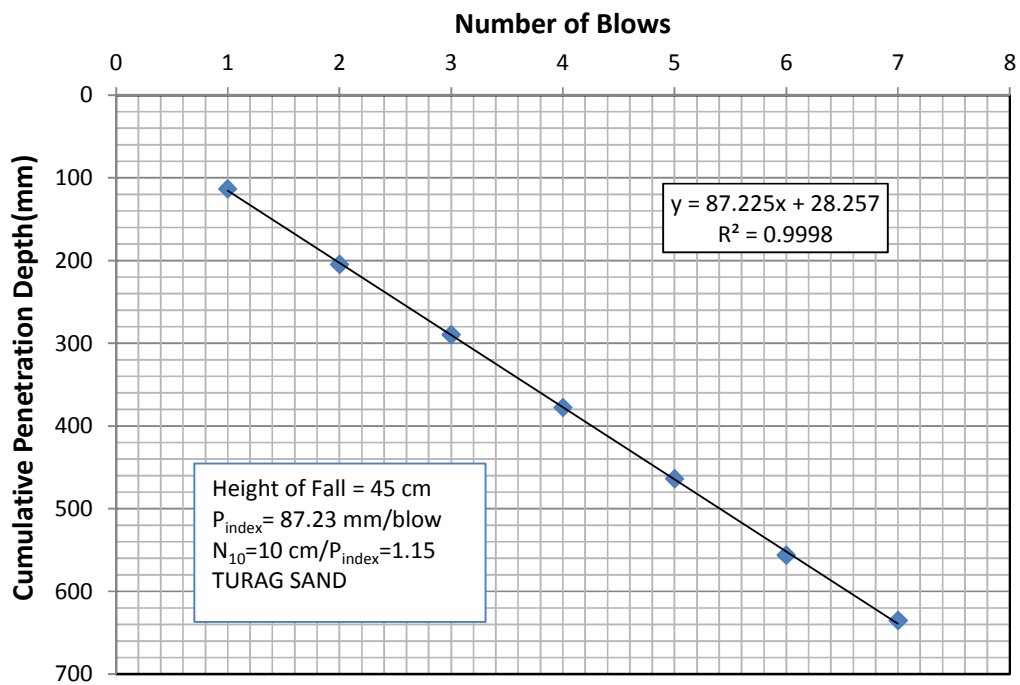


Figure 4.1(e): No. of Blows vs Cumul. Penetration Depth (Height of fall = 45 cm: TURAG SAND)

Tables 4.2 shows the data obtained for determining P_{index} and N_{10} from Cumulative Depth of Penetration (mm) vs. Number of Blows plot for 22.5 cm (9 inch), 30 cm (12 inch), 37.5 cm (15 inch) height of falls respectively for Meghna Sand.

Table 4.2: Number of Blows and Cumulative Depth of Penetration Data (in mm) for Calibration (MEGHNA SAND)

No of Blows	Height of Fall(cm)		
	22.5	30	37.5
1	155	230	270
2	295.2	370	340.5
3	425.5	490	409.5
4	530.5	550	455.5
5	611	605	502.5
6	-	-	549.5

Figures 4.2(a), 4.2(b), 4.2(c) show the graphical procedure of obtaining P_{index} and N_{10} from Cumulative Depth of Penetration (mm) vs. Number of Blows plot for 22.5 cm (9 inch), 30 cm (12 inch), 37.5 cm (15 inch) pluviation height of falls respectively.

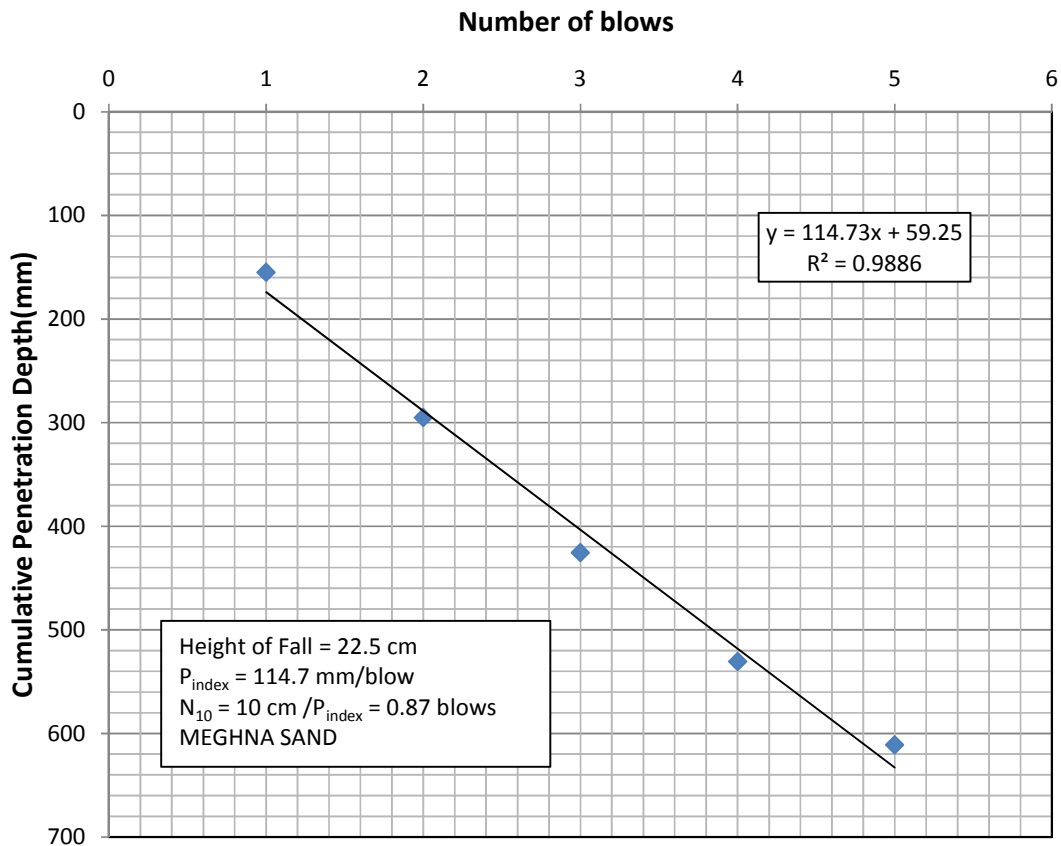


Figure 4.2 (a): No. of Blows vs Cumul. Penetration Depth(Height of fall = 22.5 cm: MEGHNA SAND)

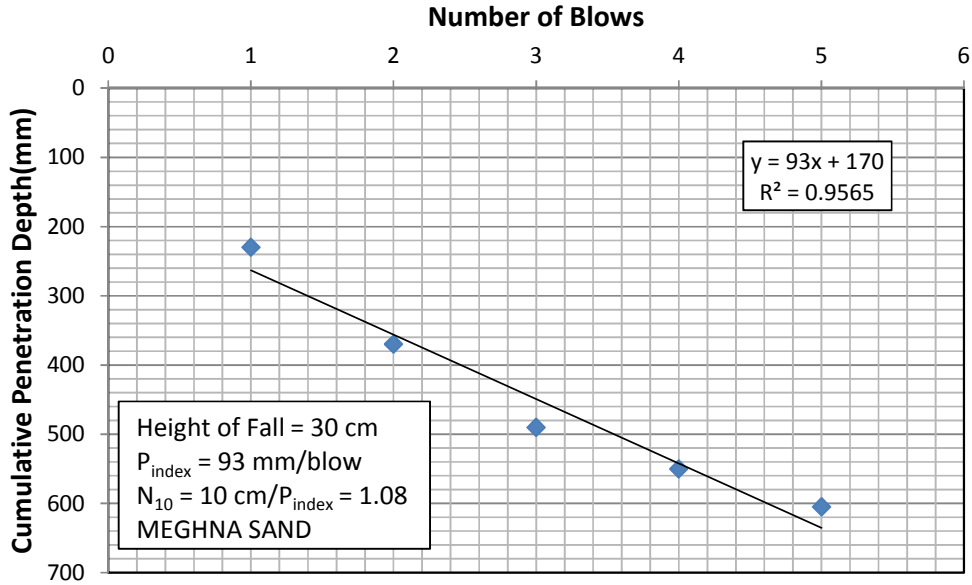


Figure 4.2(b): No. of Blows vs Cumul. Penetration Depth (Height of fall = 30 cm: MEGHNA SAND)

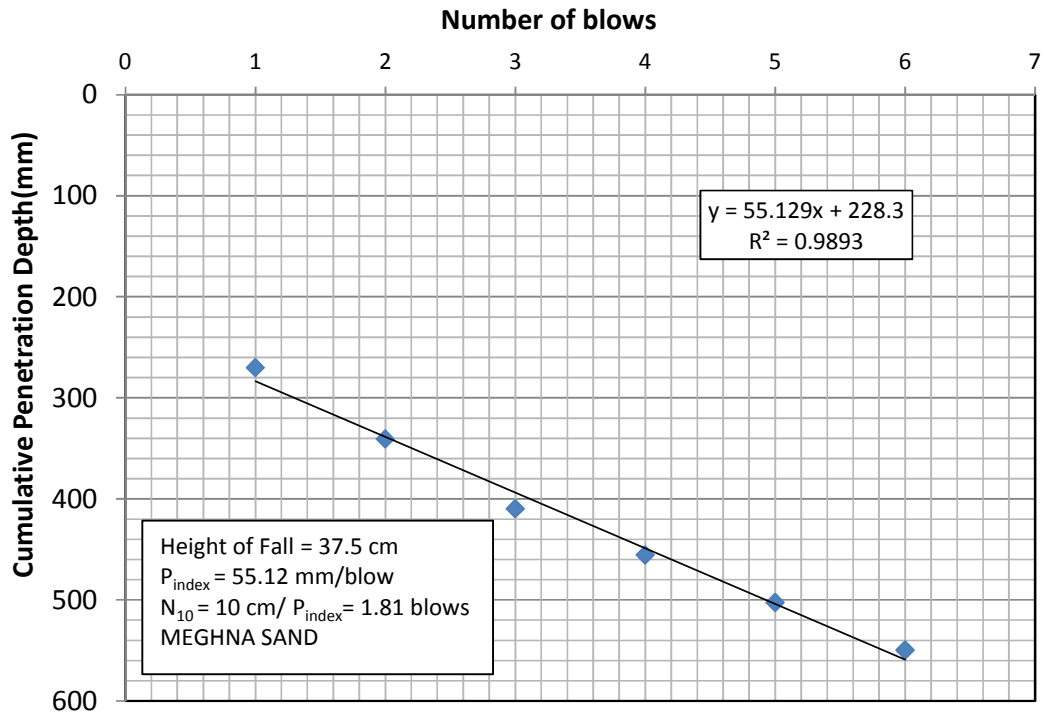


Figure 4.2(c): No. of Blows vs Cumul. Penetration Depth (Height of fall = 37.5 cm: MEGHNA SAND)

For various pluviation heights of fall relative density was obtained as presented in Table 4.3 and 4.4 for Turag and Meghna sand respectively. Their relationships are also presented in Figure 4.3 and 4.4 respectively. Versus Relative density relation of the sand beds for

Turag and Meghna sand are shown in Figure 4.5 and 4.6. Thus, correlation between Relative Density versus N_{60} was established.

Table 4.3: Various parameters for Turag sand against pluviation height of fall

Determination No.	Height of Fall (cm)	Relative Density, D_r (%)	N_{60} (mm/blow)	N_{60} / D_r
1	15.0	34.9	150.9	0.66
2	22.5	46.7	125.4	0.8
3	30.0	58.28	109.1	0.92
4	37.5	63.55	98.4	1.02
5	45.0	70.51	87.23	1.15

Table 4.4: Various parameters for Meghna sand against pluviation height of fall

Determination No.	Height of Fall (cm)	Relative Density, D_r (%)	N_{60} (mm/blow)	N_{60} / D_r
1	22.5	60.42	114.7	0.87
2	30	76.2	93	1.08
3	37.5	85.69	55.12	1.81

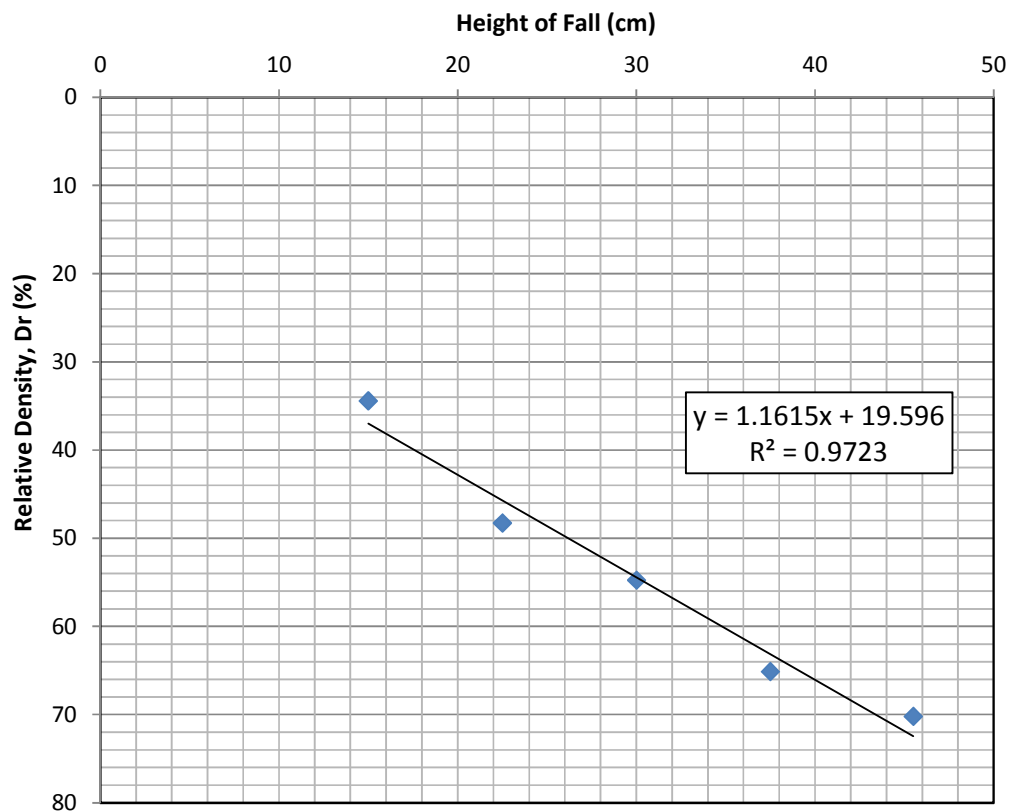


Figure 4.3: Pluviation Height of Fall versus Relative Density of Turag Sand

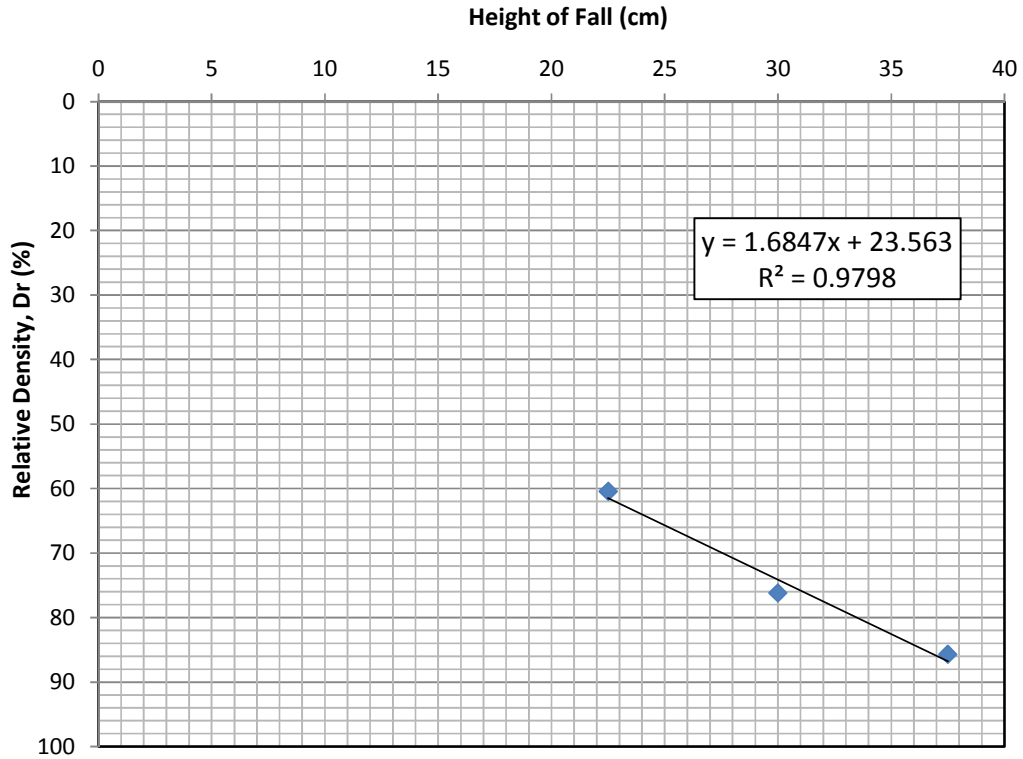


Figure 4.4: Pluviation Height of Fall versus Relative Density of Meghna Sand

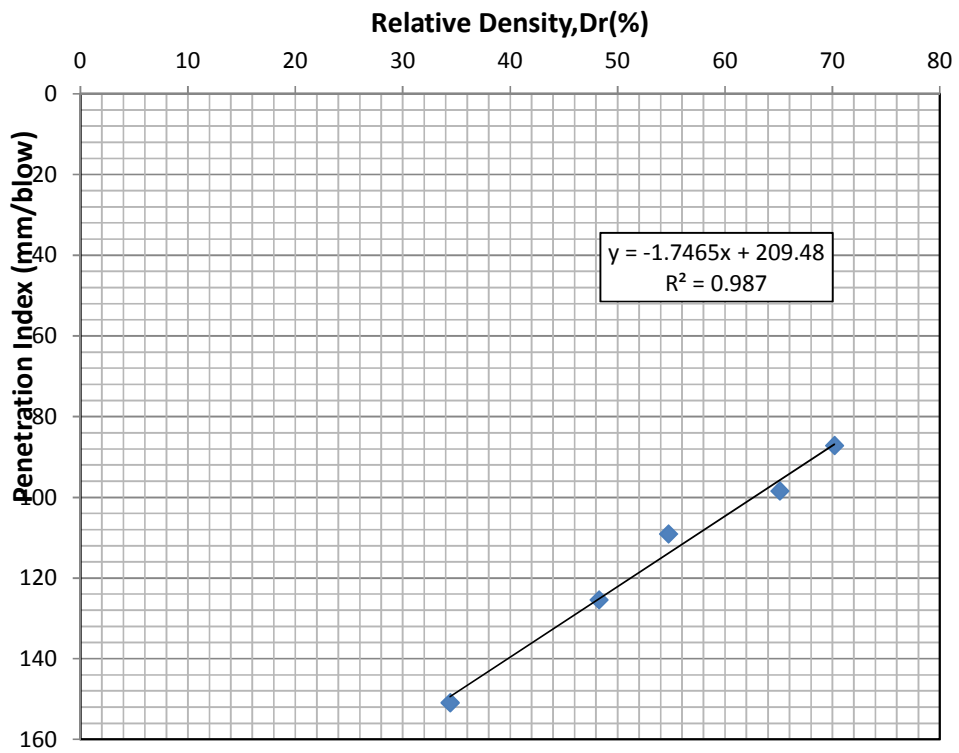


Figure 4.5: Relative Density - Relationship for Turag Sand

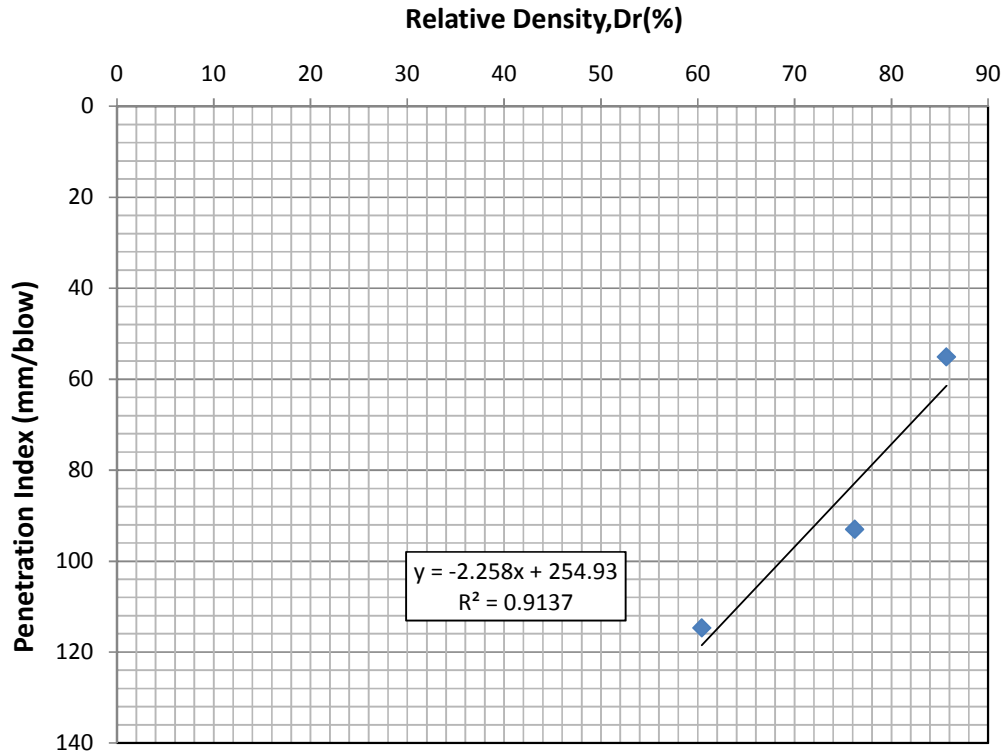


Figure 4.6: Relative Density - Relationship for Meghna Sand

4.3 Calibration Correlations

The analyses of the data suggest that there exists linear relationship between D_r and relative density, which can be expressed as:

$$\text{For Turag Sand, } D_r(\%) = 1.149h + 20.07 \quad (4.1)$$

$$= -1.746 C_p + 209.4 \quad (4.2)$$

$$\text{For Meghna Sand, } D_r(\%) = 1.684h + 23.56 \quad (4.3)$$

$$= -2.258 C_p + 254.9 \quad (4.4)$$

Where,

h =Pluviation height of fall of sand in cm

C_p =Cone penetration per blow of hammer mm/blow

4.4 Estimation of Initial Penetration Index,

As mentioned earlier, sand bed of uniform relative density was prepared in the experimental tank by air pluviation method from a height of approximately 20 cm (8 inch) for both Turag and Meghna sand samples. Sand compaction pilings were done by the fabricated SCP miniature both in square and equilateral triangular pattern in case of Turag river sand sample while in case of Meghna river sand sample, SCPs were constructed in equilateral triangular pattern only as mentioned. In each pattern, SCPs were constructed at 30 cm, 22.5 cm, and 15 cm center to center spacing. before and after the construction of SCPs for both the beds formed of Turag and Meghna River sand sample for different spacing were determined through DCP tests. of the sand beds before the construction of SCPs are more or less found to be 470 mm/blow.

4.5 Estimation of Penetration Index, for Improved Soil Bed of Turag Sand

After the improvement of the bed by sand piling, cumulative penetration depth against number of blows for each borehole was determined for piling of a particular spacing in different pattern. Then recorded cumulative penetration depths were plotted against number of blows for each borehole of different spacing of piling both in square and equilateral triangular pattern after the improvement of the bed. for each borehole is then determined from the average slope of number of blows vs. cumulative penetration depth for each plot. for each bed of particular spacing is then determined from the average of the values of the boreholes determined from that bed of particular spacing and pattern.

value of the soil was determined as 10 cm/ . Average and average values for the square and triangular patterns for Turag sand are shown in Figures 4.7 to 4.12. The effectiveness of SCP was examined by plotting P_{index} against spacing of SCPs for both square and triangular patterns as shown in Figures 4.13 and 4.14.

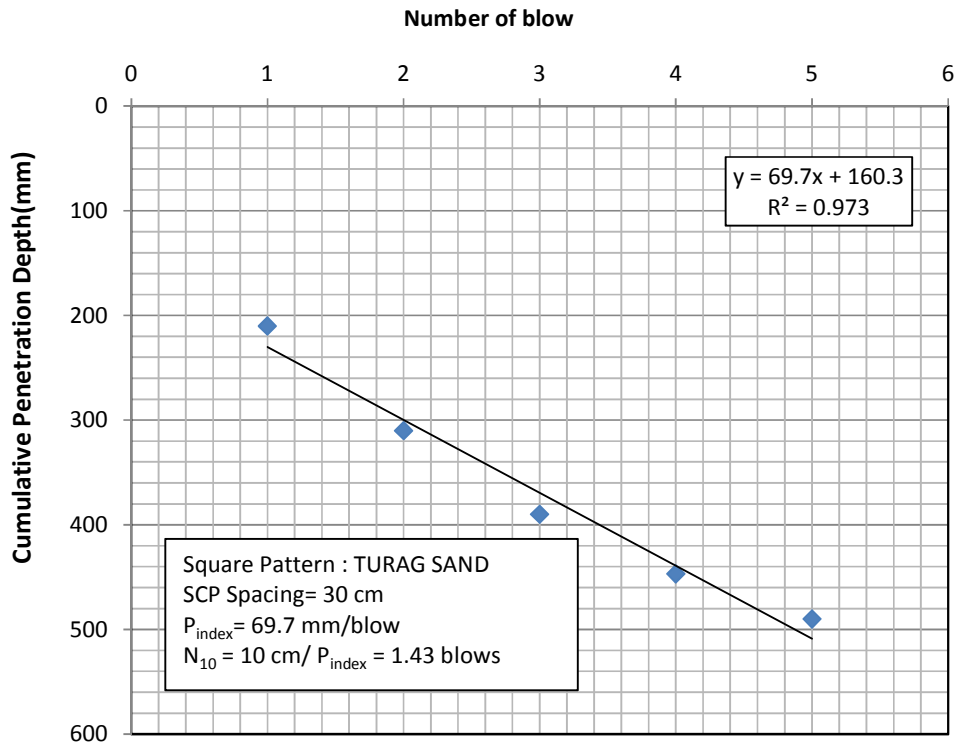


Figure 4.7: Estimation of P_{index} and N_{10} (SCP Spacing = 30 cm, Square Pattern; TURAG)

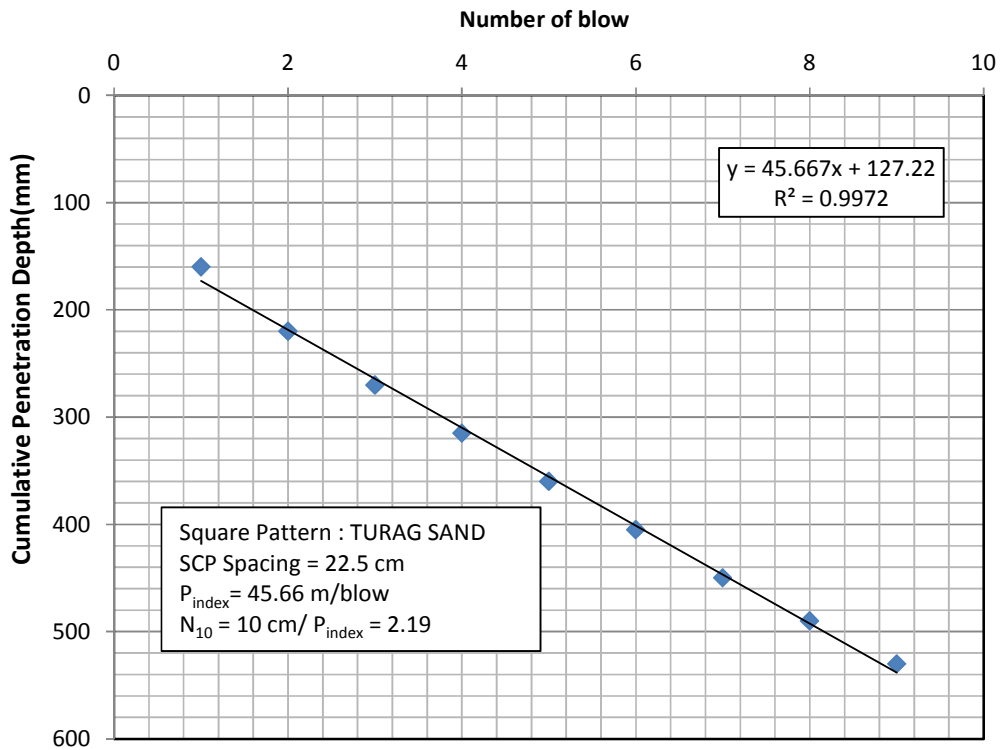


Figure 4.8: Estimation of P_{index} and N_{10} (SCP Spacing = 22.5 cm, Square Pattern; TURAG)

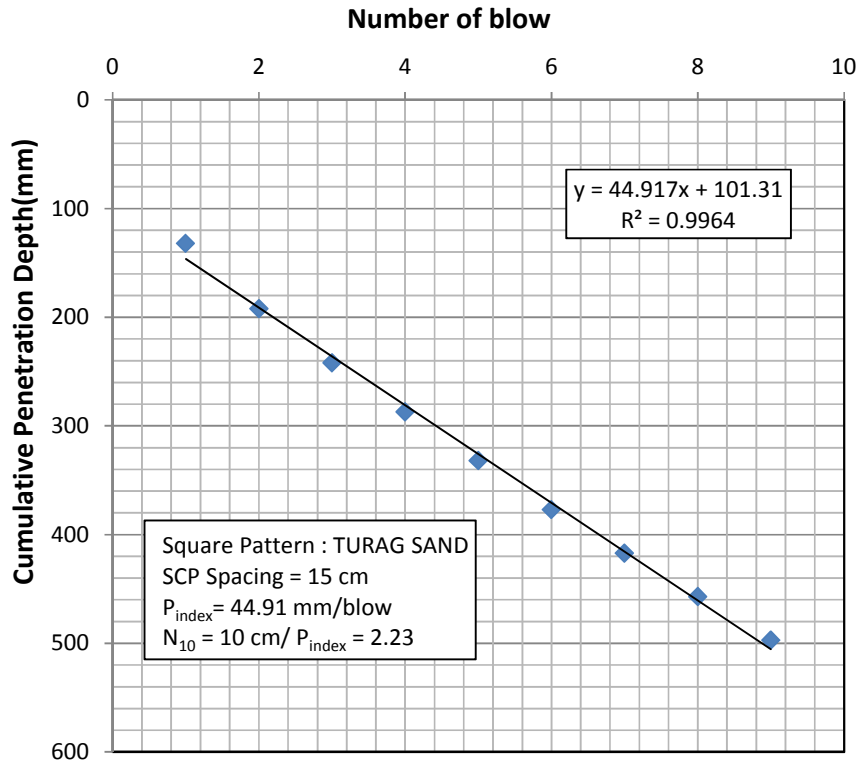


Figure 4.9: Estimation of P_{index} and N_{10} (SCP Spacing = 15 cm, Square Pattern; TURAG)

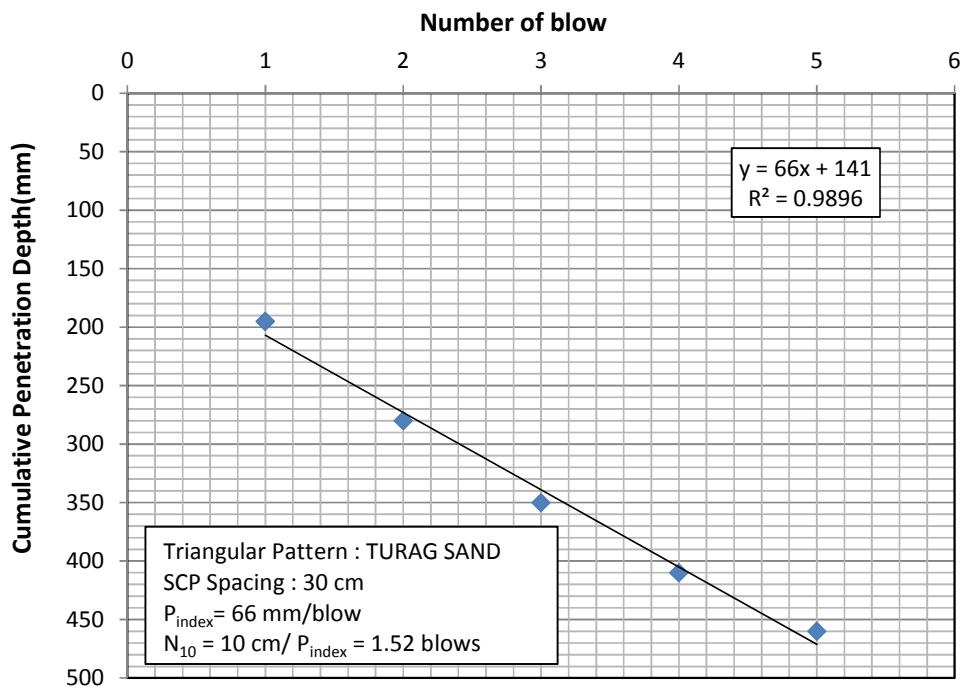


Figure 4.10: Estimation of P_{index} and N_{10} (SCP Spacing = 30 cm, Triangular Pattern; TURAG)

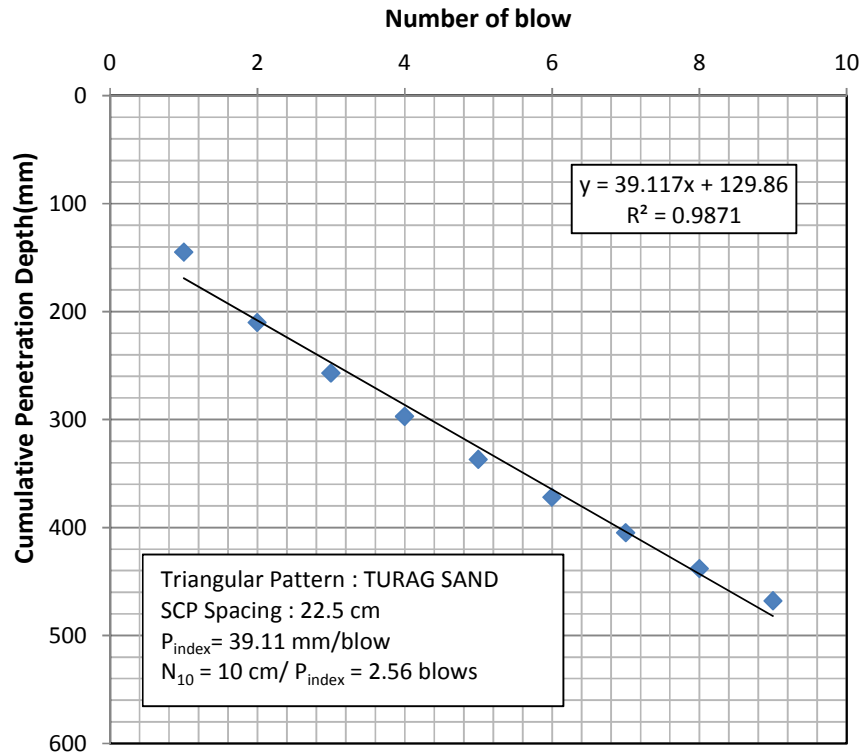


Figure 4.11: Estimation of P_{index} and N_{10} (SCP Spacing = 22.5 cm, Triangular Pattern; TURAG)

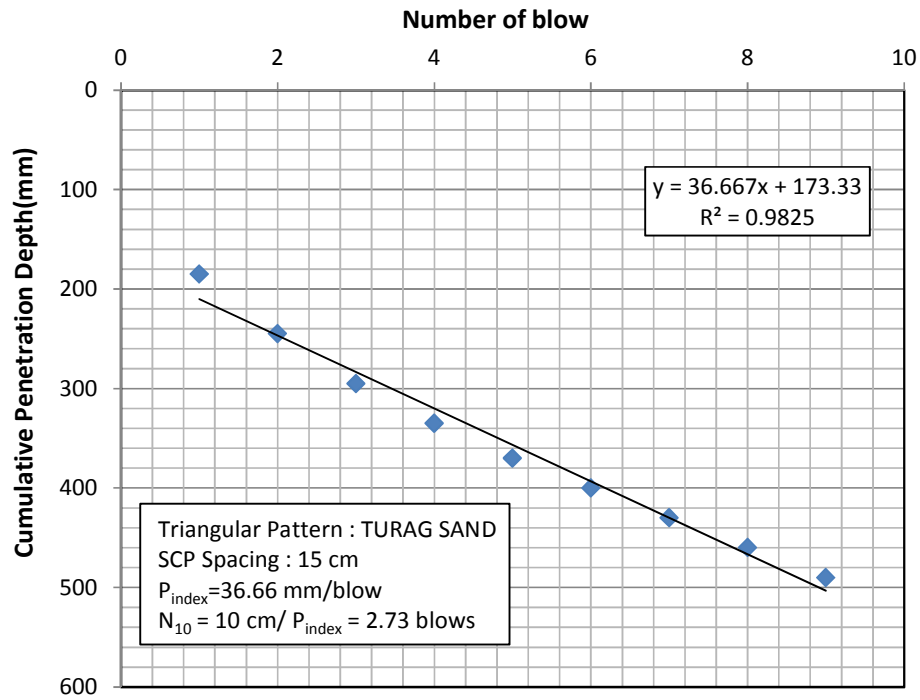


Figure 4.12: Estimation of P_{index} and N_{10} (SCP Spacing = 15 cm, Triangular Pattern; TURAG)

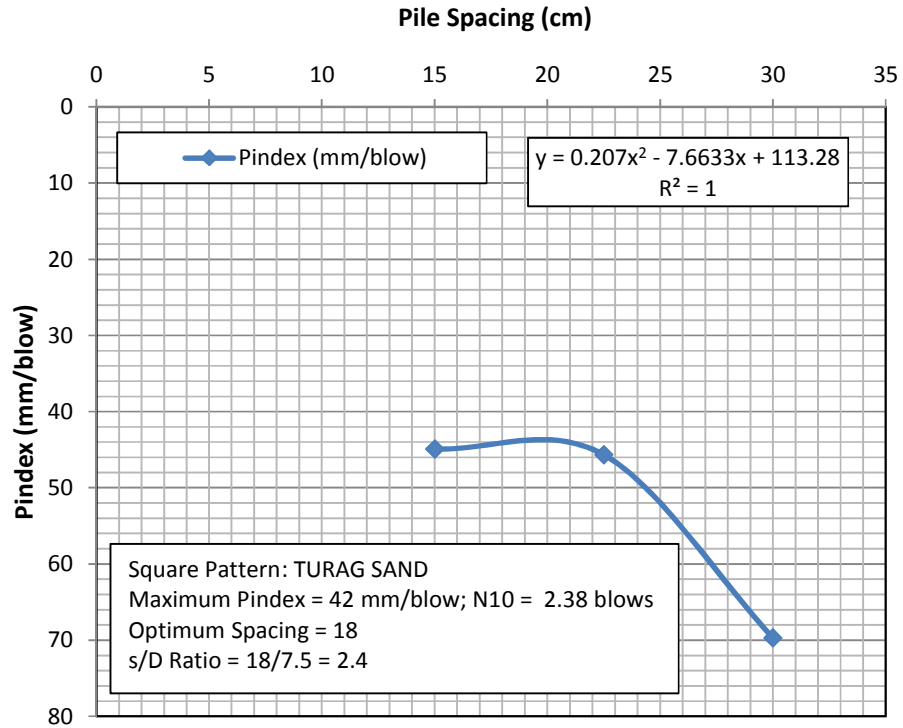


Figure 4.13: Effectiveness of SCP: Piling Spacing Vs. P_{index}, Square Pattern (TURAG)

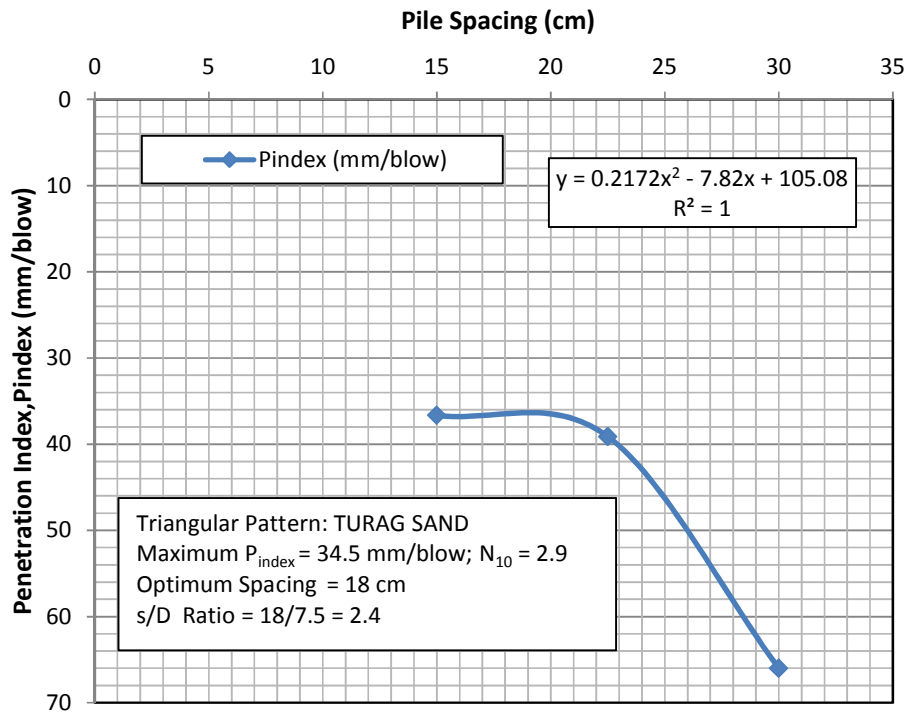


Figure 4.14: Effectiveness of SCP: Piling Spacing Vs. P_{index}, Triangular Pattern (TURAG)

4.6 Estimation of Penetration Index, P_{index} for Improved Soil Bed for Meghna Sand

Sand compaction pilings (SCPs) were constructed in equilateral triangular pattern only for the case of Meghna sand to carry out a comparative study between P_{index} value of the sand bed formed of Turag and Meghna sand in equilateral triangular pattern since equilateral triangular pattern of pilings were found to be more effective than that of square pattern of piling in the case of Turag sand sample. P_{index} of the prepared sand bed before the improvement of the bed was determined first. After the improvement of the bed by sand piling, cumulative penetration depth against number of blows was determined for piling spacing of 30 cm, 22.5 and 15 cm centre to centre respectively. Then recorded cumulative penetration depths were plotted against number of blows for different spacing of piling in equilateral triangular pattern after the improvement of the bed. P_{index} is then determined from the average slope of number of blows vs. cumulative penetration depth for each plot. P_{index} of the prepared sand bed before the improvement of the bed for the equilateral triangular pattern of piling was 470 mm/blow for 30 cm, 22.5 cm and 15 cm centre to centre spacing. Figures 4.15, 4.16 and 4.17 show plots for equilateral triangular pattern of piling in 30 cm, 22.5 cm and 15 cm spacing respectively after the improvement of the bed. N_{10} value was also calculated as 10 cm/ P_{index} for each plot. Figure 4.18 shows plot of piling spacing vs. P_{index} for equilateral triangular pattern of piling for the bed formed of Meghna sand.

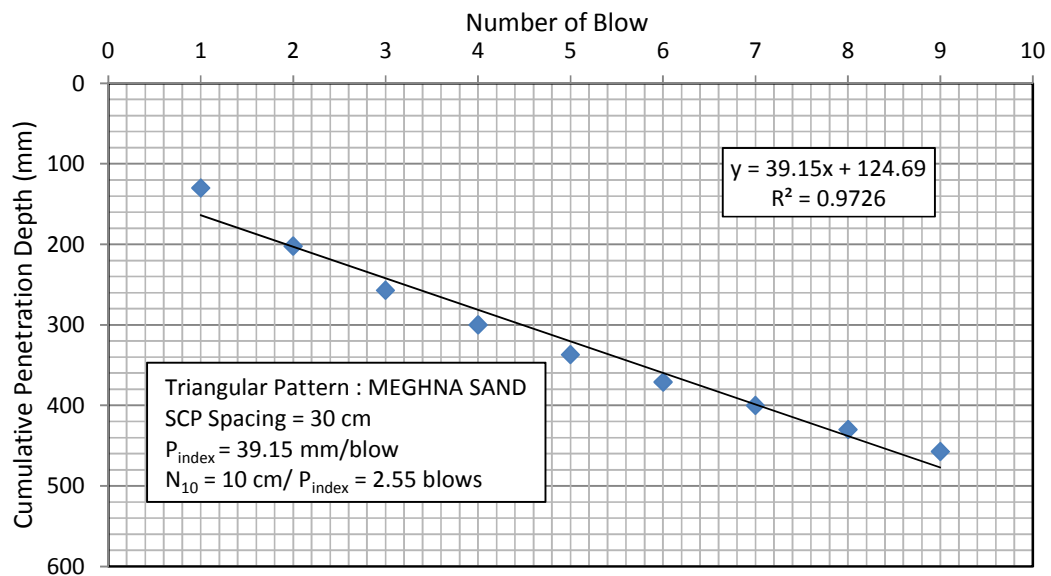


Figure 4.15: Estimation of P_{index} and N_{10} (SCP Spacing = 30 cm, Triangular Pattern; MEGHNA)

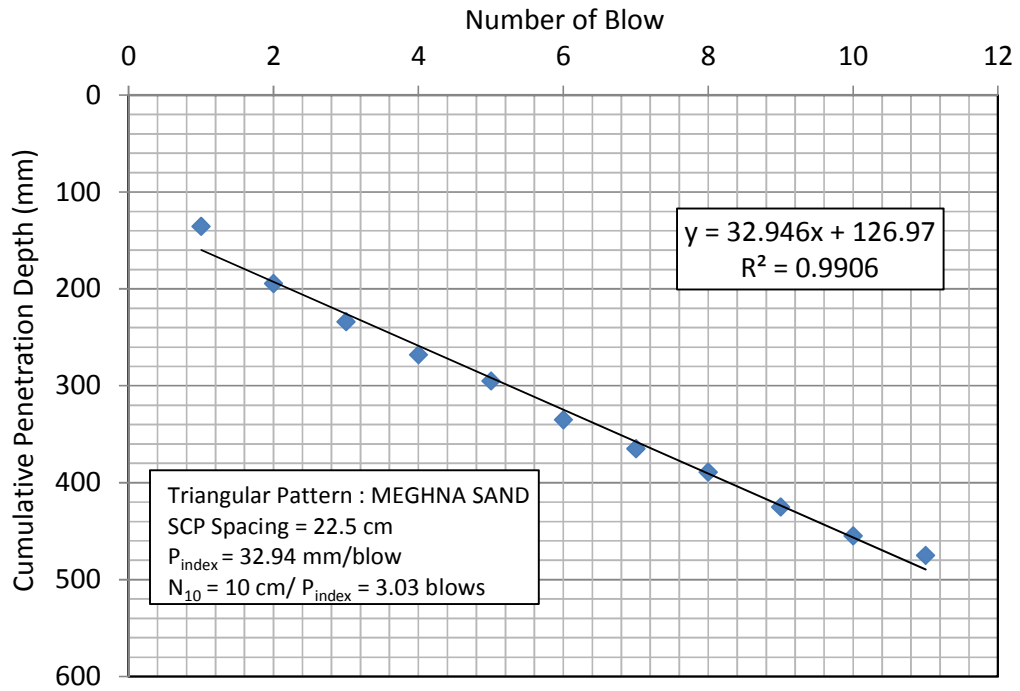


Figure 4.16: Estimation of P_{index} and N_{10} (SCP Spacing = 22.5 cm, Triangular Pattern; MEGHNA)

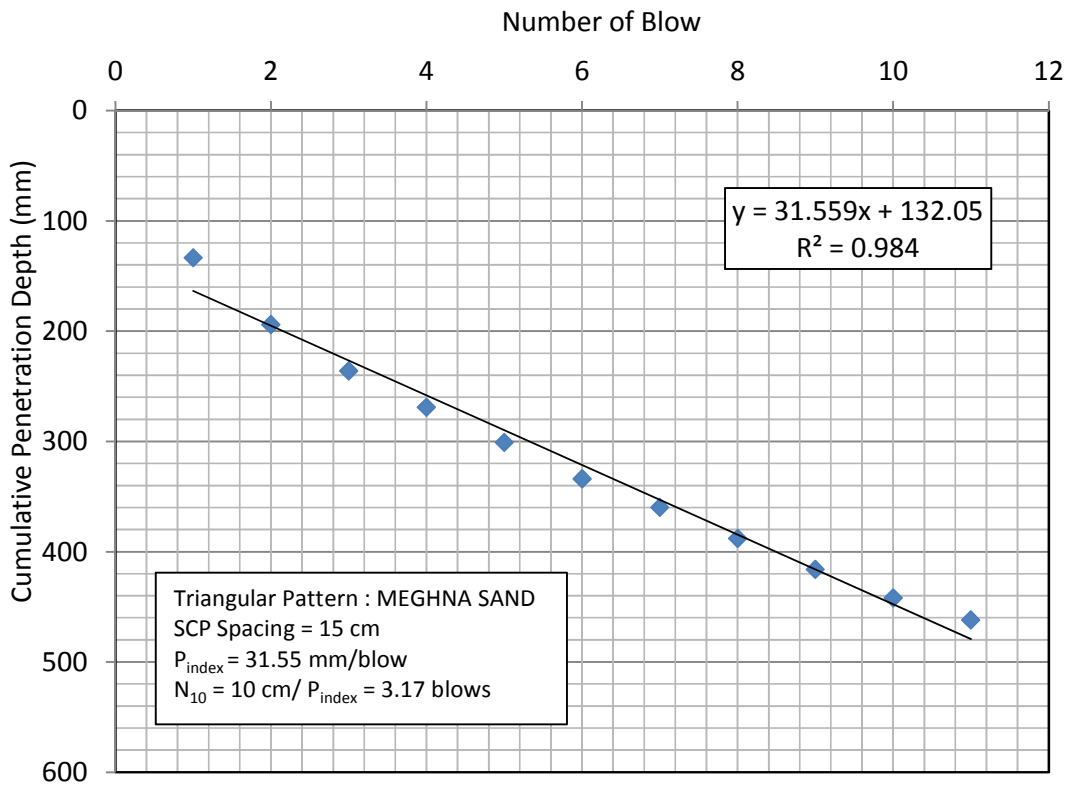


Figure 4.17: Estimation of P_{index} and N_{10} (SCP Spacing = 15 cm, Triangular Pattern; MEGHNA)

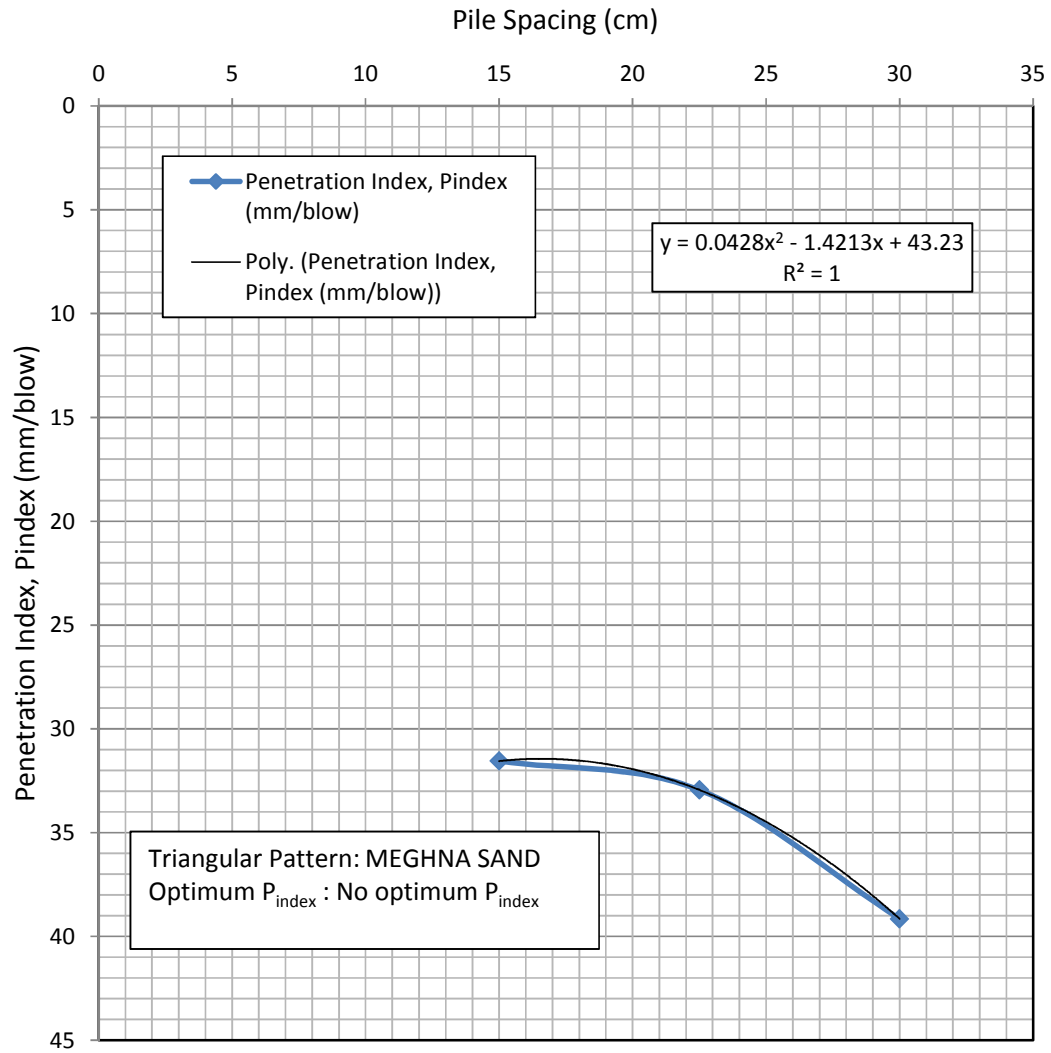


Figure 4.18: Effectiveness of SCP: Piling Spacing Vs. P_{index} , Triangular Pattern (MEGHNA)

4.7 Comparison of P_{index} Values of Sand Bed formed of Turag and Meghna Sands

With the help of calibrated DCP miniature device, penetration index of the sand bed formed of the sand of River Turag was determined both in square and equilateral triangular pattern while in case of Meghna sand it was determined in equilateral triangular pattern only. Comparative analysis data of the P_{index} value found out from the sand bed formed of the sand of River Turag and Meghna against pile spacing, in equilateral triangular pattern is shown in Table 4.5. Figure 4.19 shows the comparative graphical analysis of the P_{index} value found out from the Sand Bed formed of the Sand of River Turag and Meghna in equilateral triangular pattern.

Table 4.5: P_{index} value against pile spacing of Turag and Meghna sands for triangular pattern of SCP

Sl. No.	Item	Pile Spacing(cm)	Sand Sample	
			Turag	Meghna
1	P_{index} (mm/blow) (Triangular Pattern)	30.0	66	39.15
		22.5	39.11	32.94
		15.0	36.66	31.55

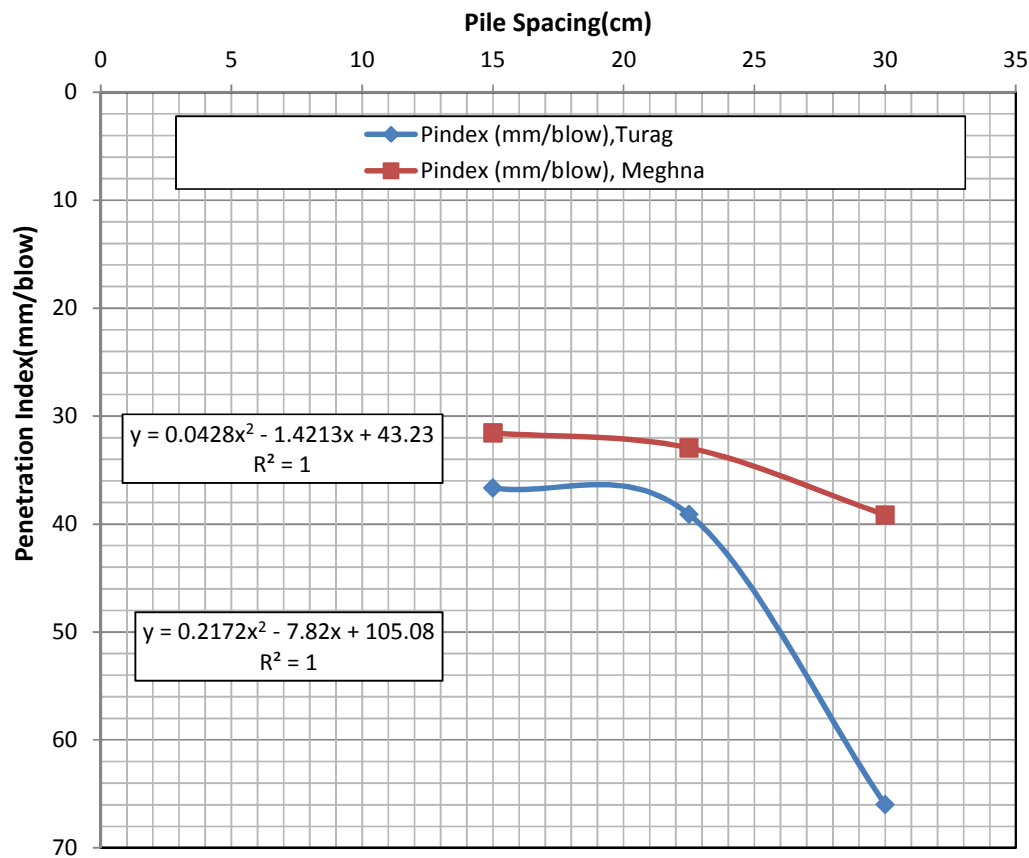


Figure 4.19: Comparison of SCP Effectiveness: Comparative Plot of Pile Spacing vs. P_{index} , between the beds formed of TURAG and MEGHNA sand (Triangular Pattern)

4.8 Prediction of Relative Density of Improved Bed

Relative density of improved bed is determined from the calibrated graph/extrapolated calibrated graph “Relative density vs. ” of the calibrated fabricated DCP miniature.

as determined from the improved bed for both square and equilateral triangular pattern in case of Turag sand and for equilateral triangular pattern only in case of Meghna sand as described earlier is used to find out the corresponding relative density. Data

analysis for establishing extrapolated calibrated correlation of the DCP miniature between relative density and P_{index} for TURAG and MEGHNA sand is shown in Table 4.6 and 4.7 respectively. Figure 4.20 and 4.21 show the extrapolated calibrated correlation plot Relative Density vs. P_{index} of the fabricated DCP miniature device for TURAG and MEGHNA sand. P_{index} and hence the relative densities determined for different spacing both in square and equilateral triangular pattern in case of Turag sand are shown in Tables 4.8 and 4.9 respectively. P_{index} and hence the relative densities determined for different spacing for equilateral triangular pattern in case of Meghna sand is shown in Table 4.10.

Table 4.6: Data for establishing extrapolated calibrated correlation of the DCP miniature between relative density and P_{index} , TURAG sand

Relative Density, D_r (%)	P_{index} (mm/blow)
34.9	150.9
46.7	125.4
58.28	109.1
63.55	98.4
70.51	87.2
100	34.8

Table 4.7: Data for establishing extrapolated calibrated correlation of the DCP miniature between relative density and P_{index} , MEGHNA sand

Relative Density, D_r (%)	P_{index} (mm/blow)
60.42	114.7
76.2	93
85.69	55.12
100	29.1

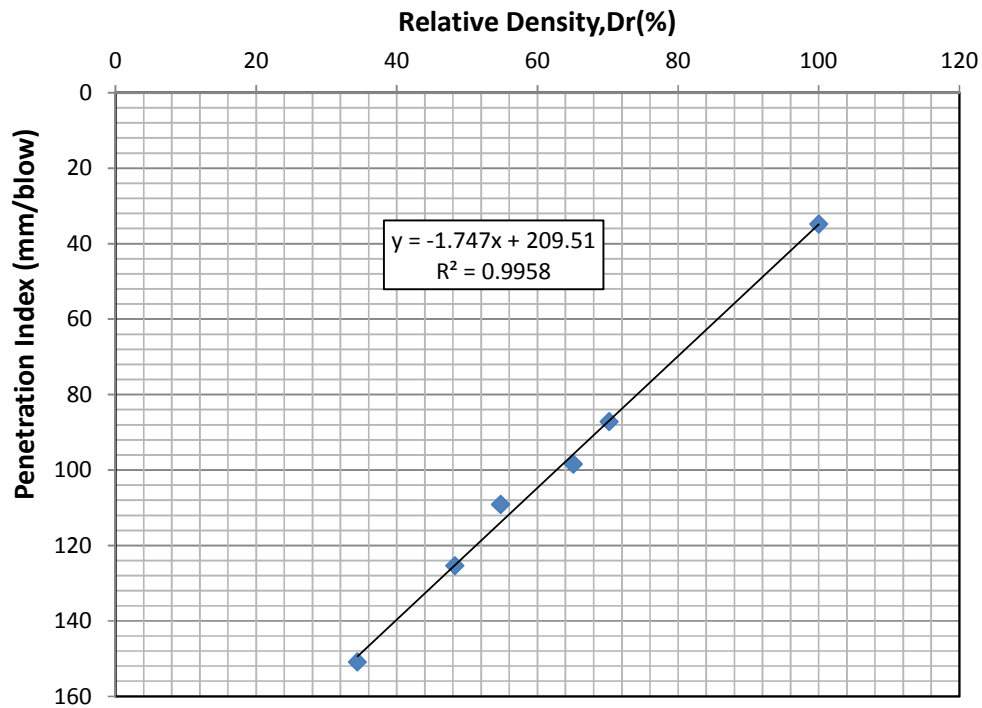


Figure 4.20: Extrapolated Correlation between Relative Density and Penetration Index, TURAG

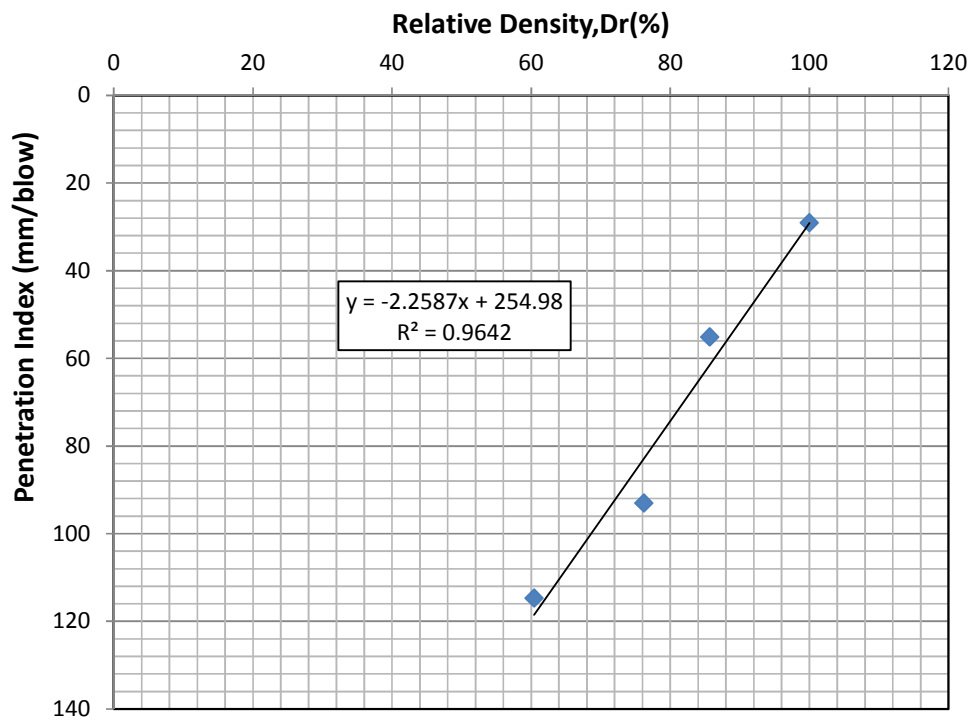


Figure 4.21: Extrapolated Correlation between Relative Density and Penetration Index, MEGHNA

Table 4.8: P_{index} and Relative Densities of Sand Bed for Square Pattern for SCP, Turag Sand

SL. No.	Pile Spacing(cm)	P_{index} (mm/blow)	Relative Densities, D_r (%)
1	30.0	69.7	80.1
2	22.5	45.66	93.8
3	15.0	44.91	94.2

Table 4.9: P_{index} and Relative Densities of Sand Bed for Triangular Pattern for SCP, Turag Sand

SL. No	Pile Spacing(cm)	P_{index} (mm/blow)	Relative Densities, D_r (%)
1	30.0	66	82.2
2	22.5	39.11	97.5
3	15.0	36.66	98.9

Table 4.10: P_{index} and Relative Densities of Sand Bed in Triangular Pattern: Meghna Sand

Sl. No	Pile Spacing(cm)	P_{index} (mm/blow)	Relative Densities, D_r (%)
1	30.0	39.15	95.5
2	22.5	32.94	98.3
3	15.0	31.55	98.9

4.9 Comparative Study for the Determination of the Most Suitable Method of SCP

Comparison of the P_{index} s and hence the relative densities as determined for both square and equilateral triangular pattern for the sand sample of River Turag is made to find out the most suitable method of SCP out of these two pattern of piling as well as the suitable spacing of SCP. Analysis of the sand sample of the River Meghna was used to confirm the suitable pattern of equilateral triangular pattern including suitable spacing of SCP. Experimental data was then compared with the practical data of equilateral triangular pattern of spacing of SCP which was carried out on the approach road project site of Padma Bridge, Janjira end as obtained by ABEDIN 2014. The comparison of the P_{index} s and Relative densities values for different piling spacing between square and equilateral

triangular pattern for Turag sand sample is shown in Table 4.11. Comparison of P_{index} and Relative Densities between Turag and Meghna Sand Sample for different Spacing in Equilateral Triangular Pattern of Piling is shown in Table 4.12.

Table 4.11: P_{index} and relative density of sand bed square and triangular patterns of SCP (Turag)

Sl. No.	Item	Pile Spacing(cm)	Pattern of Piling	
			Square	Triangular
1	P_{index} (mm/blow)	30.0	69.7	66
		22.5	45.66	39.11
		15.0	44.91	36.66
2	Relative Densities, D_r (%)	30.0	80.1	82.2
		22.5	93.8	97.5
		15.0	94.2	98.9

Table 4.12: P_{index} and relative densities of Turag and Meghna sands for triangular pattern of SCP

Sl. No.	Item	Pile Spacing(cm)	Sand Sample	
			Turag	Meghna
1	P_{index} (mm/blow) (Triangular)	30.0	66	39.15
		22.5	39.11	32.94
		15.0	36.66	31.55
2	Relative Densities, D_r (%) (Triangular)	30.0	82.2	95.5
		22.5	97.5	98.3
		15.0	98.9	98.9

4.10 Effect of SCP Pattern and Spacing on Soil Improvement

Two patterns of SCP arrangements were used in the present investigation; square and equilateral triangular. The improvement indices and for both square and triangular pattern of SCP for Turag sand are presented in Figures 4.13 and 4.14. For easy comparison the various indices obtained for Turag sand are provided in Table 4.13, and the plots are presented in Figures 4.22 to 4.25.

It was observed that there is a nonlinear variation of p_{index} with pile spacing, s/D ratio (s = SCP centre to centre spacing, D = diameter of SCP), replacement ratio, a_s . It was also observed that there is a nonlinear variation of relative density with replacement ratio, a_s .

Analysis shows that there exists a strong non-linear relationship between P_{index} and SCP pile spacing.

The relationship may be expressed as:

For Square Arrangement:

$$P_{index} = 0.227 s^2 - 8.613 s + 123.7 \quad (4.5)$$

For Triangular Arrangement:

$$P_{index} = 0.217 s^2 - 7.82 s + 105 \quad (4.6)$$

Where,

P_{index} is in mm/blow

It is to be noted from the plots that triangular arrangement of SCP always yields a lower penetration index as compared to the square arrangements giving rise to higher density of soil. This agrees with the findings of other investigators (Kitazume, 2005; Abedin, 2014).

Table 4.13: Improvement Indices for Square and Triangular SCP Arrangements (Turag Sand)

SL. No.	Pile Spacing (cm)	s/D Ratio	Area Ratio, a_s (%)		P_{index} (mm/blow)		N_{10} Values		Relative Densities, D_r (%)	
			Square	Triangle	Square	Triangle	Square	Triangle	Square	Triangle
1	30.0	4	4.91	7.56	69.7	66	1.43	1.52	80.1	82.24
2	22.5	3	8.73	13.44	45.66	39.11	2.19	2.56	93.8	97.55
3	15.0	2	19.64	30.23	44.91	36.66	2.23	2.73	94.2	98.94

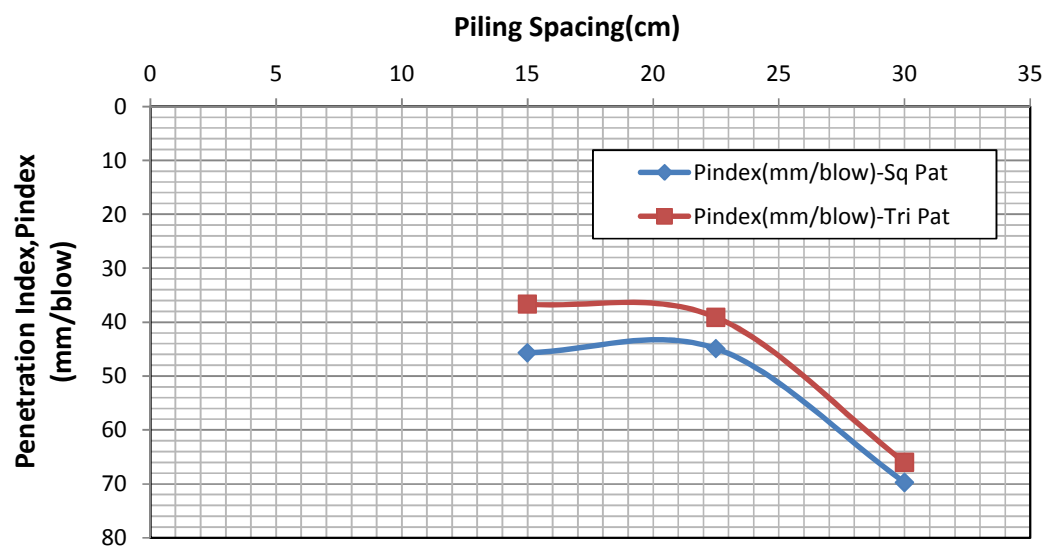


Figure 4.22: Variation of Penetration Index with SCP Spacing, Turag

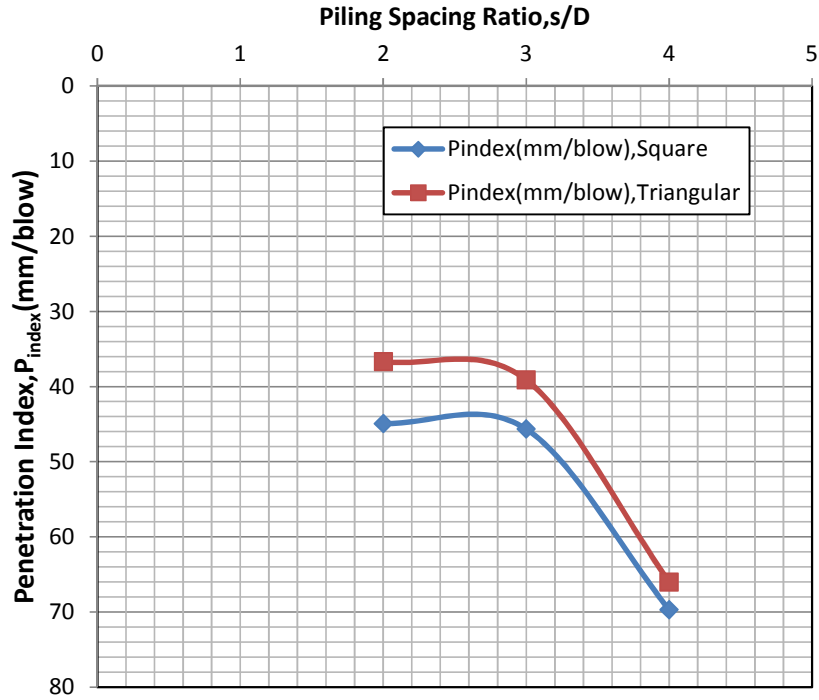


Figure 4.23: Variation of Penetration Index with SCP Spacing Ratio, Turag

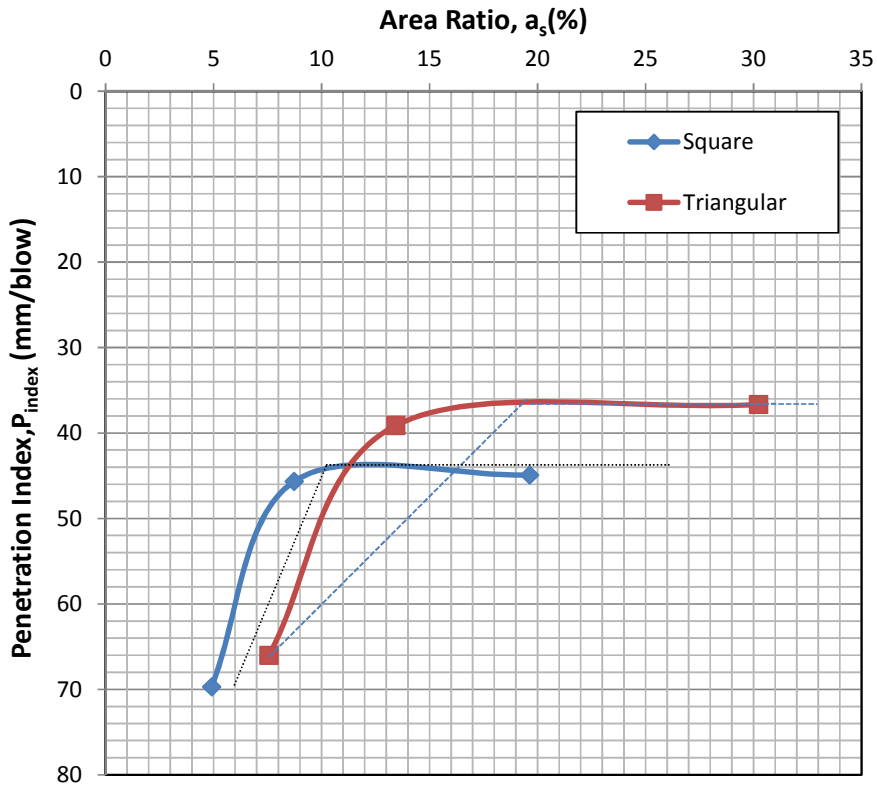


Figure 4.24: Variation of Penetration Index with Replacement Area Ratio, TURAG

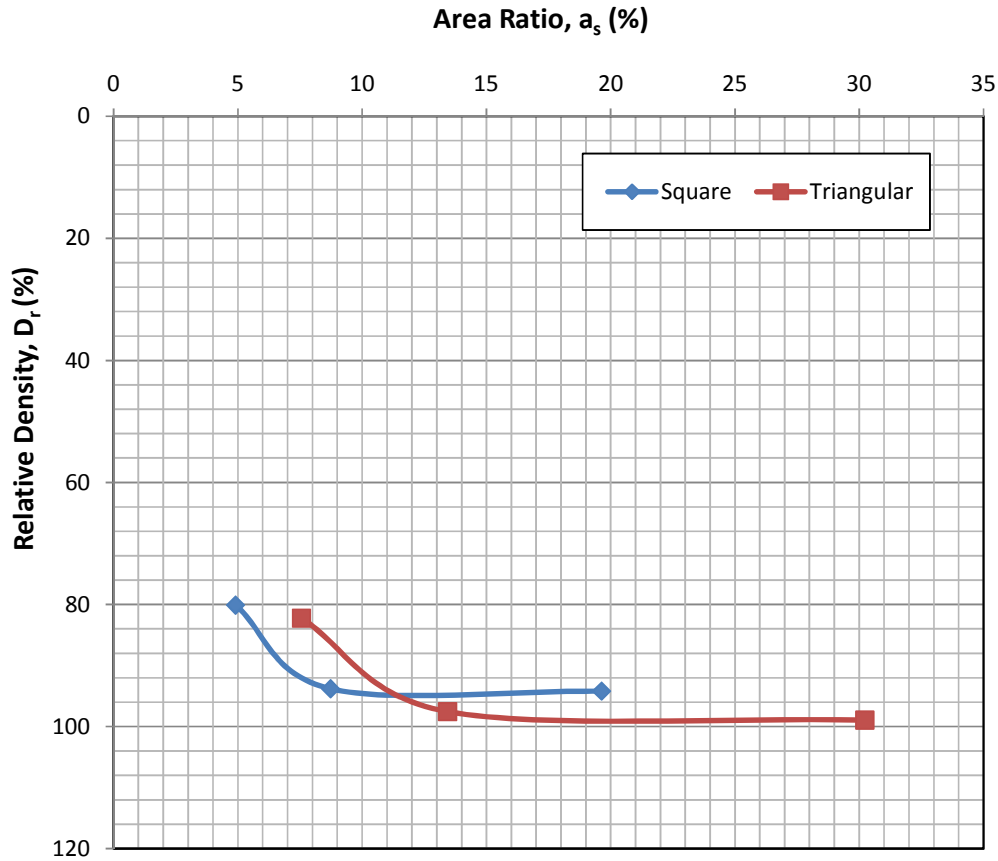


Figure 4.25: Variation of Relative Density with Replacement Area Ratio, TURAG

4.11 Effect of SCP Pattern on Replacement Ratio for Soil Improvement

It is conventional believe that soil improvement by SCP depends solely on the area replacement ratio. Contrary to that the present investigation revealed that along with the area replacement ratio, the penetration index is also sensitive to the arrangement (pattern) of SCPs. Figure 4.24 illustrates that there is an optimum p_{index} for both square and triangular arrangements, and the value is approximately 44 mm/blow and 36 mm/blow. However, the maximum penetration index reaches at a replacement ratio of approximately 10% and 20% for the cases of square and triangular arrangements.

4.12 Relation between Relative Density, and Replacement Area Ratio, a_s , of Soil

The relative density and replacement area ratio relations for Turag sand are shown in Figure 4.25. It was observed that there is a nonlinear relation between relative density and area replacement ratio. Analysis shows that with the increase of replacement area ratio relative

density of the soil increases. It was also observed that with the same replacement area ratio relative density of the triangular pattern of SCP is higher than that of square pattern.

4.13 Relation between Penetration Index, and Relative Density, of Soil

The penetration index and relative density relations for Turag sand are shown in Figure 4.26. It was observed that the data for square and triangular arrangements showed unique relationship between penetration index, P_{index} and relative density, D_r .

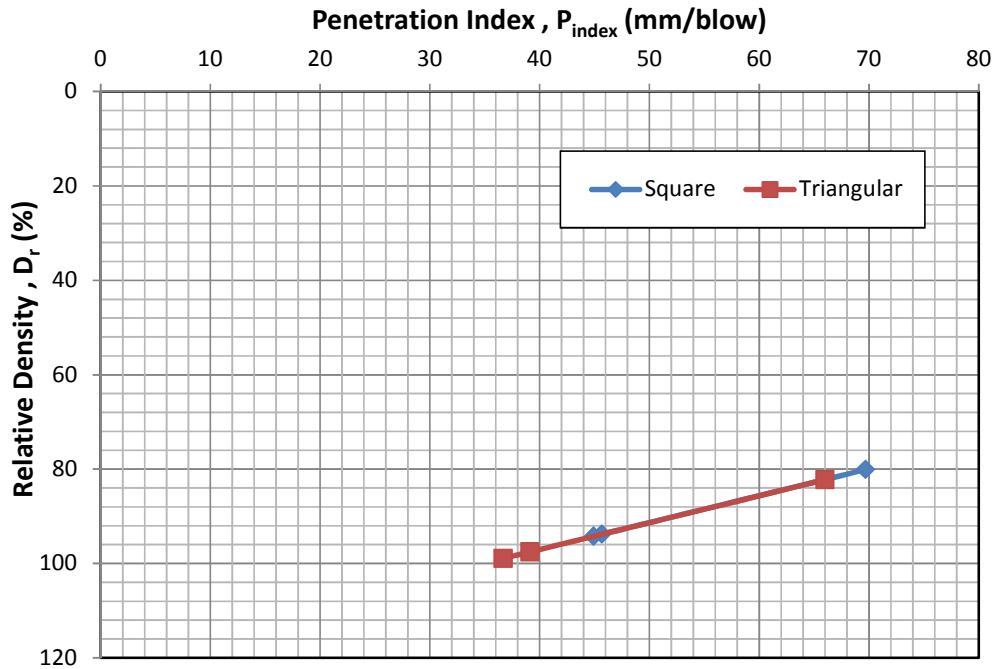


Figure 4.26: Variation of Penetration Index with Relative Density, TURAG

The relationship is linear and can be expressed by the following equation.

$$D_r (\%) = 119.7 - 0.569 P_{index} \quad (4.7)$$

Where, P_{index} is in mm/blow

4.14. Effect of Grain Characteristics on Soil Improvement due to SCP

As triangular arrangement was found to be slightly efficient as compared to the square arrangement, a coarser Meghna sand ($D_{50} = 0.20$, F.M. = 0.89) as compared to the Turag sand ($D_{50} = 0.17$, F.M. = 0.66) was taken for investigation in triangular pattern. The penetration index data are plotted in Figure 4.27 for comparison of SCP spacing - relations, and is reproduced as under. It was interesting to note that penetration index did not reach to a maximum value within the range of SCP spacing considered in this study.

This phenomenon suggests that penetration index is not uniquely related to density of soil, rather it is a function of grain characteristics of soil that needed to be investigated.

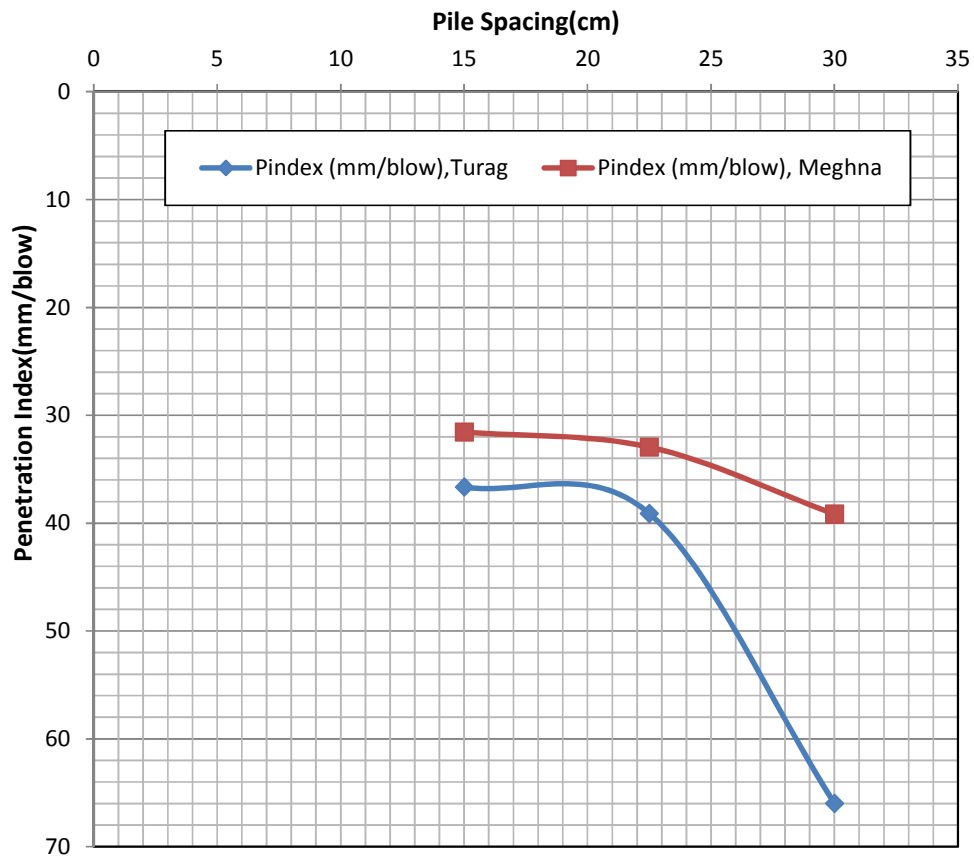


Figure 4.27: Comparison of SCP Effectiveness: Comparative Plot of Pile Spacing Vs P_{index} , TURAG and MEGHNA River (Triangular Pattern)

CHAPTER FIVE

CONCLUSIONS AND RECOMMENDATIONS

5.1 General

The present study investigated the effectiveness of using Sand Compaction Pile (SCP) in improving the loose alluvial sandy deposits of Bangladesh. This was a laboratory study on models, and two types of sand of different coarsenesses were used as soil bed materials. Artificial loose sand bed was prepared in a container tank and sand compactions piles were installed both in square and equilateral triangular patterns. The initial denseness of the soil deposits were determined using precalibrated Dynamic Cone Penetrometer (DCP). The improved soil stiffnesses were also measured in terms of penetration index using the DCP. Test data obtained for various soil and physical conditions were analysed to obtain some conclusive verdict. However, limited number of soil samples and physical conditions were considered in the investigation, and to generalize the research apprehensions, further studied should be carried out. In the following Sections the conclusion from the studies are summarized and recommendations would be made to carry out further research.

5.2 Conclusions

The study suggested the following conclusions:

- (i) With the installation of SCP the penetration index, value reaches to a constant value at an optimum replacement ratio, depending on the arrangement of sand compaction piles. The constant value of is approximately 44 mm/blow and 36 mm/blow for square and triangular pattern respectively, and the constant value reaches at a replacement ratio of 9.5% for square SCP arrangement and 13% for triangular SCP arrangement.
- (ii) The study revealed that soil improvement due to SCP is not only the function of replacement ration, but also a function of SCP arrangements.
- (iii) There is a nonlinear variation of with pile spacing. The relationship may be expressed by:

For Square Arrangement:

$$= 0.227 - 8.613 + 123.7 \quad (5.1)$$

For Triangular Arrangement:

$$= 0.217 - 7.82 + 105 \quad (5.2)$$

Where, P_{index} is in mm/blow

- (iv) Triangular arrangement of SCP always yields a lower penetration index as compared to the square arrangements giving rise to higher density of soil.

- (v) Square and triangular arrangements of SCP showed unique relationship between penetration index, P_{index} and relative density, ρ_r . The relationship is linear and can be expressed as:

$$P_{\text{index}}(\%) = 119.7 - 0.569 \rho_r \quad (5.3)$$

Where, P_{index} is in mm/blow

- (vi) This study suggests that penetration index is not uniquely related to density of soil, rather it is a function of grain characteristics of soil that needed to be investigated.
- (vii) The complexity of SCP phenomenon can be reasonably estimated using model tests in the laboratory.

5.3 Recommendations for Further Study

The following recommendation may be made to continue the present study.

- (i) The study was limited to using two types of sand with small amount of fine content. The study may be continued using varying quantities of fine.
- (ii) The study was conducted using only two types of SCP arrangements; Square and Equilateral Triangular. Further study should be done using other arrangements of SCP like rectangular, hexagonal etc.
- (iii) The study was done on dry soil sample. There may be significant effect of water content on the SCP performance. As such, study should be carried out considering the effect of water.
- (iv) In the present study only the sandy soil was considered as SCP bed material. The study should be continued on reconstituted clay sample with varying moisture content.
- (v) The present study considered only a single SCP diameter of 75 mm. To generalize, other SCP diameters of SCP should be taken in to account. It is apprehended that there must be an optimum diameter of the SCP up to which the SCP would behave like SCP.
- (vi) The present study ignored the similitude dimensions of the model. Further study should be carried out considering this important aspect of using models for laboratory tests.
- (vii) Sophisticated studies on SCP were being done by few investigators around the world using laboratory centrifuge.
- (viii) Numerical model may be developed to simulate the complexities involved in the behavior of SCP, thus addressing the problem in a refined manner. Provisions may be

kept in the model to vary any or all the parameters involved in the phenomenon of SCP.

REFERENCES

- Abedin, M.Z. (2014), Report on Geotechnical Assessment for Subsoil Improvement of Padma Bridge Approach Road Embankment at Janjira End, Unpublished Report submitted to the Bangladesh Bridge Authority, January, 2014.
- Aboshi, H., Ichimoto, E., Enoki, M. & Harada, K. (1979), The Composer- A Method to Improve Characteristics of Soft Clay by Inclusion of Large Diameter Sand Columns, Proceedings of International Conference on Soil Reinforcements, Paris, Vol. 1.
- Aboshi, H. & Suematsu, N. (1985), The State of the Art on Sand Compaction Pile method, Proc. 3rd International Geotechnical Seminar on Soil Improvement Methods, Singapore, pp. 1-12.
- Alam, M.J., Hossain, M.S. and Azad, A.K. (2012), Development of Correlation Between Dynamic Cone Resistance and Relative Density of Sand, Journal of Civil Engineering (IEB), 42 (1) (2014), pp.63-74.
- ASTM (2012a), ASTM: D 6951/D6951M: Standard Test Method for Use of the Dynamic Cone Penetrometer in Shallow Pavement Applications, American Society for Testing and Materials, 2012, West Conshohocken, PA 19428- 2959, USA.
- ASTM (2012b), ASTM D1556: Standard Test Method for Density and Unit Weight of Soil in Place by the Sand-Cone Method, American Society for Testing and Materials, 2014, West Conshohocken, PA 19428-2959, USA.
- ASTM (2012c), ASTM D2937: Standard Test Method for Density of Soil in Place by the Drive-Cylinder Method, American Society for Testing and Materials, 2012, West Conshohocken, PA 19428-2959, USA.
- ASTM (2014a), ASTM D4253: Standard Test Methods for Maximum Index Density and Unit Weight of Soils Using a Vibratory Table, American Society for Testing and Materials, 2014, West Conshohocken, PA 19428- 2959, USA.
- ASTM (2014b), ASTM D4254: Standard Test Methods for Minimum Index Density and Unit Weight of Soils and Calculation of Relative Density”, American Society for Testing and Materials, 2014, West Conshohocken, PA 19428-2959, USA.
- Barksdale, R.D. and Bachus, R.C. (1983), Design and Construction of Stone Columns, Report No. FHWA/RD-83/026, National Technical Information Service, Springfield, Virginia, USA: Cited by Jiangtao (2009).

- Baumann, V. & Bauer, G.E.A. (1974), The Performance on Various Soils Stabilized by the Vibro- Compaction Method, Canadian Geotechnical Journal, 3(2), 509-530.
- Bhandhari, R.K.M. (1983), Behaviour of a Tank Founded on Soil Reinforced with Stone Columns, Proc. 8th European Conference on Soil Mechanics and Foundation Engineering, Helsinki, pp. 209-212.
- Brauns, J. (1978), Initial Bearing Capacity of Stone Columns and Sand Piles, Symposium on Soil Reinforcing and Stabilising Techniques, Sydney, Australia, pp. 477-496.
- Cho, S.M., Kim, B.I., Kim, Y.U. and Lee, S.H. (2005), Effect of Soil Compaction Pile on Settlement Reduction in Soft Ground, Int. Journal of Offshore and Polar Engineers, Vol. 15, No. 3, Set. 2005, pp. 235-140.
- Goughnour, R.R. (1983), Settlement of Vertically Loaded Stone Columns in Soft Ground, Proceedings of the 8th European Conference on Soil Mechanics and Foundation Engineering, Helsinki, 235-240.
- Greenwood, D.A. (1970), Mechanical Improvement of Soils below Ground Surface, Proc. Of the Ground Engineering Conference, ICE, London, pp. 9-20.
- Hughes, J.M.O. and Withers, N.J. (1974), Reinforcing Soft Cohesive Soil with Stone Columns, Ground Engineering, 7(3), 42-49.
- Hwang, J.H. and Yeh, P.Y. (2012). "Assessing Improvement Effects of Sand Compaction Pile in an Ash Pond". Proc. of the Twenty-second (2012) International Offshore and Polar Engineering Conference, Rhodes, Greece, June 17-22, 2012.
- Jiangtao, Y. (2009), Centrifugr and Numerical Modelling of sand Compaction Pile Installation, Ph.D. Thesis, Dept. of Civil Engineering, National University of Singapore.
- Jung, J.B, Lee, K. and Lee, J.S. (1999), Consolidation Behaviour of Clay Ground Improved by sand Compaction Piles.
- Kempfert, H.G. (2003), Ground Improvement Methods with Special Emphasis on Column-Type Techniques, Proc. Int. Workshop on Geotechniques of Soft Soils – Theory and Practice, Vermeer, Schweiger & Cudny (Eds), VGE, Germany.
- Kitazume, M, (2005). "The Sand Compaction Pile Method", A.A. Balkema Publishers, London, UK.

- Look, B.G. (2007), Handbook of Geotechnical Investigation and Design Tables, Taylor & Francis, London.
- Moh, Z.C., Ou, C.D., Woo, S.M. and Yu, K. (1981). "Compaction Sand Piles for Soil Improvement", Proc. X International Conference on Soil Mechanics and Foundation Engineering, Stockholm, 1981, Vol. 3, pp. 749-752.
- Murali Krishna, A. and Madhav, M. R. (2008). "Treatment of Loose to Medium Dense Sands by Granular Piles: Improved SPT 'N₁' Values", Technical Note, Geotech Geol Eng (2009) 27: 455-459.
- Murayama, S. (1962), A Consideration on Vibro-compozer Method, Mechanization of Construction Work, No. 150, pp. 10-15: Cited by: Jiangtao (2009).
- Okamura, M, Ishihara, M, and Tamura, K. (2006). "Degree of Saturation and Liquefaction Resistances of Sand Improved with Sand Compaction Pile". Journal of Geotechnical and Geoenvironmental Engineering, ASCE, Vol. 132, No. 2, February 1, 2006; pp.258-264.
- Priebe, H.J. (1976), Estimating Settlements in a Gravel Column Consolidated Soil, Die Bautechnik 53, 160-162 (in German): Cited by Cited by: Jiangtao (2009).
- Prebe, H.J. (1995), The Design of Vibro-replacement, Ground Engineering, 28(10), 31-37.
- Samanta, M., Sawant, V.A. and Ramasamy, G. (2010), Ground Improvement using Displacement Type Sand Piles, Proc. Indian Geotechnical Conference, IGS Mumbai Chapter and IIT Mumbai, Dec.16-18, 2010, pp. 629-632.
- Sogabe, T. (1981), Technical Subjects on Design and Execution of Sand Compaction Pile Method, Proceedings of the Thirty-sixth Annual Conference of the Japan Society of Civil Engineers, III, 39-50: Cited by: Jiangtao (2009).
- Solyman, Z.V., Sumsudin, Osellame, J. and Purnomo, B.J. (1986), Ground Improvement by Compaction Piling, Journal of Geotechnical Engineering, ASCE, Vol. 112, No. 12, Dec. 1986, pp. 1069-1083.
- Terashi, M., Kitazume, M. & Okada, H. (1991a), Applicability of practical formula for bearing capacity of clay improved by SCP, Proceedings of the International Conference on Geotechnical Engineering for Coastal Development: Theory and Practice on Soft Ground, Yokohama, Japan, Vol. 1, 405-410. Cited by: Jiangtao (2009).
- Terashi, M., Kitazume, M. & Minagawa, S. (1991b), Bearing capacity of improved

ground by sand compaction piles, Deep Foundation Improvements: Design, Construction, and Testing, ASTM STP 1089, American Society for Testing and Materials, Philadelphia, 47-61. Cited by: Jiangtao (2009).

Tsuboi, H., Harada, K., Tanaka, Y. and Matsui, T. (2003), Construction for Judging Suitability of Filling Materials for an SCP, Int. Jnl. Of Offshore and Polar Engineering, 13(1), 66-72.

Unnikrishnan, N. and Johnson, A.S. (2009), Efficacy of Densification Techniques for Bearing Capacity Improvement, Proc. Indian Geotechnical Congress 2009, Guntur, India.

Van Impe, W.F. & De Beer, E. (1983), Improvement of Settlement Behaviour of Soft Layers by Means of Stone Columns, Proceedings of the Eighth European Conference on Soil Mechanics and Foundation Engineering, Helsinki, 309-312.

Vesic, A.S. (1972), Expansion of Cavities in Infinite Soil Mass, Journal of the Soil Mechanics and Foundations Division, ASCE 98, No. SM3, 265-290.

Weber, T.M. (2004), Development of Sand Compaction Pile Installation Tool for the Geotechnical Drum Centrifuge, XVI European Young Geotechnical Engineers Conference, 8-11 July, 2004, Vienna, Austria.